UNIVERSITY OF CALIFORNIA SAN DIEGO

Functional Characterization of Oncogenic Driver FGFR3-TACC3

A dissertation submitted in partial satisfaction of the

requirements for the degree Doctor of Philosophy

in

Chemistry

by

Katelyn N. Nelson

Committee in charge:

Professor Daniel J. Donoghue, Chair
Professor Seth M. Cohen
Professor Jack E. Dixon
Professor Seth J. Field
Professor Susan S. Taylor

2018

The Dissertation of Katelyn N. Nelson is approved, and it is acceptable in quality and form for publication on microfilm and electronically:

_____

_____

_____

_____

_____
Chair

University of California San Diego

2018

DEDICATION

This dissertation is dedicated to my parents and grandparents, without whom college and graduate school would have never been possible. Thank you for encouraging me always and teaching me the importance of hard work. This work is also dedicated to Lindsay Mitchell, Tanis Au, and Randy Au. Your love and support means more than you will ever know.

EPIGRAPH

The expert in anything was once a beginner.

-Helen Hayes

TABLE OF CONTENTS

Signature Page……..iii

Dedication…….iv

Epigraph……..v

Table of Contents……..vi

List of Figures…….viii

List of Tables....……....ix

Acknowledgements……x

Vita…….xii

Abstract of the Dissertation…….xiv

Chapter 1 Functions of Fibroblast Growth Factor Receptors in Cancer Defined by Novel Translocations……..……..…….1
1.1 Overview of Canonical FGFR Signaling……2
1.2 FGFR Translocations and Fusion Proteins in Cancer……..4
1.3 Concluding remarks……22
1.4 Acknowledgments……...22
1.5 References…….....23

Chapter 2 Oncogenic Gene Fusion FGFR3-TACC3 Regulated by Tyrosine Phosphorylation……29
2.1 Introduction……30
2.2 Results……32
2.3 Discussion .....…….……..46
2.4 Materials and Methods…….....50
2.5 Acknowledgments……...57
2.6 References……...57

Chapter 3 Oncogenic Driver FGFR3-TACC3 is dependent on membrane trafficking and MAPK signaling……61
3.1 Introduction…….....62
3.2 Results…….....63
3.3 Discussion…….……..84
3.4 Materials and Methods…….....87
3.5 Acknowledgments……...91
3.6 References……...91

Chapter 4 Receptor Tyrosine Kinases: Translocation Partners in Hematopoietic Disorders..94
4.1 Receptor Tyrosine Kinase Translocations in Cancer.…….....94
4.2 ALK Translocations: Fusion Proteins Involving the Only RTK Named for a Disease…….97
4.3 FGFR Translocations: Relatively Rare but Providing Important Insights ……..100
4.4 PDGFR Translocations: Fusion Proteins and Their Cancers …….....108
4.5 Signaling Alterations Resulting from RTK Translocations ……111
4.6 Therapeutics for Hematopoietic Cancers with RTK Translocations……116
4.7 Concluding Remarks…….122
4.8 Acknowledgments…….122
4.9 References…….123

LIST OF FIGURES

Figure 1. FGFR signaling pathways…….....3

Figure 2. Structural organization of select FGFR fusion proteins……..6

Figure 3. Increase in tyrosine phosphorylation by introduction of the TACC domain…….32

Figure 4. Phosphorylated tyrosine residues in FGFR3, FGFR3(K650E), FGFR3-TACC3 and FGFR3(K650E)-TACC3 identified by mass spectrometry analysis…..34

Figure 5. Representative spectra of selected peptides……...36

Figure 6. Transformation of NIH3T3 cells by FGFR3 and FGFR3-TACC3 derivatives.……39

Figure 7. IL-3 independent growth and MTT viability assay in 32D cells expressing FGFR3 or FGFR3-TACC3 derivatives…….....41

Figure 8. Localization and signaling of FGFR3-TACC3 fusions…….43

Figure 9. Nuclear-localized FGFR3-TACC3 does not convey cell transformation……..62

Figure 10. Plasma membrane-localized FGFR3-TACC3 conveys cell transformation.....64

Figure 11. Re-localization to the plasma membrane reinstates NLS-FGFR3-TACC3 oncogenic activity.……...……...…..66

Figure 12. FGFR3-TACC3 presence in the secretory pathway produces oncogenic effects....69

Figure 13. TACC domain mutations and their contribution to cell transformation.....72

Figure 14. Effect of MEK and FGFR inhibitors on cell transformation and MAPK pathway…….74

Figure 15. General Structural Schematic of RTK Fusion Proteins……...96

Figure 16. Cellular localization of various RTK fusion proteins……99

Figure 17. Major signaling pathways activated by common RTK fusion proteins……116

LIST OF TABLES

Table 1. FGFR fusion proteins arising from translocations…….....19

Table 2. RTK Fusion Proteins in Hematological Cancers……..104

Table 3. TKIs: Therapeutics for Hematopoietic Disorders…….121

ACKNOWLEDGEMENTS

I would like to thank Professor Daniel J. Donoghue for his invaluable support and guidance as my advisor. I am extremely grateful the opportunity to earn my degree and further my education in his laboratory. I would also like to thank April Meyer for teaching and mentoring me, and for answering countless questions, without whom my education and this project would have suffered greatly. Thank you to Asma Siari, Clark Wang, and Annie Chang for their valued contributions to this project. Thank you to everyone I have worked with in the Donoghue lab, Leandro Gallo, Juyeon Ko, Nicole Peiris, Laura Castrejon, Fangda Li, Guillermo Cardenas, and Anna Seck for the constant support, feedback, and camaraderie.

Chapter 1, in part was published as "Functions of Fibroblast Growth Factor Receptors in Cancer Defined by Novel Translocations and Mutations", in Cytokine and Growth Factor Reviews in 2015 with the authors Gallo LH, Nelson KN, Meyer AN, Donoghue DJ. The dissertation author was a co-author of this paper.

Chapter 2 was published as "Oncogenic Gene Fusion FGFR3-TACC3 Is Regulated by Tyrosine Phosphorylation", in Molecular Cancer Research in 2016, with the authors of Nelson KN, Meyer AN, Siari A, Campos AR, Motamedchaboki K, Donoghue DJ.. The dissertation author was the primary investigator and author of this material.

Chapter 3, in part is currently being prepared for submission for publication of the material, with the authors of Nelson KN, Meyer AN, Wang CG, Donoghue DJ. The dissertation author was the primary investigator and author of this material.

Chapter 4 was published as "Receptor Tyrosine Kinases: Translocation Partners in Hematopoietic Disorders", in Trends in Molecular Medicine in 2017, with the authors of

Nelson KN, Peiris MN, Meyer AN, Siari A, Donoghue DJ. The dissertation author was the primary investigator and author of this material.

VITA

2012 B. S. in Biochemistry, California State University, Long Beach, USA

2015 M. S. in Chemistry, University of California San Diego, USA

2018 Ph. D. in Chemistry, University of California San Diego, USA

PUBLICATIONS

Katelyn N. Nelson, April N. Meyer, Clark Wang, Daniel J. Donoghue**. "**Oncogenic Driver FGFR3-TACC3 is dependent on membrane trafficking and ERK signaling." *To be submitted.* 2018.

Leandro H. Gallo, Juyeon Ko, Katelyn N. Nelson, April N. Meyer, Asma Siari, and Daniel J. Donoghue. "Oncogenic mutations in IKKB signal through a UBE2N/UBE2V2 dependent mechanism." *In progress.* 2018.

Katelyn N. Nelson, Malalage N. Peiris, April N. Meyer, Asma Siari, Daniel J. Donoghue**. "**Receptor tyrosine kinases: translocation partners in hematopoietic disorders." *Trends in Molecular Medicine,* 23(1): 59-79, 2017.

Katelyn N. Nelson, April N. Meyer, Asma Siari, Alexandre R. Campos, Khatereh Motamedchaboki, Daniel J. Donoghue. "Oncogenic Gene Fusion FGFR3-TACC3 is Regulated by Tyrosine Phosphorylation." *Molecular Cancer Research,* 14(5): 458-69, 2016.

Leandro H. Gallo, Katelyn N. Nelson, April N. Meyer, and Daniel J. Donoghue. "Functions of Fibroblast Growth Factor Receptors in Cancer Defined by Novel Translocations and Mutations." *Cytokine & Growth Factor Reviews,* 26(4):425-49, 2015.

Leandro H. Gallo, April N. Meyer, Khatereh Motamedchaboki, Katelyn N. Nelson, Martin Haas, and Daniel J. Donoghue. "Novel Lys63-linked Ubiquitination of IKKβ Induces STAT3 Signaling." *Cell Cycle,*13(24):3964-76, 2014.

ABSTRACT OF THE DISSERTATION

Functional Characterization of Oncogenic Driver FGFR3-TACC3

by

Katelyn N. Nelson

Doctor of Philosophy in Chemistry

University of California San Diego, 2018

Professor Daniel J. Donoghue, Chair

Fibroblast Growth Factor Receptors (FGFRs) are critical for cell proliferation and differentiation. Mutation and/or translocation of FGFRs lead to aberrant signaling that often results in developmental syndromes or cancer growth. As sequencing of human tumors becomes more frequent, so does the emergence of FGFR translocations and fusion proteins. The research conducted in this work will focus on a frequently identified fusion protein between FGFR3 and transforming acidic coiled-coil containing protein 3 (TACC3). As detailed in this dissertation, it is apparent that the fused coiled-coil TACC3 domain results in

constitutive phosphorylation of key activating FGFR3 tyrosine residues. The presence of the TACC coiled-coil domain leads to increased and altered levels of FGFR3 activation, fusion protein phosphorylation, MAPK pathway activation, nuclear localization, cellular transformation, and IL3-independent proliferation. Introduction of K508R FGFR3 kinase dead mutation abrogates these effects, except for nuclear localization which is due solely to the TACC3 domain. We further demonstrate that the oncogenic effects initiated by FGFR3-TACC3 are dependent on the overactivation of the MAPK pathway and localization of FGFR3-TACC3 to the secretory pathway or the plasma membrane. The activation of the MAPK pathway is essential for cell transformation but involvement in the cell cycle via the canonical TACC3 pathways is not. Additionally, we have shown that kinase inhibitors for MEK (Trametinib) and FGFR (BGJ398) are effective in blocking cell transformation and MAPK pathway upregulation. The need for precision medicine is evidenced by the different effects these inhibitors have against various FGFR3-TACC3 breakpoints. The existence of FGFR3-TACC3 fusions in human cancers creates additional challenges and opportunities for identifying effective treatment strategies. The development of such personalized medicines will be essential in treating patients who harbor oncogenic drivers such as FGFR3-TACC3.

CHAPTER 1

Functions of Fibroblast Growth Factor Receptors in Cancer Defined by Novel Translocations

ABSTRACT

The four receptor tyrosine kinases (RTKs) within the family of Fibroblast Growth Factor Receptors (FGFRs) are critical for normal development but also play an enormous role in oncogenesis. Mutations and/or abnormal expression often lead to constitutive dimerization and kinase activation of FGFRs, and represent the primary mechanism for aberrant signaling. Sequencing of human tumors has revealed a plethora of somatic mutations in FGFRs that are frequently identical to germline mutations in developmental syndromes, and has also identified novel FGFR fusion proteins arising from chromosomal rearrangements that contribute to malignancy. This chapter reviews approximately 40 different fusion proteins created by translocations involving FGFRs that have been identified in human cancer. This chapter discusses the effects of these genetic alterations on downstream signaling cascades, and the challenge of drug resistance in cancer treatment with antagonists of FGFRs.

1.1 OVERVIEW OF CANONICAL FGFR SIGNALING

Receptor tyrosine kinases (RTKs) represent important signal transducers in the cell membrane and are comprised of nearly twenty families of homologous proteins in humans, with almost 60 distinct members (1). In the FGFR family, four homologous human receptors have been identified: FGFR1, FGFR2, FGFR3 and FGFR4. All of the FGFRs exhibit three extracellular immunoglobulin (Ig)-like domains, a membrane-spanning segment and a split tyrosine kinase domain. Fibroblast growth factors (FGFs), a large family of related growth factors, act in concert with heparin sulfate proteoglycans (HSPGs) as high-affinity FGFR agonists (2, 3). The splicing of FGFRs results in further distinction of ligand specificity accompanied by altered biological properties, in which the most studied splicing isoforms involve the third immunoglobulin-like domain of the receptors (4). For FGFR2 and FGFR3, the first half of third Ig domain consists of an invariant exon (IIIa), and splicing of the second half of third Ig domain results in either IIIb isoform (exons 7 and 8) or IIIc isoform (exons 7 and 9). Generally, the IIIb isoforms of FGFRs are expressed in tissues of epithelial origin whereas the IIIc isoforms are expressed in mesenchymal tissues (5).

Binding of FGF/HSPG to FGFR induces the dimerization of receptor monomers in the plasma membrane, followed by trans-autophosphorylation of tyrosine residues located in the cytoplasmic kinase domain. This tyrosine phosphorylation triggers the binding of Src homology (SH2) domain of phospholipase C gamma (PLCγ) to the receptor, resulting in the activation of PKC. Activation also induces RAS-MAPK and PI3K-AKT signaling via FRS2 and GRB2 adaptor proteins. Additional pathways activated by FGFRs include Jun N-terminal kinase and JAK/STAT pathways. FGFR signaling results in cellular proliferation and migration, anti-apoptosis, angiogenesis and wound healing (Figure 1) (6).

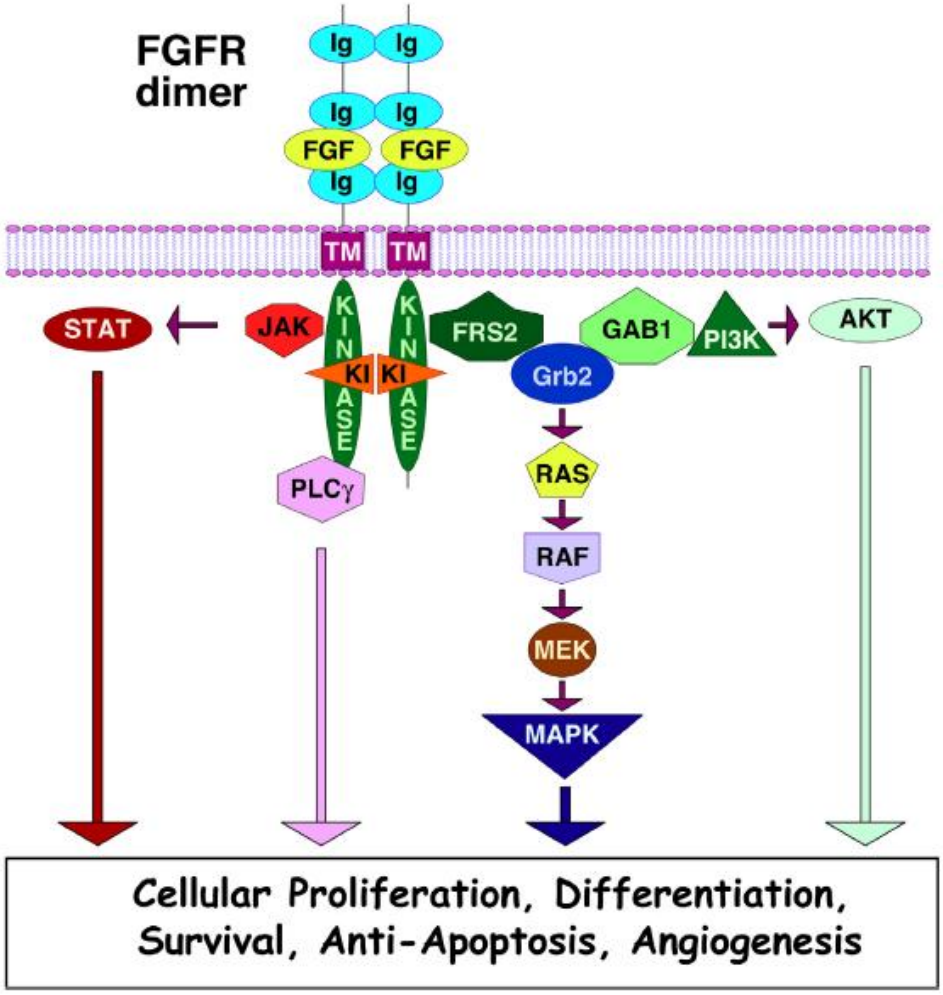

Figure 1. FGFR Signaling Pathways. FGF ligand binds to FGFR monomers, leading to the dimerization and subsequent tyrosine autophosphorylation of the receptor. This event leads to activaton of FGFRs and various downstream proteins, resulting in cellular proliferation, differentiation, survival, anti-apoptosis and angiogenesis.

1.2 FGFR TRANSLOCATIONS AND FUSION PROTEINS IN CANCER

FGFR fusion protein discovery across a variety of cancers

Fusion proteins are continually being discovered in a variety of human cancers. Particularly, fusions involving FGFRs are prevalent in hematological cancers and solid tumors. The existence of translocations involving FGFRs has been known since the late 1990s, when a patient with T-cell lymphoblastic lymphoma was found to harbor a ZNF198-FGFR1 fusion, now also referred to as ZMYM2-FGFR1. Lymphoma or leukemia cases from the 1970s and 1980s described disease characteristics similar to the now well-defined disease, 8p11 myeloproliferative syndrome (EMS). This correlation may arise because FGFR1 fusions in leukemia and lymphoma often originate as EMS. According to the World Health Organization, EMS is classified as "myeloid and lymphoid neoplasms with FGFR1 abnormalities," and has also been called "stem cell leukemia/lymphoma" (7).

In EMS, FGFR1 located at 8p11.22 is often disrupted by chromosomal translocation, resulting in a fused coding region. The fusions in EMS consistently result in FGFR1 fused to an N-terminal dimerization domain (Figure 2), an alteration that has also been found in breast cancer, lung squamous cell carcinoma, phosphaturic mesenchymal tumor, rhabdomyosarcoma and leukemia (Table 1) (8-11). With FGFR as the 3' partner, the ligand-binding extracellular domain and transmembrane domain are excluded from the fusion protein, with only the FGFR kinase domain attached to the 5' protein partner. Dimerization of this fusion type would result only from the N-terminal oligomerization domain, not FGF ligand binding. In solid tumors, it is more common to find FGFR as the 5' fusion gene, with the breakpoint consistently found in exons 17, 18, or 19, leaving the extracellular, transmembrane and kinase domains intact. When the extracellular domain is present, dimerization is thought to increase with the addition

of FGF ligand. Although the domains present in fusion proteins vary, the intact FGFR kinase domain is always retained, indicating this domain is critical for a functioning fusion protein and cancer progression. It is rare to see an FGFR fusion protein with an additional FGFR activating mutation. The reason may be that either event alone may be sufficient for cancer to progress, although the dual activation of an FGFR both by mutation and translocation could provide additional oncogenic potential. Additionally, while some FGFR fusions occur with high tissue specificity, others occur across many cancer types (12).

Dimerization of FGFR induced by the fusion partner

In FGFR fusion proteins, almost all fusion partners contribute a known dimerization domain which allows the FGFR to dimerize and autophosphorylate the kinase domain, leading to activation and downstream signaling, increased cell proliferation and cancer progression (Figure 1). Recently, an FGFR3 fused to transforming acidic coiled-coil containing 3 (TACC3) has been discovered in glioblastoma, bladder cancer, lung cancer, oral cancer, head and neck squamous cell carcinoma and gallbladder cancer (8, 9, 13-19) (Table 1). Additionally, FGFR1-TACC1 has been identified in glioblastoma (18, 20). The coiled-coil domain of TACC3 is assumed to bring the FGFR3 portion of the fusion proteins close together, inducing activation. FGFR3-TACC3, FGFR3-BAIAP2L1, and FGFR2-CCDC6 have been shown to dimerize presumably through their coiled-coil domains (8). The FGFR2-BICC1 gene fusion has been found in cholangiocarcinoma, colorectal cancer and hepatocellular carcinoma (8, 21-23). The self-associating sterile alpha motif domain (SAM) of BICC1, containing a helix-loop-helix domain, fused 3' to FGFR2, is believed to instigate constitutive dimerization of FGFR2 in order to produce an active receptor (12) (Figure 2).

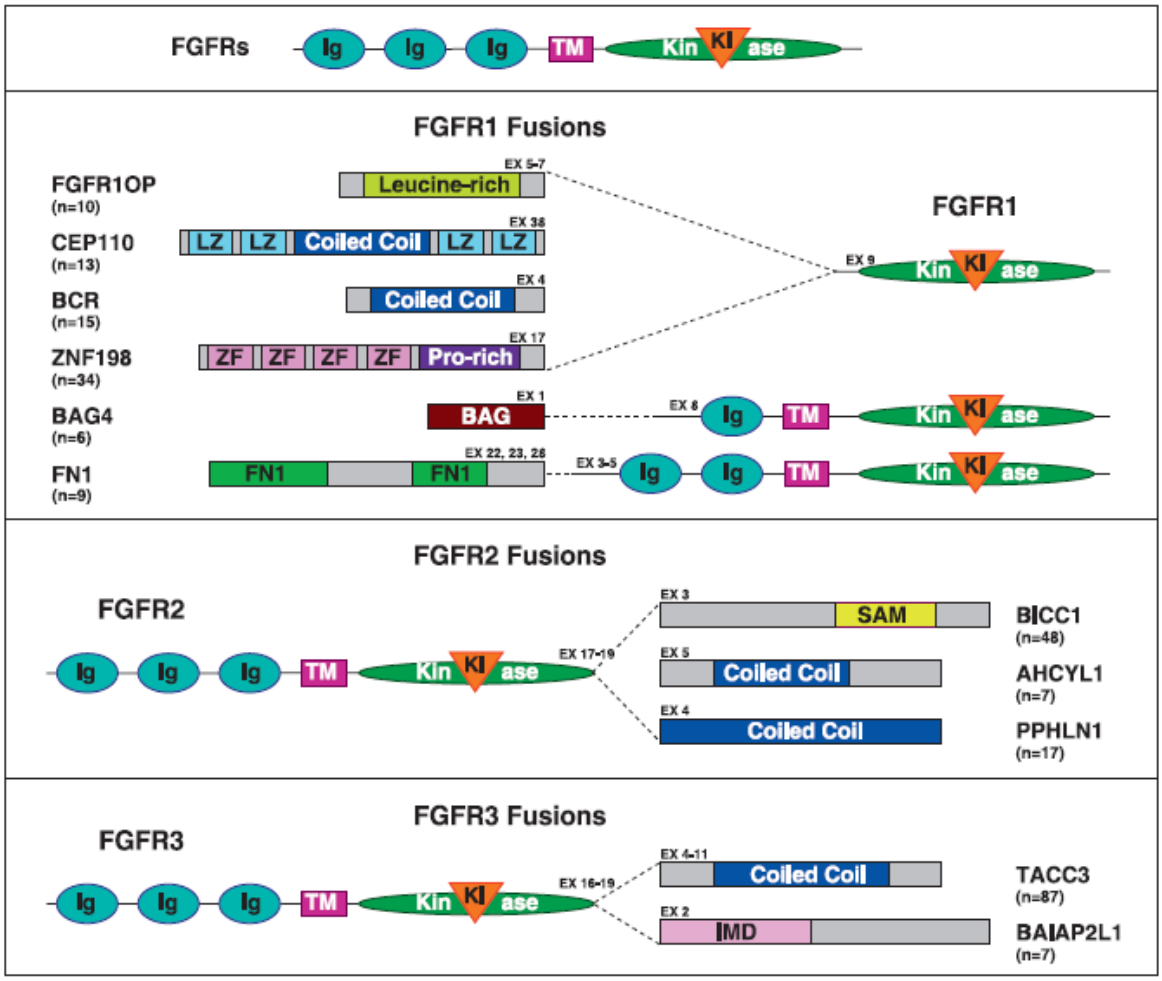

Figure 2. Structural Organization of Select FGFR Fusion Proteins**.** Schematic representations are presented for the more common (n>5) FGFR fusions identified in human cancers and cell lines. The most common breakpoint of each fusion is shown. Occurrence numbers (n) indicate the total number of times the fusion has been identified, including breakpoints not shown in the figure. See Table 3 for full list of FGFR fusions and translocations.

Other dimerization domains found in FGFR fusion proteins are believed to have the same function. FGFR fusion partner domains include zinc-finger, leucine zipper, coiled-coil, SAM, LIS1-homologous (LIsH), IRSp53/MIM (IMD), BAG, FN1, AFF3, and stomatin/prohibitin/flotillin/HflK/C (SPFH) domains (also known as the prohibitin PHB

domain) (Table 1). Other fusions thought to dimerize by self-association domain include FGFR2-CASP7 in breast cancer, which dimerizes through active site loops, and CPSF6-FGFR1, which dimerizes through a RNA recognition motif (7, 8, 24). The most frequent fusion partner domain is the coiled-coil, occurring in the proteins mentioned above; in addition, the other coiled-coil fusion proteins are BCR-FGFR1 (25), CEP110-FGFR1 (7), CUX1-FGFR1 (26), FGFR1OP2-FGFR1 (27), FGFR2-AHCYL1 (21), FGFR2-CIT (28), FGFR2-FAM76A (29), FGFR2-KIAA1598 (22), FGFR2-KIAA1967 (8), FGFR2-OFD1 (8), FGFR2-PPHLN1 (30), FGFR2-TACC3 (23), LRRFIP1-FGFR1 (7), MYO18A-FGFR1 (7), TRIM24-FGFR1 (7), and TPR-FGFR1 (31).

In order for autophosphorylation to occur, RTKs need to be exactly aligned. It has been shown that dimerization of the intracellular domain alone will not activate the receptor. Ligand binding rotates and aligns the extracellular juxtamembrane domain and intramembrane α-helices, leading to intracellular kinase domain alignment, dimerization and activation (24). To create an active FGFR fusion protein, the dimerization domain must provide the correct alignment. The most common FGFR1 fusion in EMS is ZNF198-FGFR1, which contains either 4 or 10 zinc finger domains and a proline-rich domain from ZNF198, followed by the tyrosine kinase domain of FGFR1 (Figure 2) (7). The proline-rich domain is a self association domain and is essential for dimerization and activation of FGFR1 (32).

An exception to the activation-by-oligomerization theme is an internal tandem duplication (ITD) of FGFR1 in a patient with pilocytic astrocytoma, resulting in a duplication of the FGFR1 kinase domain. ITD has previously been observed in Acute Myeloid Leukemia with FLT3, another receptor tyrosine kinase. This ITD, which occurs in the juxtamembrane

domain of FLT3, leads to enhanced receptor activation and increased downstream signaling of MAPK and STAT5 (33).

Altered cellular localization of FGFR by the fusion partner

Often, the creation of FGFR fusion proteins not only activates FGFR and its canonical pathways, but results in an incongruous FGFR localization as well. Some partner proteins can lead to localization of FGFR to a cellular compartment other than the plasma membrane. Fusion proteins that have been shown to have irregular localization include FGFR1OP-FGFR1, CEP110-FGFR1, ZNF198-FGFR1, and TEL-FGFR3 in lymphoma and FGFR3-TACC3 in glioblastoma. Wild-type FGFR1OP (FGFR1 oncogenic partner) and CEP110 (centriolin) are centrosomal proteins. Once engaged in a fusion with FGFR1, FGFR1OP localizes the kinase domain to the centrosome through a CAP350 interaction (34). CEP110 is involved in centriole maturation and localizes to the centrosome via an 170-amino acid region in the C-terminus, a region retained in the CEP110-FGFR1 fusion. Instead of the expected localization to the centrosome, cytoplasmic expression of the fusion protein was observed (35). Continuous kinase activity and inappropriate cytoplasmic localization due to CEP110-FGFR1 fusion formation may result in increased cell viability and hematopoietic stem cell growth. The fusion proteins ZNF198-FGFR1 and TEL-FGFR1 have been identified as cytoplasmic proteins (7, 11). The translocation of ZNF198 and FGFR1 genes removes the FGFR1 transmembrane domain and the C-terminal nuclear localization signal of ZNF198, which most likely leads to cytoplasmic localization.

Expressed FGFR3-TACC3 has been shown to localize to the mitotic spindle poles in dividing mouse astrocytes, most likely due to recruiting effects of TACC3. In addition, the fusion protein increased the percentage of aneuploidy by greater than 2.5-fold (18). As TACC3 is an important component of mitotic spindle assembly and is involved with the attachment of chromosomes to microtubules, it is most likely playing a role in chromosomal segregation errors. During mitosis, wild-type TACC3 is strongly diffused around centrosomes, due to the localizing effects of the C-terminal coiled-coil (36). As this domain is present in the FGFR3 fusion, multiple effects could be implicated by the fusion protein such as localization of FGFR3-TACC3 to the centrosome or a novel biochemical activity. During interphase, wild-type TACC3 has been found to be concentrated in the nucleus (36). The location of the FGFR3-TACC3 fusion in non-dividing cells has not yet been identified.

Although the localization of ERLIN2-FGFR1 has not yet been investigated, wild-type ERLIN2 anchors to the ER membrane via an N-terminal binding motif. This motif is still present when ERLIN2 is fused to FGFR1, and may be affecting fusion protein location (37). The fusion results in the SPFH oligomerization domain of ERLIN2 fused 5' to exon 4 of FGFR1, and was detected in breast cancer.

Thus, for these and other FGFR fusion proteins discussed: is the salient biological feature the localization of the FGFR kinase domain to a novel cellular compartment? Or, is it the constitutive dimerization and activation of the FGFR kinase domain, regardless of the localization of the normal fusion partner, that is determinative? Much further experimental research will be required to arrive at a definitive answer.

Downstream signaling impacts of fusion proteins

FGFR fusion proteins have been shown to activate the normal FGFR pathways, specifically the PI3K/AKT, MAPK, and JAK/STAT pathways (Figure 1). FGFR3-TACC3, FGFR3-BAIAP2L1, and FGFR2-CCDC6 increase activation of PI3K/AKT and MAPK pathways (12). FGFR2-TACC3 has also been shown to increase MAPK activation, but only a moderate increase of FRS2 phosphorylation of the PI3K pathway has been seen (23). In wild-type FGFR1, FRS2 normally binds to the juxtamembrane domain between amino acids 407 and 433. In many FGFR1 fusions, this domain is either fully or partially disrupted by translocation of the fusion partner, which results in an inability to recruit FRS2. This has been shown to occur in ZNF198-FGFR1, but may occur in other fusion proteins with FGFR as the 3' partner. However, although FRS2 interaction with ZNF198-FGFR1 was undetectable, the PI3K pathway remained active (7).

In addition to the activation of MAPK and PI3K pathways, cells expressing FGFR1OP-FGFR1 exhibit increased phosphorylation of STAT1 and STAT3, but not STAT5 (38). Furthermore, ZNF198-FGFR1 activates STAT5, FGFR3-TACC3 activates STAT3, and FGFR3-BAIAP2L1 and FGFR2-CCDC6 increase STAT1 activation (12, 34). ERLIN2-FGFR1 and CEP110-FGFR1 have been shown to be biologically active through tyrosine phosphorylation of the respective fusion proteins, but further downstream signaling activation has not been explored (8, 35). Despite an overall increase in cell proliferation pathway activation, a contrasting study reports a failure to over-activate MAPK and AKT by FGFR3-TACC3 (18). Studies exploring FGFR2-AHCYL1 and FGFR2-BICC1 fusions report an absence of AKT and STAT3 phosphorylation, although the MAPK pathway remained active (21). Additionally, TEL-FGFR3 directly interacts with and activates STAT3 and STAT5,

presumably through the FGFR3 portion of the protein, an interaction that has not been shown with other fusion proteins (11).

Fusions with FGFR as the 5' partner usually result in a deletion of the last exon of FGFR, which includes the tyrosine residue important for PLCγ binding (39). In bladder cancer, cells transfected with FGFR3-TACC3 or FGFR3-BAIAP2L1 were unable to activate PLCγ, due to a deletion of the last exon of FGFR3 in both fusion proteins (14) (Figure 2) Chromosomal rearrangements such as these also result in the loss of the 3' UTR (untranslated region) of FGFR, significant as a region that contains various microRNA (miRNA) regulation sites. MiR-99a is normally present at high levels in the brain and results in a downregulation of FGFR3 translation. The formation of FGFR3-TACC3 fusion in glioblastoma results in a loss of the miR-99a site, which leads to the overexpression of FGFR3-TACC3. This miRNA site is unique to FGFR3, but overexpression due to a loss of miRNA regulation could occur in any FGFR fusion where the 3' UTR region contains a regulatory miRNA site (17).

Interestingly, nuclear pore complex proteins have been identified in fusion proteins with FGFR1. RANBP2-FGFR1, TPR-FGFR1, and NUP98-FGFR1 have all been identified in EMS (7, 31, 40). Mechanistically, these may be similar to other fusion proteins discussed previously in that two of these possess dimerization domains, with RANBP2 (RAN binding protein 2, also NUP358) containing a leucine zipper domain and TPR (Translocated Promoter Region) containing a coiled-coil domain (Table 1). A dimerization motif in NUP98 has not yet been identified, however. Also mechanistically unclear is the fusion partner AFF3 (AF4/FMR2 Family, Member 3, also known as LAF4), a nuclear transcriptional activator, which has been identified as the 3' fusion partner with FGFR2 (Table 1). AFF3 has also been found fused to the MLL gene in acute lymphoblastic leukemia (41). It is unclear whether the

significant biochemical consequence of these fusion proteins is manifested in the dimerization and activation of the FGFR partner, or whether the abnormal nuclear localization of the FGFR component represents the key event.

All EMS cases with FGFR1 fusions have thus far been negative for the BCR-ABL fusion gene, which occurs in 85-90% of CML. The remaining cases either contain other translocations or are classified as BCR-ABL negative CML, or atypical CML. Some of these atypical CML cases are now linked to the broad spectrum of EMS cases, due to the presence of a translocation involving the 8p11 region (42). Patients with BCR-FGFR1 [t(8;22)(p11;q11)] fusion are often referred to as CML-like due to their greater resemblance to CML than to EMS. BCR has been shown to interact with Grb2 by phosphorylation of Y177 (7). This interaction is thought to be important for BCR-ABL signaling in CML patients, and may be playing a role in EMS patients with BCR-FGFR1 as well.

Inhibition of FGFR fusion proteins

Through the use of various drug treatments, a reduction of cell proliferation and FGFR fusion protein activity has been accomplished. Studies indicate that an active FGFR kinase domain drives cancer progression, thus the goal of many cancer treatments is to inhibit the FGFR portion of the fusion (18) (21). FGFR inhibitors have been used *in vitro* to reduce phosphorylation of FGFR and subsequent downstream signaling proteins. FGFR kinase inhibitors AZD4547, BGJ398, and PD173074 have inhibited growth of FGFR3-TACC3-expressing Rat1A and glioma stem-like cells (GSC-1123). PD173074 and AZD4547 both resulted in tumor shrinkage during *in vivo* mouse xenograft studies as well (18). For fusions FGFR2-AHCYL1 and FGFR2-BHCC1, both BGJ398 and PD173074 were successful in

reducing *in vitro* fusion activity and cell growth (21). In bladder cancer, sensitivity of FGFR3-TACC3 and FGFR3-BAIAP2L1 to the kinase inhibitors PD173074, dovitinib, SU5402, and BGJ398 has been reported (14). BGJ398 and dovitinib are currently involved in numerous clinical trials (clinicaltrials.gov).

FGFR3 translocations were also targeted using the heat shock protein 90 (HSP90) inhibitor, ganetespib (STA-9090). By inhibiting HSP90, hundreds of proteins soon become degraded, which disrupts oncogenic signaling pathways. Ganetespib treatment of bladder cancer cell line RT112, which contains FGFR3-TACC3, resulted in a decrease of fusion protein expression and cell viability. Expression of the apoptosis facilitator protein BIM (BCL2-Like 11, or BLC2L11) was induced, indicative of apoptotic pathway activation. Combination of ganetespib with BGJ398 proved to be the most effective in causing cell death. However, ganetespib had differential effects on protein expression and cell viability in RT4 and SW780 cell lines, which contain FGFR3-TACC3 and FGFR3-BAI1AP2L1, respectively. While HSP90 inhibitors 17-AAG and 17-DMAG reduced cell viability, resistance to ganetespib was exhibited. This discrepancy may be due to differences in drug movement or metabolism (43). Other HSP90 inhibitory compounds were effective in killing cells expressing BCR-ABL *in vitro* (34). These results collectively indicate the potential of HSP90 inhibitors against fusion positive cases.

In cholangiocarcinoma, pazopanib (GW786034B) followed by ponatinib (AP24534) treatment, both RTK inhibitors, induced anti-tumor activity in a patient with FGFR2-TACC3. Ponatinib treatment also led to anti-tumor activity in a patient exhibiting FGFR2-MGEA5 fusion. Ponatinib has been FDA approved for treatment of the drug resistant T315I mutation in BCR-ABL fusion protein in CML (23).

In EMS, the small number of patients who have achieved long term remission have received hematopoietic stem cell transplantation. Many therapies used for acute lymphoblastic leukemia, acute myeloid leukemia, and myeloproliferative neoplasms have proven unsuccessful or display only short term remission against EMS. FGFR1 kinase inhibitor SU5402 has shown promise, demonstrating inhibitory effects in cells expressing BCR-FGFR1 or ZNF198-FGFR1. Interestingly, PI3K, farnesyltransferase, and p38 inhibitors were also successful in reducing growth of these cells, whereas MEK inhibitor PD98059 was not (130). This is distinct from the MEK inhibitor U0126, which was shown to inhibit growth of cells expressing FGFR3-TACC3 (17). While dovitinib has been successful in inhibiting the proliferation of Ba/F3 cells transfected with ZNF198-FGFR1 or BCR-FGFR1 and cell lines expressing FGFR1OP2-FGFR1, a push for effective FGFR1 inhibitors is needed for EMS cases (44).

Translocations leading to FGFR overexpression

Some translocations do not create a novel fusion protein; rather, these result in overexpression of FGFR. In the translocations of SLC45A3-FGFR2 in prostate cancer and IgH-MMSET-FGFR3 in Multiple Myeloma (MM), the partner gene promoter now controls FGFR transcription, which alters the expression levels of the receptor. SLC45A3-FGFR2 translocation results in the endogenous promoter and exon 1 noncoding region of SLC45A3 attached 5' to the FGFR2 gene, which places FGFR2 transcription under the control of an androgen-regulated promoter. This leads to FGFR2 overexpression and oncogenicity (8).

Multiple Myeloma (MM) is characterized by a growth of malignant cells in the bone marrow. In approximately 20% of MM cases, a t(4;14) (p16.3;q32) translocation places

MMSET and FGFR3 under the control of the IgH promoter, leading to overexpression of FGFR3 (45). The overexpressed FGFR3 often contains an additional mutation, resulting in functional changes such as resistance to tyrosine kinase inhibitors (V557M), constitutive dimerization (Y375C), or constitutive kinase activation (K652E) (95). However, one third of cases with this translocation lose FGFR3 expression while IgH is overexpressed. Additionally, although rare, translocations between FGFR3 and an immunoglobulin gene enhancer have been found in chronic lymphocytic leukemia (CLL), including t(4;14) (p16;q32) between FGFR3 and IgH, and t(4;22) (p16;q11.2) involving FGFR3 and IgL (46, 47).

MM cases with the t(4;14) translocation have shown partial responsiveness to the FGFR3 inhibitor PD173074 and RTK inhibitor sunitinib (SU-11248). During *in vitro* studies, both inhibitors halted cell growth and inhibited FGFR3 activity, inducing an apoptotic response. However, during *in vivo* studies, tumor growth in the translocation-positive model was not inhibited by sunitinib, even though sunitinib was active in the translocation-negative tumors. The difference between the *in vitro* and *in vivo* data may be due to a difference in tumor microenvironment (45). These studies also revealed that RTK inhibitors PD173074, sunitinib, and vandetanib (ZD6474) inhibited viability of Ba/F3 cells transformed with ZNF198-FGFR1. Sunitinib, which inhibits many RTKs, is approved for metastatic renal cell carcinoma treatment (45), and is being examined in clinical trials for relapsed multiple myeloma patients. Additionally, masitinib (AB1010, a TK inhibitor) has entered phase II clinical trials for MM patients with the t(4;14) translocation. [clinicaltrials.gov]

Genomic events that contribute to FGFR fusion proteins

Although the occurrence of FGFR fusion proteins may be rare, there are similarities between fusions. Fusions with FGFR as the 5' partner have only been found in solid tumors so far. In contrast, fusions with FGFR as the 3' partner have consistently been found in EMS, which predisposes patients to either lymphoma, leukemia, or both. A few exceptions have been ERLIN2-FGFR1 found in breast cancer (8), BAG4-FGFR1 in lung squamous cell carcinoma (LUSC) (8), FOXO1-FGFR1 in rhabdomyosarcoma (48), TEL-FGFR3 in lymphoma (11), FN1-FGFR1 in phosphaturic mesenchymal tumor (49), and SQSTM1-FGFR1 in leukemia (50) (Table 1).

While the mechanism and cause of gene rearrangements is unknown, both intrachromosomal and interchromosomal rearrangements have been identified. Rearrangements in the form of tandem duplication, inversion, deletion, or translocation have all been identified as FGFR fusion formation events. Translocations occur when two double stranded breaks on different chromosomes rearrange and repair (12). Fusion genes joined by a translocation can result in the formation of a reciprocal gene (i.e. FGFR2-BICC1 and BICC1-FGFR2 genes). This has been reported in some cases, such as BCR-FGFR1, CEP110-FGFR1, FGFR1OP-FGFR1, FGFR2-AHCYL1, FGFR2-BICC1, HERVK-FGFR1, LRRFIP1-FGFR1, RANBP2-FGFR1, SQSTM1-FGFR1, TIF1-FGFR1, and ZNF198-FGFR1 fusions (7, 21-23, 35, 40, 50, 51). However, reciprocal translocations have not been shown to be translated into functional proteins. The majority of these studies do not report the presence of a reciprocal fusion gene, and this may be indicative of another genetic alteration, such as an insertion or complex rearrangement, which would preclude the formation of the reciprocal gene (7).

The formation of these chromosomal rearrangements may occur due to common chromosomal fragile sites (CFSs). An increasing number of studies have identified CFSs as areas commonly affected by deletions, amplifications, and rearrangements in cancer (52). CFSs have become linked to genomic instability, the driving force of cancer. Chromosomal breakpoints identified in cancer match to 67% of fragile sites induced *in vitro* (52). All individuals posses CFSs, and these regions have been identified as evolutionarily conserved. CFSs contain tandem repeat sequences, often flexible AT-rich repeats and the formation of non-B-DNA secondary structures. Additionally, the fragile nature of CFSs has been linked to a lack of replicating origins within the CFS region, which may lead to incomplete replication. CFS expression is also specific to tissue or cell type. An investigation should be made into the correlation between CFS and tumor-specific gene rearrangements, as seen with some FGFR fusion protein expression. Mutagens and carcinogens often target CFS regions. Regulation of CFS occurs by DNA damage response proteins, including the ataxia telangiectasia mutated (ATM) pathway. This pathway is downregulated in cholangiocarcinoma patients with FGFR2 fusions (30).

CFS FRA10F has been identified at 10q26, a region which contains the FGFR2 gene (23), though some indicate FGFR2 is proximal to FRA10F (52). FGFR2 is also surrounded by ribosomal protein pseudogenes (RPS15AP5 and RPL19P16), which contain repetitive bases, leading to genomic instability (23). Although not thoroughly investigated, these factors could be an indication of the high level of genomic rearrangements seen in the FGFR2 region. In this regard, it may be noteworthy that 10 of 107 cholangiocarcinoma patients simultaneously exhibited two different fusions, FGFR2-BICC1 and FGFR2-PPHLN1 (30). CFS regions have also been identified on the X chromosome, in regions flanking the ODF1 gene, which has

been identified in a FGFR2-ODF1 fusion in thyroid cancer (8, 52). As seen (Table 1), FGFR1, FGFR2, and FGFR3 rearrangements predominate while, for unknown reasons, FGFR4 fusions are strikingly absent.

Table 1: FGFR Fusion Proteins Arising From Translocations

5′ gene	Disease	FGFR isoform	5′ gene exon fusion point	3′ gene	3′ gene exon fusion point	Occurrences	Translocation	Normal biological function/ pathway of FGFR fusion partner	Fusion description
Fusions with FGFRs as 5′ gene									
FGFR1	Glioblastoma		17	TACC1	7	2	t(8,8) (p11;p11)	Microtubule interaction	TK domain: coiled coil domain
	Pilocytic astrocytoma	αA1	18	FGFR1	11	1	duplication	Regulation of various cellular processes	ITD of TK domain
FGFR2	Breast cancer	IIIc	19	AFF3	8	1	t(2;10) (q11;q26)	Nuclear transcriptional activator	TK domain: AFF3 domain
		IIIc	19	CASP7	4	1	t(10;10) (q25;q26)	Caspase involved in apoptosis, inflammation	TK domain: self association domain
		IIIc	19	CCDC6	2	1	t(10;10) (q21;q26)	Coiled-coil domain containing protein	TK domain: coiled coil domain
	Cholangiocarcinoma		19	AHCYL1	5	7	t(10;1) (q26.1;p13.2)	Adenosylhomocysteinase activity/IP3 binding	TK domain: coiled coil domain
		IIIb	17	BICC1	1	1	t(10;10) (q21.1;q26.1)	RNA binding protein	TK domain: SAM
			17	BICC1	3	1	t(10;10) (q21.1;q26.1)	RNA binding protein	TK domain: SAM
		IIIb	19	BICC1	3	4	t(10;10) (q21.1;q26.1)	RNA binding protein	TK domain: SAM
			Not ID'd	BICC1	Not ID'd	40	t(10;10) (q21.1;q26.1)	RNA binding protein	TK domain: SAM
			18	KIAA1598/SHOOTIN1	7	1	t(10;10) (q25;q26)	Needed for neuronal polarization	TK domain: coiled coil domain
		IIIb	17	MGEA5	12	1	t(10;10) (q24;q26)	O-GlcNAc transferase	Unknown
		IIIb	19	PPHLN1	4	17	t(10;12) (q26;q12)	Epithelial differentiation	TK domain: coiled coil domain
		IIIb	17	TACC3	11	2	t(4;10) (p16;q26)	Stabilization of mitotic spindle	TK domain: coiled coil domain
	Colorectal cancer		19	BICC1	3	1	t(10;10) (q26.1;q21.1)	RNA binding protein	TK domain: SAM
	Hepatocellular carcinoma		19	BICC1	3	1	t(10;10) (q26.1;q21.1)	RNA binding protein	TK domain: SAM
	Lung adenocarcinoma	IIIb	17	CIT	23	1	t(10;12) (q26;q24)	Cell division	TK domain: coiled coil domain
	Lung squamous cell carcinoma	IIIc	19	KIAA1967/CCAR2	5	1	t(8;10) (p21;q26)	Cell cycle and apoptosis regulator	TK domain: coiled coil domain
		IIIc	Not ID'd	KIAA1967/CCAR2	Not ID'd	1	t(8;10) (p21;q26)	Cell cycle and apoptosis regulator	TK domain: coiled coil domain
	Ovarian cancer		17	FAM76A	2	1	t(1;10) (p35;q26)	Unknown	TK domain: coiled coil domain
	Thyroid cancer	IIIc	19	OFD1	3	1	t(10;X) (q26;p22)	Centriolar component, regulates Wnt signaling	TK domain: coiled coil; LisH domain

Gallo LH, Nelson KN, Meyer AN, Donoghue DJ. Functons of Fibroblast Growth Factor Receptors in cancer defined by novel translocations and mutations. Cytokine Growth Factor Rev. 2015.

Table 1: FGFR Fusion Proteins Arising From Translocations. Continued

5′ gene	Disease	FGFR isoform	5′ gene exon fusion point	3′ gene	3′ gene exon fusion point	Occurrences	Translocation	Normal biological function/ pathway of FGFR fusion partner	Fusion description
FGFR3	Bladder cancer	IIIb	18	BAIAP2L1	2	2	t(4;7)(p16;q22)	Formation of actin	TK domain: coiled coil; IMD domain
			Not ID'd	BAIAP2L1	Not ID'd	3	t(4;7)(p16;q22)	Formation of actin	TK domain: coiled coil; IMD domain
			16	TACC3	11	3	t(4;4)(p16;p16)	Stabilization of mitotic spindle	TK domain: coiled coil domain
			17	TACC3	4	1	t(4;4)(p16;p16)	Stabilization of mitotic spindle	TK domain: coiled coil domain
			17	TACC3	11	1	t(4;4)(p16;p16)	Stabilization of mitotic spindle	TK domain: coiled coil domain
		IIIb	18	TACC3	4	1	t(4;4)(p16;p16)	Stabilization of mitotic spindle	TK domain: coiled coil domain
		IIIb	18	TACC3	8	1	t(4;4)(p16;p16)	Stabilization of mitotic spindle	TK domain: coiled coil domain
		IIIb/IIIc	18	TACC3	11	5	t(4;4)(p16;p16)	Stabilization of mitotic spindle	TK domain: coiled coil domain
	Gallbladder cancer		17	TACC3	11	1	t(4;4)(p16;p16)	Stabilization of mitotic spindle	TK domain: coiled coil domain
	Glioblastoma		16	TACC3	8	3	t(4;4)(p16;p16)	Stabilization of mitotic spindle	TK domain: coiled coil domain
			16	TACC3	9	1	t(4;4)(p16;p16)	Stabilization of mitotic spindle	TK domain: coiled coil domain
			16	TACC3	10	1	t(4;4)(p16;p16)	Stabilization of mitotic spindle	TK domain: coiled coil domain
			16	TACC3	11	1	t(4;4)(p16;p16)	Stabilization of mitotic spindle	TK domain: coiled coil domain
			17	TACC3	6	2	t(4;4)(p16;p16)	Stabilization of mitotic spindle	TK domain: coiled coil domain
			17	TACC3	8	5	t(4;4)(p16;p16)	Stabilization of mitotic spindle	TK domain: coiled coil domain
			17	TACC3	10	4	t(4;4)(p16;p16)	Stabilization of mitotic spindle	TK domain: coiled coil domain
			17	TACC3	11	7	t(4;4)(p16;p16)	Stabilization of mitotic spindle	TK domain: coiled coil domain
			18	TACC3	4	1	t(4;4)(p16;p16)	Stabilization of mitotic spindle	TK domain: coiled coil domain
			18	TACC3	5	2	t(4;4)(p16;p16)	Stabilization of mitotic spindle	TK domain: coiled coil domain
			18	TACC3	9	1	t(4;4)(p16;p16)	Stabilization of mitotic spindle	TK domain: coiled coil domain
			18	TACC3	10	1	t(4;4)(p16;p16)	Stabilization of mitotic spindle	TK domain: coiled coil domain
			18	TACC3	11	4	t(4;4)(p16;p16)	Stabilization of mitotic spindle	TK domain: coiled coil domain
			18	TACC3	13	1	t(4;4)(p16;p16)	Stabilization of mitotic spindle	TK domain: coiled coil domain
		IIIc	19	TACC3	4	1	t(4;4)(p16;p16)	Stabilization of mitotic spindle	TK domain: coiled coil domain
	Head and neck		18	TACC3	6	1	t(4;4)(p16;p16)	Stabilization of mitotic spindle	TK domain: coiled coil domain
	squamous cell	IIIb	18	TACC3	10	2	t(4;4)(p16;p16)	Stabilization of mitotic spindle	TK domain: coiled coil domain
	carcinoma		18	TACC3	14	1	t(4;4)(p16;p16)	Stabilization of mitotic spindle	TK domain: coiled coil domain
			19	TACC3	11	1	t(4;4)(p16;p16)	Stabilization of mitotic spindle	TK domain: coiled coil domain
	Lung		Not ID'd	BAIAP2L1	Not ID'd	1	t(4;7)(p16;q22)	Formation of actin	TK domain: coiled coil; IMD domain
	adenocarcinoma		17	TACC3	4	1	t(4;4)(p16;p16)	Stabilization of mitotic spindle	TK domain: coiled coil domain
			17	TACC3	8	1	t(4;4)(p16;p16)	Stabilization of mitotic spindle	TK domain: coiled coil domain
			17	TACC3	10	1	t(4;4)(p16;p16)	Stabilization of mitotic spindle	TK domain: coiled coil domain
			17	TACC3	11	8	t(4;4)(p16;p16)	Stabilization of mitotic spindle	TK domain: coiled coil domain
	Lung squamous cell		Not ID'd	BAIAP2L1	Not ID'd	1	t(4;7)(p16;q22)	Formation of actin	TK domain: coiled coil; IMD domain
	carcinoma		17	TACC3	5	1	t(4;4)(p16;p16)	Stabilization of mitotic spindle	TK domain: coiled coil domain
			17	TACC3	7	1	t(4;4)(p16;p16)	Stabilization of mitotic spindle	TK domain: coiled coil domain
			17	TACC3	8	2	t(4;4)(p16;p16)	Stabilization of mitotic spindle	TK domain: coiled coil domain
			17	TACC3	10	2	t(4;4)(p16;p16)	Stabilization of mitotic spindle	TK domain: coiled coil domain
			17	TACC3	11	7	t(4;4)(p16;p16)	Stabilization of mitotic spindle	TK domain: coiled coil domain
			18	TACC3	9	1	t(4;4)(p16;p16)	Stabilization of mitotic spindle	TK domain: coiled coil domain
			18	TACC3	10	2	t(4;4)(p16;p16)	Stabilization of mitotic spindle	TK domain: coiled coil domain
		IIIb	18	TACC3	11	6	t(4;4)(p16;p16)	Stabilization of mitotic spindle	TK domain: coiled coil domain
	Oral cancer	IIIb	18	TACC3	10	1	t(4;4)(p16;p16)	Stabilization of mitotic spindle	TK domain: coiled coil domain
Fusions with FGFRs as 3′ gene									
BAG4	Lung squamous cell		1	FGFR1	8	2	t(8;8)(p11;p11)	Anti-apoptotic protein	BAG domain: Ig,TM,TK domains
	carcinoma	IIIc	2	FGFR1	9	1	t(8;8)(p11;p11)	Anti-apoptotic protein	BAG domain: Ig,TM,TK domains
			Not ID'd	FGFR1	Not ID'd	3	t(8;8)(p11;p11)	Anti-apoptotic protein	BAG domain: Ig,TM,TK domains
ERLIN2	Breast cancer	IIIc	10	FGFR1	4	1	t(8;8)(p11;p11)	Lipid raft associated protein family	SPFH domain: Ig, TM, TK domain
FN1	Phosphaturic		22	FGFR1	3,4	1	t(2;8)(q35;p11)	Cell adhesion	FN domain: Ig, TM, TK domain
	mesenchymal		23	FGFR1	3,4	1	t(2;8)(q35;p11)	Cell adhesion	FN domain: Ig, TM, TK domain
	tumor		28	FGFR1	5	1	t(2;8)(q35;p11)	Cell adhesion	FN domain: Ig, TM, TK domain
			Not ID'd	FGFR1	Not ID'd	6	t(2;8)(q35;p11)	Cell adhesion	FN domain: Ig, TM, TK domain

Table 1: FGFR Fusion Proteins Arising From Translocations. Continued

5′ gene	Disease	FGFR isoform	5′ gene exon fusion point	3′ gene	3′ gene exon fusion point	Occurrences	Translocation	Normal biological function/ pathway of FGFR fusion partner	Fusion description
FOXO1	Rhabdomyosarcoma		Not ID'd	FGFR1	Not ID'd	1	t(8;13;9) (p11.2;q14; q32)	Transcription factor	Unknown
SQSTM1	Leukemia		9	FGFR1	9	1	t(5;8) (q35;p11)	Ubiquitin binding, NFκB regulation	PB1-ZF: TK domain
TEL/ETV6	Lymphoma		5	FGFR3	10	1	t(4;12) (p16;p13)	ETS family of transcription regulators	SAM: TK domain
8p11 myeloproliferative syndrome (EMS) resulting from fusions of FGFR1									
BCR	8p11 myeloproliferative syndrome (EMS)		4	FGFR1	9	10	t(8;22) (p11;q11)	Serine/Threonine kinase	Coiled coil domain: TK domain
			Not ID'd	FGFR1	Not ID'd	5	t(8;22) (p11;q11)	Serine/Threonine kinase	Coiled coil domain: TK domain
CEP110/ centriolin			Not ID'd	FGFR1	8	2	t(8;9) (p11;q33)	Required for centrosome function	LZ/coiled coil domain: TK domain
			38(15)(40)	FGFR1	9	4	t(8;9) (p11;q33)	Required for centrosome function	LZ/coiled coil domain: TK domain
			Not ID'd	FGFR1	Not ID'd	7	t(8;9) (p11;q33)	Required for centrosome function	LZ/coiled coil domain: TK domain
CPSF6			8	FGFR1	9	1	t(8;12) (p11;q15)	RNA processing	RNA recognition motif: TK domain
			Not ID'd	FGFR1	Not ID'd	2	t(8;12) (p11;q15)/ dic(8;12) (p11;p11)	RNA processing	RNA recognition motif: TK domain
CUX1			11	FGFR1	10	1	t(7;8) (q22;p11)	Homeodomain family of DNA binding proteins	Coiled coil domain: TK domain
FGFR1OP (FOP)			5	FGFR1	9	1	t(6;8) (q27;p11-12)	Microtubule anchoring	Leu rich domain: TK domain
			6	FGFR1	9	4	t(6;8) (q27;p11-12)	Microtubule anchoring	Leu rich domain: TK domain
			7	FGFR1	9	2	t(6;8) (q27;p11-12)	Microtubule anchoring	Leu rich domain: TK domain
			Not ID'd	FGFR1	Not ID'd	3	t(6;8) (q27;p11-12)	Microtubule anchoring	Leu rich domain: TK domain
FGFR1OP2			4	FGFR1	9	3	t(8;12) (p11;p12)/ ins(12;8) (p11;p11p22)	Wound healing	Coiled coil domain: TK domain
HERV-K			3	FGFR1	9	1	t(8;19) (p12; q13.3)	Retroviral sequence	LTR: TK domain
			Not ID'd	FGFR1	Not ID'd	1	t(8;19) (p12; q13.3)	Retroviral sequence	LTR: TK domain
LRRFIP1			9	FGFR1	9	1	t(2;8) (q37;p11)	Transcriptional repressor	Coiled coil domain: TK domain
MYO18A			32	FGFR1	9	1	t(8;17) (p11;q23)	Golgi membrane trafficking and shape	Coiled coil domain: TK domain
NUP98			Not ID'd	FGFR1	Not ID'd	1	t(8;11) (p11;p15)	Nuclear pore complex component	Unknown
RANBP2/ NUP358			20	FGFR1	9	1	t(2;8) (q12;p11)	Nuclear pore complex component	LZ: TK domain
TRIM24 (TIF1)			12	FGFR1	9	1	t(7;8) (q34;p11)	Transcription control	Coiled coil domain: TK domain
TPR			22	FGFR1	13	1	t(1;8) (q25;p11.2)	Nuclear pore complex component	Coiled coil domain: TK domain
			23	FGFR1	13	1	t(1;8) (q25;p11.2)	Nuclear pore complex component	Coiled coil domain: TK domain
			Not ID'd	FGFR1	Not ID'd	1	t(1;8) (q25;p11.2)	Nuclear pore complex component	Coiled coil domain: TK domain
ZNF198/ ZMYM2			17	FGFR1	9	34	t(8;13) (p11;q12)	Transcription factor	ZF: TK domain

1.3 CONCLUDING REMARKS

Aberrant FGFR signaling, either due to activating mutations or the presence of fusion proteins, supports cellular proliferation, tumorigenesis, and cancer progression. Although extensive research has shown that targeting FGFRs with small molecule inhibitors halts receptor activation, downstream signaling and results in tumor shrinkage, secondary mutations that contribute to drug resistance in tumors are challenges to successful clinical treatment. In addition, FGFRs fused to dimerizing partners brings a new level of complexity in terms of receptor activation and the specificity of small-molecule inhibitors. The development of FGFR therapeutics with personalized specificity will advance treatments of patients whose tumors harbor activated FGFRs via mutation or fusion protein.

1.4 ACKNOWLEDGEMENTS

Chapter 1 in part was published as “Functions of Fibroblast Growth Factor Receptors in Cancer Defined by Novel Translocations and Mutations”, in Cytokine and Growth Factor Reviews in 2015 with the authors Gallo LH, Nelson KN, Meyer AN, Donoghue DJ. Table 1 is a reprint of Table 3 from this manuscript. The dissertation author was a co-author of this paper.

The dissertation author was a co-author of this review, but not the research described by the review. The dissertation author was responsible for the section reproduced here in its entirety as well as assisting with editing and formatting all other figures, tables, and sections. Co-authors include Leandro H. Gallo, April N. Meyer, and Daniel J. Donoghue.

1.5 REFERENCES

1. Robertson S.C., Tynan J., Donoghue D.J., RTK mutations and human syndromes: when good receptors turn bad. Trends Genet 2000, 16, 368.

2. Wilkie A.O., Bad bones, absent smell, selfish testes: the pleiotropic consequences of human FGF receptor mutations. Cytokine Growth Factor Rev 2005, 16, 187-203.

3. Dailey L., Ambrosetti D., Mansukhani A., Basilico C., Mechanisms underlying differential responses to FGF signaling. Cytokine Growth Factor Rev 2005, 16, 233-247.

4. Eswarakumar V.P., Lax I., Schlessinger J., Cellular signaling by fibroblast growth factor receptors. Cytokine Growth Factor Rev 2005, 16, 139-149.

5. Turner N., Grose R., Fibroblast growth factor signalling: from development to cancer. Nat Rev Cancer 2010, 10, 116-129.

6. Ahmad I., Iwata T., Leung H.Y., Mechanisms of FGFR-mediated carcinogenesis. Biochim Biophys Acta 2012, 1823, 850-860.

7. Jackson C.C., Medeiros L.J., Miranda R.N., 8p11 myeloproliferative syndrome: a review. Hum Pathol 2010, 41, 461-476.

8. Wu Y.M., Su F., Kalyana-Sundaram S, Khazanov N, Ateeq B, Cao X, Lonigro RJ, Vats P, Wang R, Lin SF, Cheng AJ, Kunju LP, Siddiqui J, Tomlins SA, Wyngaard P, Sadis S, Roychowdhury S, Hussain MH, Feng FY, Zalupski MM, Talpaz M, Pienta KJ, Rhodes DR, Robinson DR, Chinnaiyan AM. Identification of targetable FGFR gene fusions in diverse cancers. Cancer Discov 2013, 3, 636-647.

9. Wang R, Wang L, Li Y, Hu H, Shen L, Shen X, Pan Y, Ye T, Zhang Y, Luo X, Zhang Y, Pan B, Li B, Li H, Zhang J, Pao W, Ji H, Sun Y, Chen H. FGFR1/3 tyrosine kinase fusions define a unique molecular subtype of non-small cell lung cancer. Clin Cancer Res 2014, 20, 4107-4114.

98. Comprehensive genomic characterization of squamous cell lung cancers. Nature 2012, 489, 519-525.

11 Maeda T., Yagasaki F., Ishikawa M., Takahashi N., Bessho M., Transforming property of TEL-FGFR3 mediated through PI3-K in a T-cell lymphoma that subsequently progressed to AML. Blood 2005, 105, 2115-2123.

12. Parker B.C., Engels M., Annala M., Zhang W., Emergence of FGFR family gene fusions as therapeutic targets in a wide spectrum of solid tumours. J Pathol 2014, 232, 4-15.

13. Guo G, Sun X, Chen C, Wu S, Huang P, Li Z, Dean M, Huang Y, Jia W, Zhou Q, Tang A, Yang Z, Li X, Song P, Zhao X, Ye R, Zhang S, Lin Z, Qi M, Wan S, Xie L, Fan F, Nickerson ML, Zou X, Hu X, Xing L, Lv Z, Mei H, Gao S, Liang C, Gao Z, Lu J, Yu Y, Liu C, Li L, Fang X, Jiang Z, Yang J, Li C, Zhao X, Chen J, Zhang F, Lai Y, Lin Z, Zhou F, Chen H, Chan HC, Tsang S, Theodorescu D, Li Y, Zhang X, Wang J, Yang H, Gui Y, Wang J, Cai Z. Whole-genome and whole-exome sequencing of bladder cancer identifies frequent alterations in genes involved in sister chromatid cohesion and segregation. Nat Genet 2013, 45, 1459-1463.

14. Williams S.V., Hurst C.D., Knowles M.A., Oncogenic FGFR3 gene fusions in bladder cancer. Hum Mol Genet 2013, 22, 795-803.

15. Kim Y, Hammerman PS, Kim J, Yoon JA, Lee Y, Sun JM, Wilkerson MD, Pedamallu CS, Cibulskis K, Yoo YK, Lawrence MS, Stojanov P, Carter SL, McKenna A, Stewart C, Sivachenko AY, Oh IJ, Kim HK, Choi YS, Kim K, Shim YM, Kim KS, Song SY, Na KJ, Choi YL, Hayes DN, Kim J, Cho S, Kim YC, Ahn JS, Ahn MJ, Getz G, Meyerson M, Park K. Integrative and comparative genomic analysis of lung squamous cell carcinomas in East Asian patients. J Clin Oncol 2014, 32, 121-128.

16. Majewski IJ, Mittempergher L, Davidson NM, Bosma A, Willems SM, Horlings HM, de Rink I, Greger L, Hooijer GK, Peters D, Nederlof PM, Hofland I, de Jong J, Wesseling J, Kluin RJ, Brugman W, Kerkhoven R, Nieboer F, Roepman P, Broeks A, Muley TR, Jassem J, Niklinski J, van Zandwijk N, Brazma A, Oshlack A, van den Heuvel M, Bernards R. Identification of recurrent FGFR3 fusion genes in lung cancer through kinome-centred RNA sequencing. J Pathol 2013, 230, 270-276.

17. Parker BC, Annala MJ, Cogdell DE, Granberg KJ, Sun Y, Ji P, Li X, Gumin J, Zheng H, Hu L, Yli-Harja O, Haapasalo H, Visakorpi T, Liu X, Liu CG, Sawaya R, Fuller GN, Chen K, Lang FF, Nykter M, Zhang W. The tumorigenic FGFR3-TACC3 gene fusion escapes miR-99a regulation in glioblastoma. J Clin Invest 2013, 123, 855-865.

18. Singh D, Chan JM, Zoppoli P, Niola F, Sullivan R, Castano A, Liu EM, Reichel J, Porrati P, Pellegatta S, Qiu K, Gao Z, Ceccarelli M, Riccardi R, Brat DJ, Guha A, Aldape K, Golfinos JG, Zagzag D, Mikkelsen T, Finocchiaro G, Lasorella A, Rabadan R, Iavarone A. Transforming fusions of FGFR and TACC genes in human glioblastoma. Science 2012, 337, 1231-1235.

19. Javle M, Rashid A, Churi C, Kar S, Zuo M, Eterovic AK, Nogueras-Gonzalez GM, Janku F, Shroff RT, Aloia TA, Vauthey JN, Curley S, Mills G, Roa I. Molecular characterization of gallbladder cancer using somatic mutation profiling. Hum Pathol 2014, 45, 701-708.

20. Di Stefano AL, Fucci A, Frattini V, Labussiere M, Mokhtari K, Zoppoli P, Marie Y, Bruno A, Boisselier B, Giry M, Savatovsky J, Touat M, Belaid H, Kamoun A, Idbaih A, Houillier C, Luo FR, Soria JC, Tabernero J, Eoli M, Paterra R, Yip S, Petrecca K, Chan JA,

Finocchiaro G, Lasorella A, Sanson M, Iavarone A. Detection, characterization and inhibition of FGFR-TACC fusions in IDH wild type glioma. Clin Cancer Res 2015.

21. Arai Y, Totoki Y, Hosoda F, Shirota T, Hama N, Nakamura H, Ojima H, Furuta K, Shimada K, Okusaka T, Kosuge T, Shibata T. Fibroblast growth factor receptor 2 tyrosine kinase fusions define a unique molecular subtype of cholangiocarcinoma. Hepatology 2014, 59, 1427-1434.

22. Ross JS, Wang K, Gay L, Al-Rohil R, Rand JV, Jones DM, Lee HJ, Sheehan CE, Otto GA, Palmer G, Yelensky R, Lipson D, Morosini D, Hawryluk M, Catenacci DV, Miller VA, Churi C, Ali S, Stephens PJ. New routes to targeted therapy of intrahepatic cholangiocarcinomas revealed by next-generation sequencing. Oncologist 2014, 19, 235-242.

23. Borad MJ, Champion MD, Egan JB, Liang WS, Fonseca R, Bryce AH, McCullough AE, Barrett MT, Hunt K, Patel MD, Young SW, Collins JM, Silva AC, Condjella RM, Block M, McWilliams RR, Lazaridis KN, Klee EW, Bible KC, Harris P, Oliver GR, Bhavsar JD, Nair AA, Middha S, Asmann Y, Kocher JP, Schahl K, Kipp BR, Barr Fritcher EG, Baker A, Aldrich J, Kurdoglu A, Izatt T, Christoforides A, Cherni I, Nasser S, Reiman R, Phillips L, McDonald J, Adkins J, Mastrian SD, Placek P, Watanabe AT, Lobello J, Han H, Von Hoff D6, Craig DW, Stewart AK, Carpten JD. Integrated genomic characterization reveals novel, therapeutically relevant drug targets in FGFR and EGFR pathways in sporadic intrahepatic cholangiocarcinoma. PLoS Genet 2014, 10, e1004135.

24. Witkowski W.A., Hardy J.A., L2' loop is critical for caspase-7 active site formation. Protein Sci 2009, 18, 1459-1468.

25. Matikas A., Tzannou I., Oikonomopoulou D., Bakiri M., A case of acute myelogenous leukaemia characterised by the BCR-FGFR1 translocation. BMJ Case Rep 2013, 2013.

26. Wasag B., Lierman E., Meeus P., Cools J., Vandenberghe P., The kinase inhibitor TKI258 is active against the novel CUX1-FGFR1 fusion detected in a patient with T-lymphoblastic leukemia/lymphoma and t(7;8)(q22;p11). Haematologica 2011, 96, 922-926.

27. Onozawa M, Ohmura K, Ibata M, Iwasaki J, Okada K, Kasahara I, Yamaguchi K, Kubota K, Fujisawa S, Shigematsu A, Endo T, Kondo T, Hashino S, Tanaka J, Matsuno Y, Asaka M, Imamura M. The 8p11 myeloproliferative syndrome owing to rare FGFR1OP2-FGFR1 fusion. Eur J Haematol 2011, 86, 347-349.

28. Seo JS, Ju YS, Lee WC, Shin JY, Lee JK, Bleazard T, Lee J, Jung YJ, Kim JO, Shin JY, Yu SB, Kim J, Lee ER, Kang CH, Park IK, Rhee H, Lee SH, Kim JI, Kang JH, Kim YT. The transcriptional landscape and mutational profile of lung adenocarcinoma. Genome Res 2012, 22, 2109-2119.

29. Martignetti J.A., Camacho-Vanegas O., Priedigkeit N. *et al.*, Personalized ovarian cancer disease surveillance and detection of candidate therapeutic drug target in circulating tumor DNA. Neoplasia 2014, 16, 97-103.

30. Sia D, Losic B, Moeini A, Cabellos L, Hao K, Revill K, Bonal D, Miltiadous O, Zhang Z, Hoshida Y, Cornella H, Castillo-Martin M, Pinyol R, Kasai Y, Roayaie S, Thung SN, Fuster J, Schwartz ME, Waxman S, Cordon-Cardo C, Schadt E, Mazzaferro V, Llovet JM. Massive parallel sequencing uncovers actionable FGFR2-PPHLN1 fusion and ARAF mutations in intrahepatic cholangiocarcinoma. Nat Commun 2015, 6, 6087.

31. Li F., Zhai Y.P., Tang Y.M., Wang L.P., Wan P.J., Identification of a novel partner gene, TPR, fused to FGFR1 in 8p11 myeloproliferative syndrome. Genes Chromosomes Cancer 2012, 51, 890-897.

32. Xiao S., McCarthy J.G., Aster J.C., Fletcher J.A., ZNF198-FGFR1 transforming activity depends on a novel proline-rich ZNF198 oligomerization domain. Blood 2000, 96, 699-704.

33. Kiyoi H., Naoe T., FLT3 in human hematologic malignancies. Leuk Lymphoma 2002, 43, 1541-1547.

34. Medves S., Demoulin J.B., Tyrosine kinase gene fusions in cancer: translating mechanisms into targeted therapies. J Cell Mol Med 2012, 16, 237-248.

35. Guasch G, Mack GJ, Popovici C, Dastugue N, Birnbaum D, Rattner JB, Pébusque MJ. FGFR1 is fused to the centrosome-associated protein CEP110 in the 8p12 stem cell myeloproliferative disorder with t(8;9)(p12;q33). Blood 2000, 95, 1788-1796.

36. Gergely F., Karlsson C., Still I., Cowell J., Kilmartin J., Raff J.W., The TACC domain identifies a family of centrosomal proteins that can interact with microtubules. Proc Natl Acad Sci U S A 2000, 97, 14352-14357.

37. Browman D.T., Resek M.E., Zajchowski L.D., Robbins S.M., Erlin-1 and erlin-2 are novel members of the prohibitin family of proteins that define lipid-raft-like domains of the ER. J Cell Sci 2006, 119, 3149-3160.

38. Guasch G., Ollendorff V., Borg J.P., Birnbaum D., Pebusque M.J., 8p12 stem cell myeloproliferative disorder: the FOP-fibroblast growth factor receptor 1 fusion protein of the t(6;8) translocation induces cell survival mediated by mitogen-activated protein kinase and phosphatidylinositol 3-kinase/Akt/mTOR pathways. Mol Cell Biol 2001, 21, 8129-8142.

39. Chen J, Williams IR, Lee BH, Duclos N, Huntly BJ, Donoghue DJ, Gilliland DG.Constitutively activated FGFR3 mutants signal through PLC{gamma}-dependent and -independent pathways for hematopoietic transformation. Blood, 2005, 106,328-37

40. Gervais C, Dano L, Perrusson N, Hélias C, Jeandidier E, Galoisy AC, Ittel A, Herbrecht R, Bilger K, Mauvieux L. A translocation t(2;8)(q12;p11) fuses FGFR1 to a novel partner gene, RANBP2/NUP358, in a myeloproliferative/myelodysplastic neoplasm. Leukemia 2013, 27, 1186-1188.

41. Hiwatari M, Taki T, Taketani T, Taniwaki M, Sugita K, Okuya M, Eguchi M, Ida K, Hayashi Y. Fusion of an AF4-related gene, LAF4, to MLL in childhood acute lymphoblastic leukemia with t(2;11)(q11;q23). Oncogene 2003, 22, 2851-2855.

42. Demiroglu A, Steer EJ, Heath C, Taylor K, Bentley M, Allen SL, Koduru P, Brody JP, Hawson G, Rodwell R, Doody ML, Carnicero F, Reiter A, Goldman JM, Melo JV, Cross NC. The t(8;22) in chronic myeloid leukemia fuses BCR to FGFR1: transforming activity and specific inhibition of FGFR1 fusion proteins. Blood 2001, 98, 3778-3783.

43. Acquaviva J, He S, Zhang C, Jimenez JP, Nagai M, Sang J, Sequeira M, Smith DL, Ogawa LS, Inoue T, Tatsuta N, Knowles MA, Bates RC, Proia DA. FGFR3 translocations in bladder cancer: differential sensitivity to HSP90 inhibition based on drug metabolism. Mol Cancer Res 2014, 12, 1042-1054.

44. Chase A., Grand F.H., Cross N.C., Activity of TKI258 against primary cells and cell lines with FGFR1 fusion genes associated with the 8p11 myeloproliferative syndrome. Blood 2007, 110, 3729-3734.

45. de Brito LR, Batey MA, Zhao Y, Squires MS, Maitland H, Leung HY, Hall AG, Jackson G, Newell DR, Irving JA. Comparative pre-clinical evaluation of receptor tyrosine kinase inhibitors for the treatment of multiple myeloma. Leuk Res 2011, 35, 1233-1240.

46. Bacher U, Haferlach T, Schnittger S, Weiss T, Burkhard O, Bechtel B, Kern W, Haferlach C. Detection of a t(4;14)(p16;q32) in two cases of lymphoma showing both the immunophenotype of chronic lymphocytic leukemia. Cancer Genet Cytogenet 2010, 200, 170-174.

47. Cerny J., Yu H., Miron P.M., Novel FGFR3 rearrangement t(4;22)(p16;q11.2) in a patient with chronic lymphocytic leukemia/small lymphocytic lymphoma. Ann Hematol 2013, 92, 1433-1435.

48. Liu J, Guzman MA, Pezanowski D, Patel D, Hauptman J, Keisling M, Hou SJ, Papenhausen PR, Pascasio JM, Punnett HH, Halligan GE, de Chadarévian JP. FOXO1-FGFR1 fusion and amplification in a solid variant of alveolar rhabdomyosarcoma. Mod Pathol 2011, 24, 1327-1335.

49. Lee JC, Jeng YM, Su SY, Wu CT, Tsai KS, Lee CH, Lin CY, Carter JM, Huang JW, Chen SH, Shih SR, Mariño-Enríquez A, Chen CC, Folpe AL, Chang YL, Liang CW. Identification of a novel FN1-FGFR1 genetic fusion as a frequent event in phosphaturic mesenchymal tumour. J Pathol 2014.

50 Nakamura Y., Ito Y., Wakimoto N., Kakegawa E., Uchida Y., Bessho M., A novel fusion of SQSTM1 and FGFR1 in a patient with acute myelomonocytic leukemia with t(5;8)(q35;p11) translocation. Blood Cancer J 2014, 4, e265.

51 Duckworth C.B., Zhang L., Li S., Systemic mastocytosis with associated myeloproliferative neoplasm with t(8;19)(p12;q13.1) and abnormality of FGFR1: report of a unique case. Int J Clin Exp Pathol 2014, 7, 801-807.

52. Ma K, Qiu L, Mrasek K, Zhang J, Liehr T, Quintana LG, Li Z. Common fragile sites: genomic hotspots of DNA damage and carcinogenesis. Int J Mol Sci 2012, 13, 11974-11999.

CHAPTER 2

Oncogenic Gene Fusion FGFR3-TACC3 Regulated by Tyrosine Phosphorylation

ABSTRACT

The discovery of translocations and fusion proteins involving Fibroblast Growth Factor Receptors (FGFRs) are becoming increasingly common in human cancers. Their presence leads to aberrant signaling that contributes to cell proliferation and cancer growth. A fusion protein between FGFR3 and transforming acidic coiled-coil containing protein 3 (TACC3) has become frequently identified in glioblastoma, lung cancer, bladder cancer, oral cancer, head and neck squamous cell carcinoma, gallbladder cancer, and cervical cancer. Through extensive analysis of the FGFR3-TACC3 fusion protein by titanium dioxide-based phosphopeptide enrichment (TiO2)-liquid chromatography (LC)-high mass accuracy tandem mass spectrometry (MS/MS), it was demonstrated that the fused coiled-coil TACC3 domain results in constitutive phosphorylation of key activating FGFR3 tyrosine residues. The presence of the TACC coiled-coil domain leads to increased and altered levels of FGFR3 activation, fusion protein phosphorylation, MAPK pathway activation, nuclear localization, cellular transformation, and IL3-independent proliferation. Introduction of K508R FGFR3 kinase-dead mutation abrogates these effects, except for nuclear localization which is due

solely to the TACC3 domain. These results demonstrate that FGFR3 kinase activity is essential for the oncogenic effects of the FGFR3-TACC3 fusion protein and could serve as a therapeutic target, but that phosphorylated tyrosine residues within the TACC3-derived portion are not critical for activity.

2.1 INTRODUCTION

A subset of the Receptor Tyrosine Kinase (RTK) family is the Fibroblast Growth Factor Receptor (FGFR) family, which contains four homologous receptors: FGFR1, FGFR2, FGFR3, and FGFR4. FGFR activation results in changes in cellular proliferation and migration, anti-apoptosis, angiogenesis, and wound healing. All FGFRs contain three immunoglobulin-like (Ig) domains, a transmembrane (TM) domain, and a split tyrosine kinase (TK) domain. Binding of Fibroblast Growth Factors (FGFs) and heparin sulfate proteoglycans (HSPGs) to the extracellular Ig domains collectively induces FGFR activation through dimerization of receptor monomers and trans-autophosphorylation of kinase domain activation loop tyrosine residues. Tyrosine phosphorylation of the kinase domain initiates activation of RAS-MAPK, PI3K-AKT, and JAK/STAT pathways (1).

Mutations in FGFRs have been linked to numerous human cancers and somatic disorders, many of which have been extensively studied. More recently, FGFR fusion proteins have also begun to emerge in multiple cases of human cancers (1). Since their initial discovery in the late 1990s, the detection of these fusion proteins has steadily increased at an alarming rate. The focus of this chapter is a fusion protein consisting of FGFR3 fused to transforming acidic coiled-coil containing protein 3 (TACC3) that has been identified in

glioblastoma, lung cancer, bladder cancer, oral cancer, head and neck squamous cell carcinoma, gallbladder cancer, and cervical cancer (1,2). The FGFR3-TACC3 fusion protein is a consequence of a 70 kb tandem duplication at 4p16.3 (3). This causes a reversal of the two genes, as TACC3 is normally upstream of FGFR3. TACC3 is a member of the TACC family, which consists of 3 known human proteins, TACC1, TACC2, and TACC3, all of which are involved in key roles of microtubule organization during mitosis. TACC3 is believed to be essential for the stabilization of kinetochore fibers and the mitotic spindle. A particularly important domain of this family is the C-terminal coiled coil domain (named TACC domain), which is highly conserved in all family members. This domain is believed to play an important role in localization of the protein during mitosis (4).

The frequent occurrence of this fusion protein across many cancer types leads to the question of how this protein is contributing to cancer progression. Is FGFR3 becoming constitutively activated due to the presence of the TACC domain? Is the presence of the coiled-coil domain able to stimulate activation loop phosphorylation in the FGFR3 kinase domain? Does the TACC3 domain play an important role in advancing cancer progression, or is its key role to activate the tyrosine kinase? While studies have investigated FGFR3 and TACC3 as separate entities, little has been defined about the FGFR3-TACC3 fusion protein. This chapter investigates various properties of this fusion protein and its contribution to cancer progression, including mass spectrometry analysis of phosphorylation of key tyrosine residues, downstream signaling, cell transformation, and localization.

2.2 RESULTS

Constitutive phosphorylation of FGFR3-TACC3 fusion protein

In the FGFR3-TACC3 fusion protein, tyrosine kinase domain dimerization and autophosphorylation may be elevated by the presence of the TACC3 coiled coil domain, which could be crucial to cancer progression. To investigate changes in phosphorylation and biological activity, various FGFR3-TACC3 DNA derivatives were constructed. All fusion constructs contain the breakpoint between exon 18 of FGFR3 to exon 11 of TACC3 as shown in Figure 3, chosen due to the high occurrence of this particular fusion breakpoint (3,5). This fusion is predicted to contain the extracellular, transmembrane, and intracellular kinase domains of FGFR3 fused 5' to the coiled-coil domain of TACC3 (6). Constitutively activated FGFR3 clones were produced by the K650E mutation. This mutation is known to cause Thanatophoric Dysplasia type II (TDII), a lethal form of achondroplasia, and is a highly activating and pathogenic FGFR3 mutation (1). The kinase activity of FGFR3 was abrogated by K508 to R mutation, known as the "kinase-dead" (KD) mutant (Figure 3A).

To examine the phosphorylation of each fusion construct compared to FGFR3 WT, FGFR3(K650E), and FGFR3(K508R), constructs were expressed in HEK293 cells, collected and immunoprecipitated with an N-terminal FGFR3 antibody (Figure 3B, top panel). An increase in tyrosine phosphorylation was seen in FGFR3-TACC3 compared to FGFR3 WT (lanes 2 and 6). No phosphorylation signal could be detected for the kinase-dead FGFR3 with or without the fused TACC3 (Figure 3B). These results show that tyrosine phosphorylation of the fusion protein was increased by the presence of dimerizing TACC3 coiled coil and can be amplified by the presence of the activating K650E mutation. Quantitation of phosphorylation

levels shows a 2-fold increase in tyrosine phsophorylation on the FGFR3-TACC3 fusion protein compared to FGFR3 WT (Figure 3C).

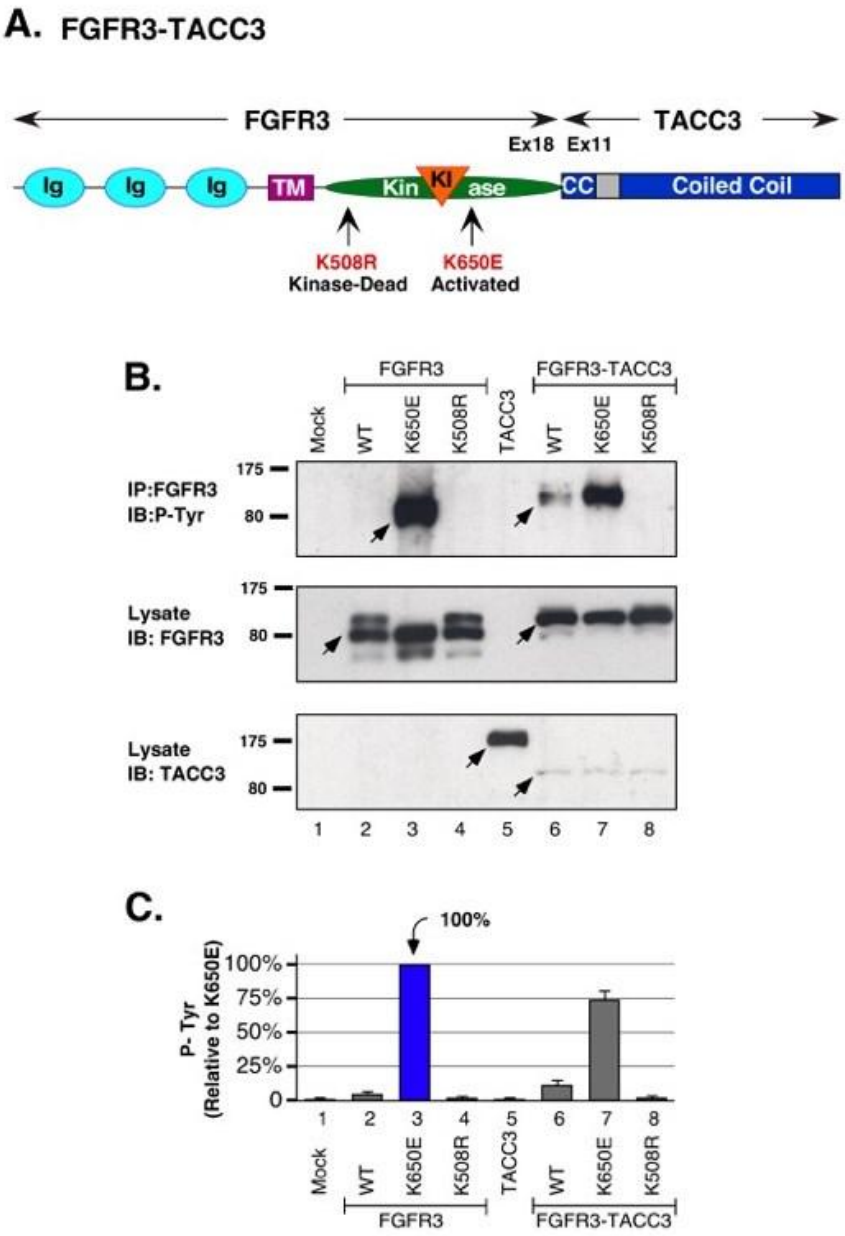

Figure 3. Increase in tyrosine phosphorylation by introduction of the TACC domain. (**A**) Schematic of FGFR3-TACC3 fusion protein. The N-terminal extracellular ligand-binding domain, transmembrane (TM), kinase, and kinase insert (KI) domains of FGFR3 are followed by a 3 amino acid linker (residues ASM), and fused to TACC3 starting at exon 11, which contains a coiled-coil domain. The location of K508 and K650 are shown. (**B**) Various mutation and fusions with FGFR3 were expressed in HEK293 cells, immunoprecipitated with FGFR3 antibody, and immunoblotted with phosphotyrosine antibody (top panel). Expression of the constructs were visualized in the lysates by immunoblotting with FGFR3 antisera (middle panel) and TACC3 antisera (bottom panel). (**C**) Quantification of tyrosine phosphorylation showing the standard error of the mean for 3 independent repeats, normalized to FGFR3(K650E).

LC-MS/MS analysis identifies elevated and novel phosphorylation sites

The strong increase in tyrosine phosphorylation seen by Western blot led to the question of whether TACC3 leads to a constitutively phosphorylated FGFR3 kinase and if additional or novel phosphorylation sites exist on the fusion protein. In order to explore this possibility, titanium dioxide-based phosphopeptide enrichment (TiO_2)-liquid chromatography (LC)-high mass accuracy tandem mass spectrometry (MS/MS) was used with samples from HEK293T cells expressing FGFR3 or FGFR3-TACC3 derivatives to identify significant phosphorylation sites. Immunoprecipitation with the FGFR3 N-terminal antibody and on-bead tryptic digestion revealed strong FGFR3 activation loop phosphorylation at residues Y647 and Y648 in both fusion proteins and non-fused FGFR3 and FGFR3(K650E) (Figure 4B), indicating the receptor was constitutively active in all samples. Mass spectrometry analysis performed on the FGFR3 (K508R) derivatives detected no phosphorylated tyrosine residues (data not shown). All tyrosine phosphorylation sites detected on the fusion protein are indicated in Figure 4C.

By comparing non-fused FGFR3 to FGFR3-TACC3, the effect of the coiled-coil domain on receptor phosphorylation and activation can be seen (Figure 4A, 4B). Not only are phosphorylation levels more robust, but additional phosphorylation sites can be detected in the FGFR3 portion of the fusion, such as Y577, Y599, and Y607 (Figure 4B, 1st and 3rd panels), indicating that receptor phosphorylation is over-stimulated in a ligand independent manner due to the presence of the TACC domain. The presence of the activating mutation K650E in FGFR3-TACC3 shows that the presence of the TACC domain leads to higher phosphorylation intensity levels of the receptor (Figure 4A, 2nd and 4th panels).

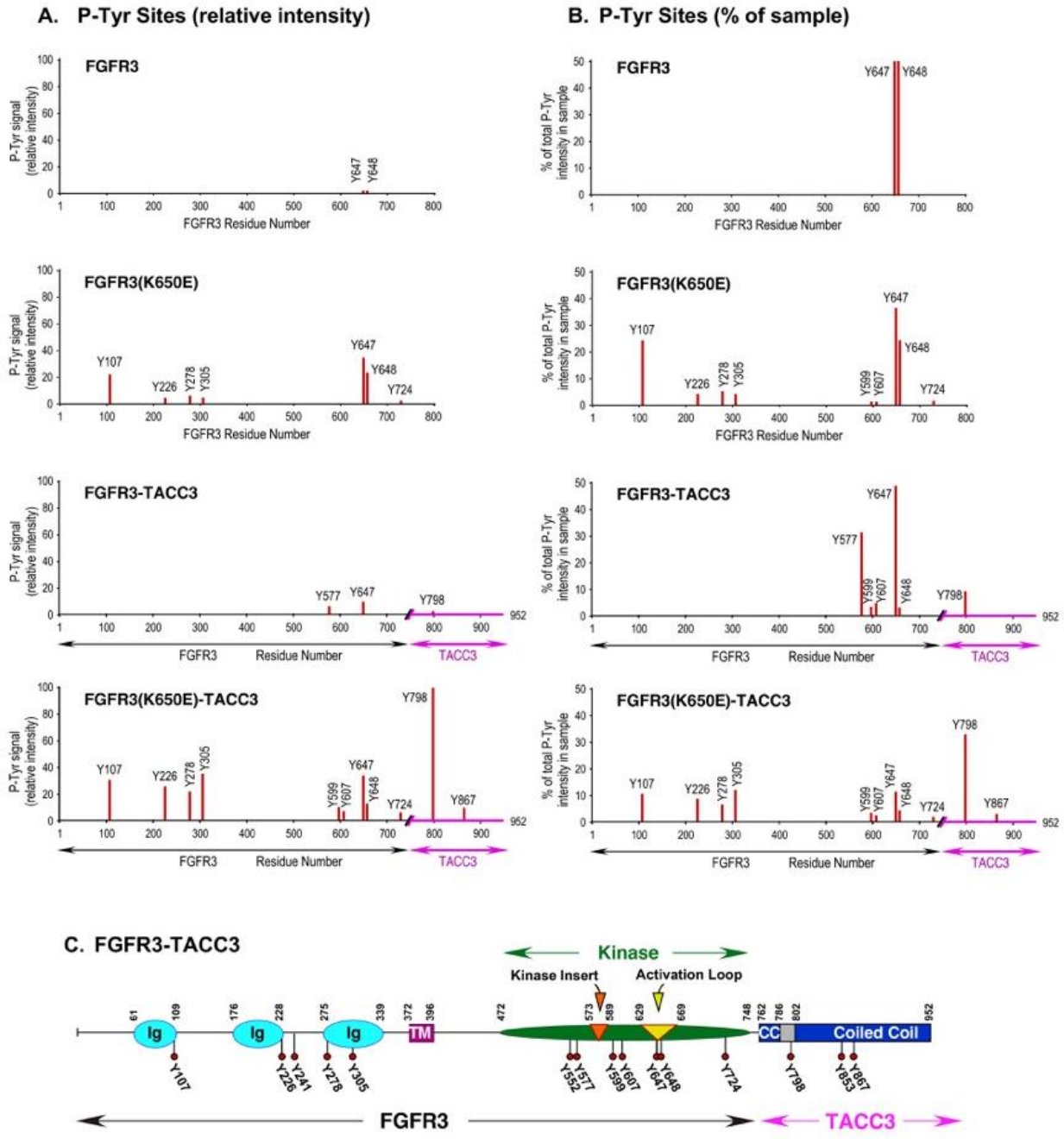

Figure 4. Phosphorylated tyrosine residues in FGFR3, FGFR3(K650E), FGFR3-TACC3, and FGFR3(K650E)-TACC3 identified by mass spectrometry analysis. **(A)** The intensity of the phosphotyrosine residues detected are presented normalized to 2 phosphoserine residues (S424 and S444) which were found to be constitutively phosphorylated across all samples. Duplicate, independent samples were subjected to mass spectrometry analysis. **(B)** For each phosphotyrosine residue detected, the percentage of intensity within the total protein is presented. **(C)** Schematic of FGFR3-TACC3 with the location of all tyrosine phosphorylation sites identified by LC-MS/MS.

Representative phosphorylated spectra are shown in Figure 5. A commonly identified FGFR3 WT peptide containing double phosphorylation of Y647 and Y648 in the activation loop is shown in panel A. In FGFR3-TACC3 fusion protein constructs, this double phosphorylated peptide becomes less frequent, with detection of peptides containing single Y647 phosphorylation becoming more common (Figure 4, 5B, 7C). Also shown are spectra containing primary phosphorylation sites Y577, Y798, and Y867 in FGFR3-TACC3 and FGFR3(K650E)-TACC3 (Figure 5D, 5E, 5F).

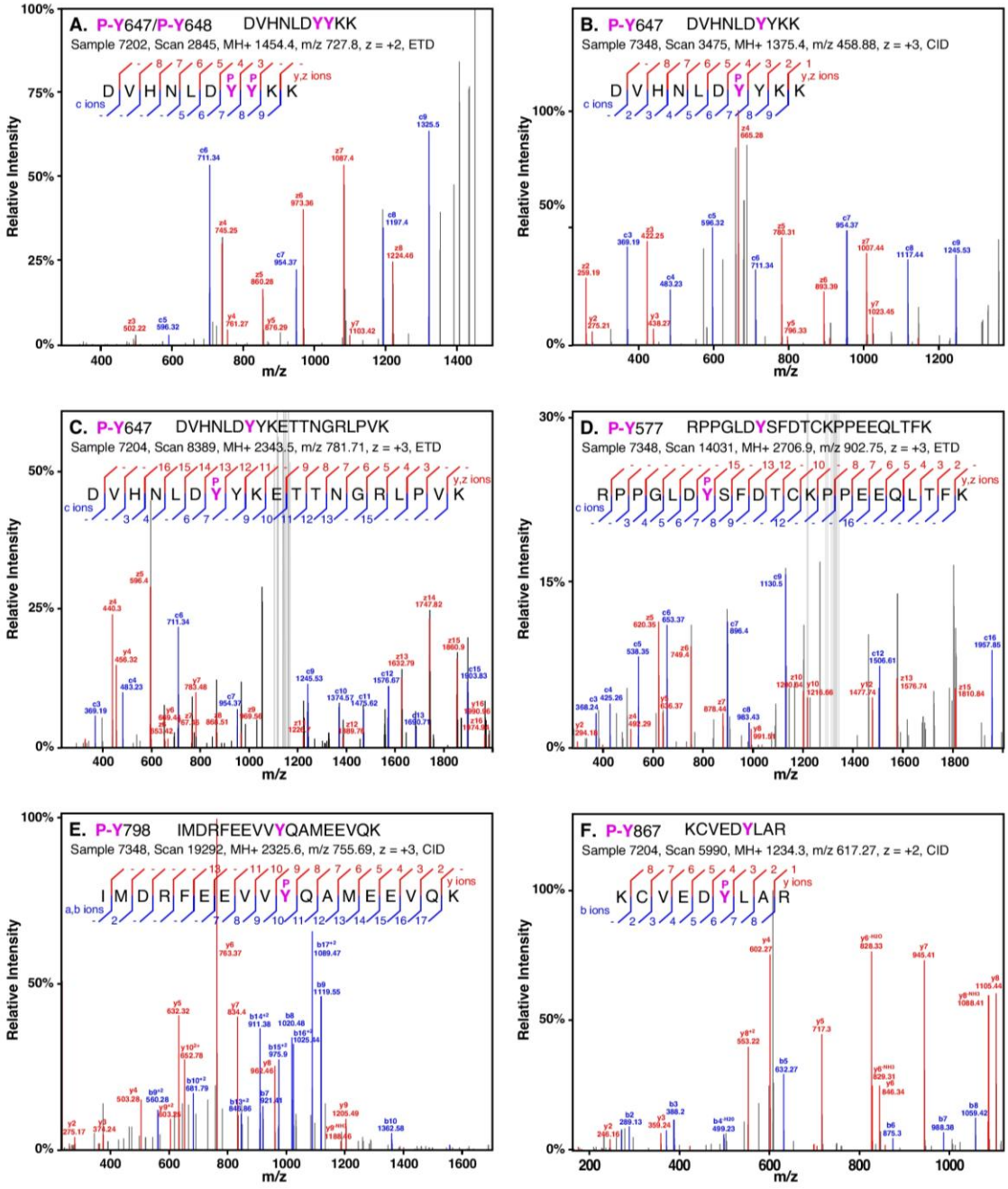

Figure 5. Representative spectra of selected peptides. The relative intensity of select ions of major phosphorylation sites are shown. Due to space constraints, not all identified ions are labeled. Identification of samples are as follows: **(A)** FGFR3 WT **(B)** FGFR3-TACC3 **(C)** FGFR3(K650E)-TACC3 **(D)** FGFR3-TACC3 **(E)** FGFR3-TACC3 **(F)** FGFR3(K650E)-TACC3.

There are four tyrosine residues in the TACC3 portion of the FGFR3-TACC3 fusion protein: Y798, Y853, Y867, and Y878, corresponding to residues Y684, Y739, Y753, and Y764 in TACC3 WT. In FGFR3-TACC3, it was previously unknown if these tyrosine residues were also phosphorylated, possibly by the fused kinase domain, and if they play a role in cancer development. Through MS analysis, phosphorylation sites Y798, Y853, and Y867 were identified in FGFR3-TACC3 (Figure 4C). Due to tryptic digest peptide size, Y853 was only recovered by a peptide miscleavage and Y878 was unable to be recovered. Increasing receptor activation by K650E mutation led to an increase in intensity levels of TACC3 tyrosine phosphorylation (Figure 4A, 3rd and 4th panels).

Of the phosphorylation sites detected in the TACC3 portion of the fusion protein, Y798 and Y853 have been previously identified as a phosphorylation sites in TACC3 WT. The function of these sites is unclear and these residues are not conserved in the TACC family (7,8). However, Y867 is a conserved tyrosine residue in the TACC family and our data has identified it as a novel phosphorylation site for the FGFR3(K650E)-TACC3 fusion protein.

As mentioned above, mass spectroscopy of HEK293T cells expressing FGFR3(K508R)-TACC3 (kinase dead mutation) revealed no phosphorylated peptides within the FGFR3 or TACC3 domains. This indicates that receptor activation is required for tyrosine phosphorylation of the fusion proteins, and the TACC domain is most likely phosphorylated by the FGFR3 kinase domain, not another tyrosine kinase.

Cell transforming ability of FGFR3-TACC3 by focus assay

To examine the transforming activity of FGFR3-TACC3 and subsequent mutants, focus-forming assays with NIH3T3 cells were performed. FGFR3-TACC3 and FGFR3(K650E)-TACC3 produced extremely high foci formation and cell transformation compared to FGFR3 WT or FGFR3(K650E) (Figure 6). Expression of PR/neu*, a focus assay positive control, displayed less transformation than FGFR3-TACC3, the latter of which also consistently produced much larger foci. PR/neu* is a Platelet-Derived Growth Factor Receptor, Beta (PDGFR-β) with a Neu receptor transmembrane domain with the activating V664E mutation ($p185^{neu*}$) (9). Despite the previously demonstrated elevated activation of PR/neu*, its transforming ability was dwarfed by the foci formation seen by FGFR3(K650E)-TACC3. As a result, samples were normalized to FGFR3(K650E)-TACC3 (Figure 6). Expression of FGFR3(K508R)-TACC3 (kinase-dead mutation) and TACC3 WT in NIH3T3 cells did not produce significant foci formation, indicating that an active FGFR3 kinase domain is essential for cell transforming ability of FGFR3-TACC3.

Within the coiled-coil domain in FGFR3-TACC3, there are four tyrosine residues. Three of these residues were found to be phosphorylated by MS analysis, as discussed above, and the fourth tyrosine, Y878, undetectable by trypic digest, is believed to be phosphorylated as well (10). In order to assess the importance of these FGFR3-TACC3 phosphorylation sites, all four TACC3 tyrosine residues were mutated to phenylalanine (Y798F, Y853F, Y867F, Y878F) with and without the activating FGFR3 K650E mutation by site-directed mutagenesis and analyzed for focus forming ability. NIH3T3 cells expressing the fusion constructs with all four tyrosine mutations, FGFR3-TACC3 4xYF and FGFR3(K650E)-TACC3 4xYF,

displayed high foci formation when compared to FGFR3-TACC3 or FGFR3(K650E)-TACC3 with no additional mutations (Figure 6).

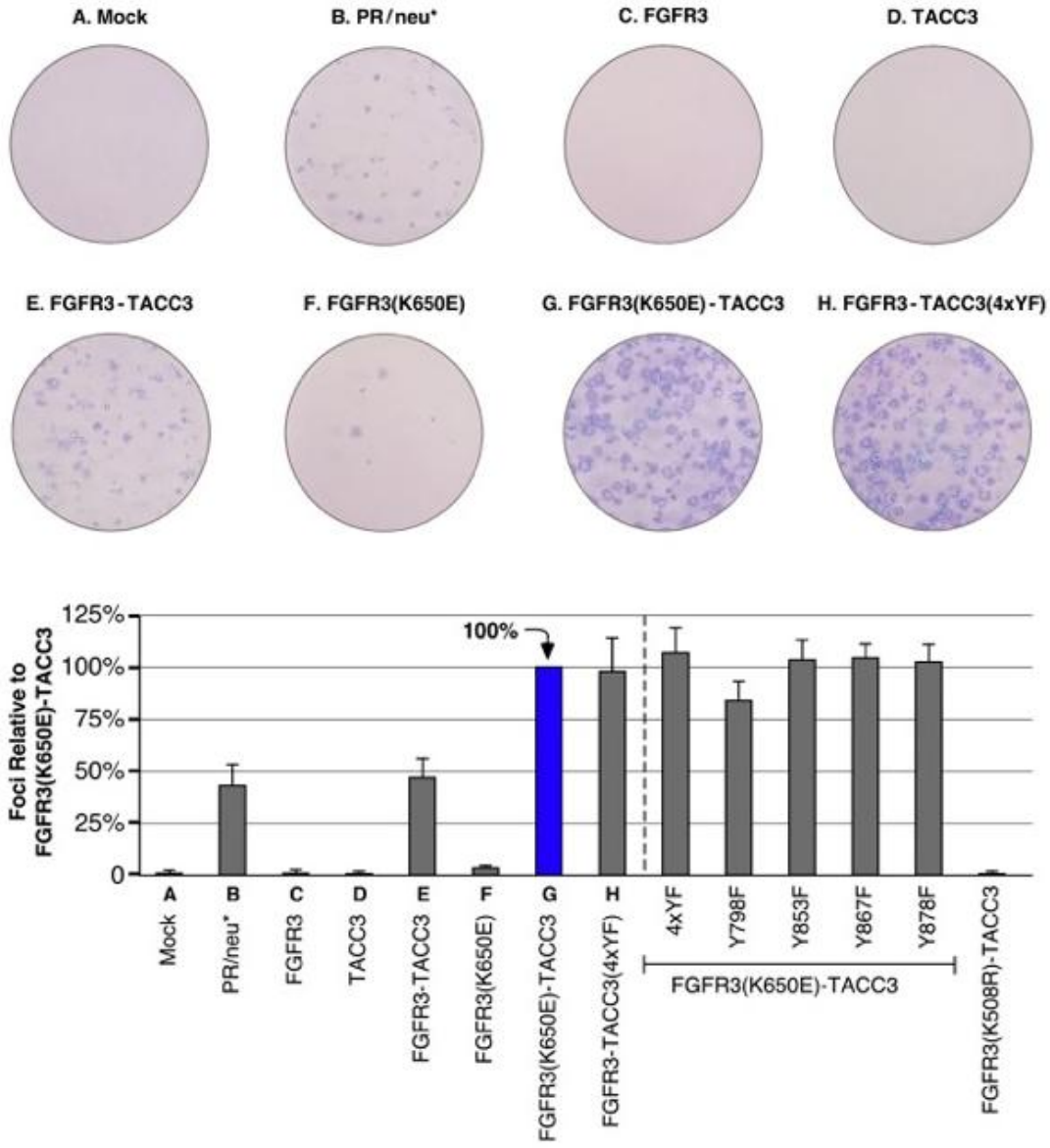

Figure 6. Transformation of NIH3T3 cells by FGFR3 and FGFR3-TACC3 derivatives. Representative plates from a focus assay are shown, with transfected constructs indicated. Number of foci were scored, normalized by transfection efficiency, and quantitated relative to FGFR3(K650E)-TACC3 +/- standard error of the mean. PR/neu* is a positive control. Assays were performed a minimum of three times per DNA construct.

To assess the effects of each individual phosphorylation site, single Y to F mutants were made in combination with activating mutation K650E. As shown in Figure 6, three of the mutations (Y853F, Y867F, Y878F) increased foci formation at an even higher rate than K650E mutation alone, indicating an inhibitory role on cell growth when phosphorylated in the FGFR3-TACC3 fusion. An exception may be FGFR3(K650E)-TACC3(Y798F), which displayed a slightly lower transformation ability than FGFR3(K650E)-TACC3, indicating this phosphorylation site may be important to cell proliferation.

FGFR3-TACC3 promotes IL-3 independent cell growth

The transforming potential of select fusion proteins was also examined in the murine myeloid cell line 32D which is dependent on Interluekin-3 (IL-3) for growth (11-13). FGFR3 WT, FGFR3-TACC3, FGFR3(K650E), FGFR3(K650E)-TACC3, FGFR3-TACC3(4xYF) and PR/neu* were electroporated into the 32D cell line and selected as described in the Materials and Methods. As seen in Figure 7A, in the absence of IL-3 all the clones expressed were able to lead to IL-3 independent growth indicating their transforming potential. Interestingly, the FGFR3-TACC3(4xYF) clone had the highest proliferation even without the activating K650E mutation. This could support the suggestion of the TACC3 tyrosine residues as being inhibitory. In addition, even in the presence of IL-3 (Figure 7B) the expression some of the clones enhanced the proliferation of the 32D cells compared to nonexpressing cells. The viability assays performed on days 3 and 7 shown in Figure 7C support the cell population assay results. All transfected constructs display cell viability, whereas 32D control cells do not, indicating that FGFR3-TACC3 and other constructs promote cell proliferation.

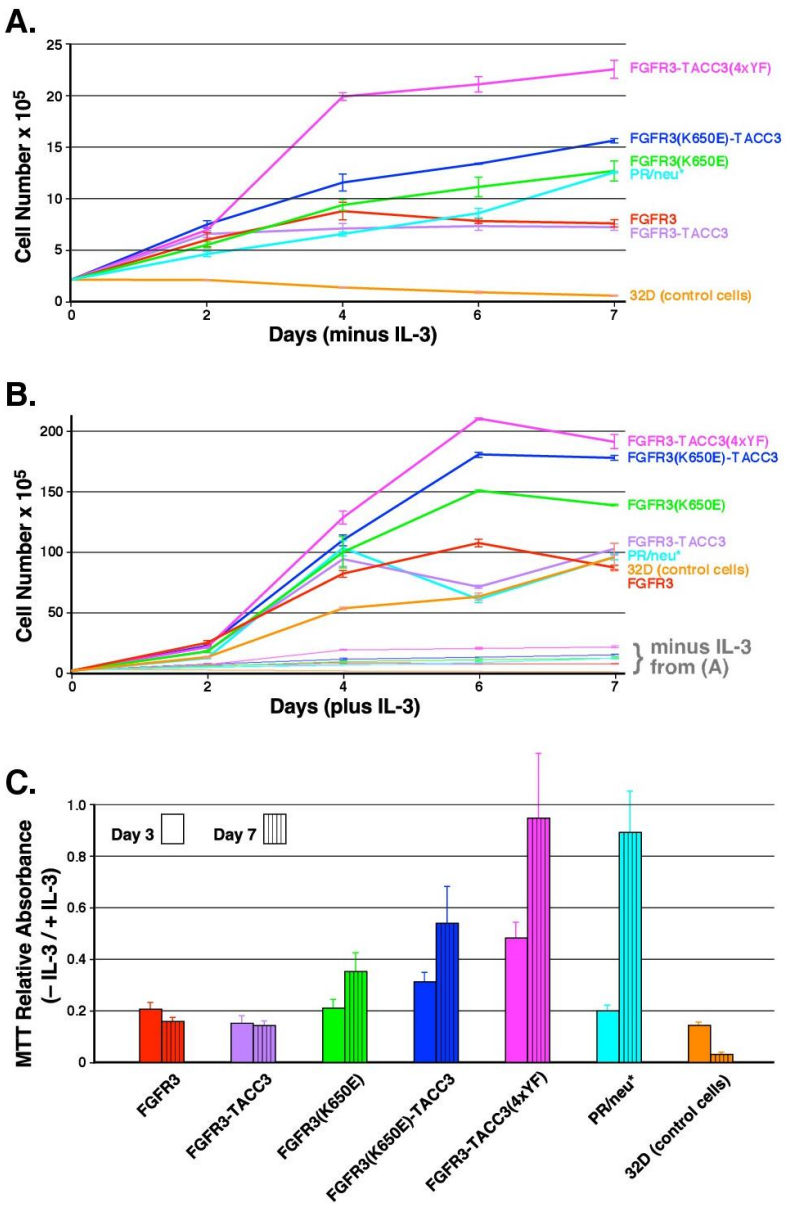

Figure 7. IL-3 independent growth and MTT viability assay in 32D cells expressing FGFR3 or FGFR3-TACC3 derivatives. PR/neu* is a positive control. **(A)** 32D cells selectively expressing FGFR3, FGFR3-TACC3, FGFR3(K650E), FGFR3(K650E)-TACC3, FGFR3-TACC3(4xYF), or PR/neu* were cultered in the absence of IL-3. The total number of viable cells were determined by trypan blue exclusion. Experiments were performed in triplicate, standard deviation is shown. **(B)** Cell counts of cultures in (A) in the presence of IL-3. Experiments were performed in triplicate, standard deviation is shown. Inset of growth from (A) without IL-3 is shown for comparison. **(C)** Cell viability as determined by MTT assay by 3 independent repeats on days 3 and 7. Relative absorbance was obtained by ratio of –IL-3 to +IL-3 absorbances read at 570 nm. Standard deviation is shown.

FGFR3-TACC3 displays nuclear localization

The presence of TACC3, a nuclear localizing protein (4), led to the question of whether a delocalization of the over activated FGFR3 kinase to the nucleus was occurring. Indeed, fractionation of MCF7 cells expressing FGFR3 WT, FGFR3(K650E), FGFR3(K508R), and their fusion counterparts displayed a clear difference in localization (Figure 8A). All three fusions, FGFR3-TACC3, FGFR3(K650E)-TACC3, FGFR3(K508R)-TACC3 (nuclear fraction, lanes 5, 6 & 7) displayed strong nuclear localization. The non-fused tyrosine kinase domains (lanes 2, 3 & 4) were present mainly in the cytoplasmic fraction. Perinuclear localization of FGFR3(K650E) has been demonstrated previously (14), but fusion of FGFR3(K650E) to TACC3 dramatically increased nuclear localization. These results indicate the presence of the TACC3 coiled coil domain is responsible for nuclear localization of the FGFR3 kinase, regardless of receptor activation. Immunoblotting for nuclear localizing mSin3A and cytoplasmic β-tubulin confirmed separation of nuclear and cytoplasmic fractions.

Downstream signaling activation by FGFR3-TACC3

It has been shown previously that FGFR3 WT and FGFR3(K650E) activate the signal transducer and activator of transcription (STAT) pathway and mitogen activated protein kinase (MAPK) pathway, but it is not clear how this activation compares to our constructed FGFR3-TACC3 or FGFR3(K650E)-TACC3 fusions. HEK293 cells expressing these fusions and their non-fused counterparts were analyzed for STAT1 and STAT3 activation. Both FGFR3(K650E) and FGFR3(K650E)-TACC3 led to phosphorylation of STAT1 and STAT3, but a significant increase in phosphorylation was not seen for the fusion constructs (Figure

8B). However, MAPK phosphorylation was strongly elevated by FGFR3-TACC3 and FGFR3(K650E)-TACC3 (Figure 8C, lanes 6 & 7), compared to non-fused FGFR3 WT and FGFR3(K650E) (lanes 2 & 3), indicating that FGFR3-TACC3 induces MAPK pathway activation. The kinase-dead FGFR3(K508R)-TACC3 did not display this activation (lane 8), indicating that FGFR3 kinase activity in the fusion protein is essential to downstream signaling activation.

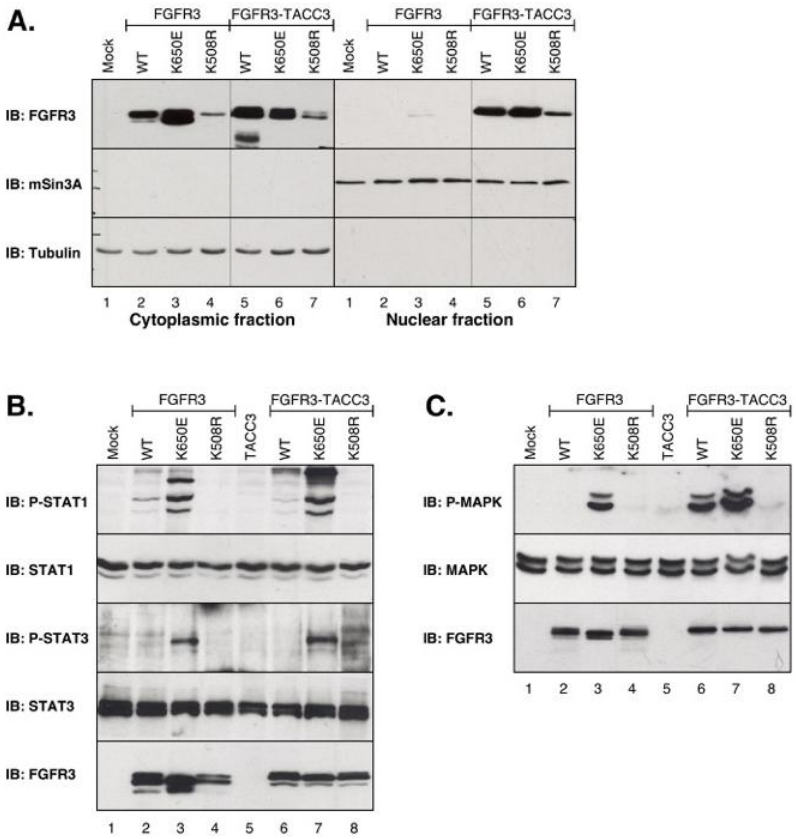

Figure 8. Localization and signaling of FGFR3-TACC3 fusions. **(A)** Fractionation of MCF7 cells expressing FGFR3 or FGFR3-TACC3 derivatives. Cells were separated into cytoplasmic (left) and nuclear (right) fractions. Immunoblotting with FGFR3 antibody shows nuclear localization of FGFR3-TACC3 fusions (top panels). Immunoblotting for mSin3A and β-Tubulin confirm fractionation (2nd and 3rd panels). **(B)** Lysates of HEK293 cells expressing FGFR3 or FGFR3-TACC3 derivatives were immunoblotted for Phospho-STAT1 (Y701) (top), STAT1 (2nd panel), Phospho-STAT3 (Y705) (3rd panel), STAT3 (4th panel), and FGFR3 (bottom). **(C)** HEK293 cell lysates expressing FGFR3 or FGFR3-TACC3 derivatives were immunoblotted for Phospho-MAPK (T202/Y204) (top), MAPK (2nd panel), and FGFR3 (bottom).

2.3 DISCUSSION

We extensively analyzed the FGFR3-TACC3 fusion protein by tyrosine residue phosphorylation changes and the impacts on cancer progression. We demonstrate that introduction of a 3' TACC3 coiled-coil domain results in constitutive activation and phosphorylation of key residues in FGFR3. Clearly, the TACC domain over-stimulates kinase activity, as shown by the additional phosphorylation sites detected by LC-MS/MS. Activation by this coiled coil domain has a more severe impact on cell transformation and downstream signaling than the activating K650E mutation alone, which causes the lethal syndrome Thanatophoric Dysplasia type II. By focus, proliferation, and viability assay, the high cell transformation, proliferation, and oncogenic potential of the fusion protein was demonstrated. The absence of biological activity shown by FGFR3(K508R)-TACC3 kinase dead mutant indicates that kinase activity is required for gain of function and cancer progression, but not required for nuclear localization of the fusion protein, as shown by cellular fractionation.

Examining the nonfused FGFR3 proteins, the analysis by LCMS/MS indicates key FGFR3 residues are being phosphorylated, primarily residues Y647 and Y648 as part of the YYKK activation loop motif essential to FGFR kinase activity (15). In the fusion protein FGFR3-TACC3, Y647 was the major site of phosphorylation within the activation loop, and phosphorylation of additional sites such as Y577, Y599, Y607, Y724, and Y798 was also observed. Introduction of the K650E mutation into the fusion protein FGFR3(K650E)-TACC3 resulted in increased phosphorylation of all the sites seen in the FGFR3-(K650E) as well as the sites seen in the FGFR3-TACC3 sample, with the additional appearance of phosphorylation at Y867 in the TACC3 domain. Residue Y724 has been shown to be critical

for activation of downstream signaling pathways, such as MAPK, STAT, and PI3K, and cell transformation (16).

Although the function has not been thoroughly explored for all the phosphotyrosine sites detected by MS analysis (Figure 4C), all sites are highly conserved in the four FGFRs, with the exception of Y577 which is not conserved in FGFR4. Interestingly, it has been suggested that Y577 is a key residue for the activation of FGFR3(K650E). Upon phosphorylation at Y577 the active state confirmation of the receptor is stabilized, independent of activation loop phosphorylation (17). The strong peak intensity seen for Y577 in FGFR3-TACC3 could indicate a change in the mechanism of activation in a ligand independent manner due to the TACC domain (Figure 6B).

The fusion breakpoint of exon 18 in FGFR3 excludes the binding site for PLCγ (Y760), thus PLCγ is no longer recruited by FGFR3-TACC3, as previously shown (5). Additionally, Y760 may contribute to maximal STAT activation (16). The removal of this site from FGFR3-TACC3 may be contributing to the absence of STAT pathway overactivation. However, significant increase of downstream signaling activation was seen in the MAPK pathway independent of FGF ligand stimulation, which correlates with previous findings and further indicates ligand-independent activation and cell growth (3,5,18).

Overexpression of TACC3 WT has been shown to increase activation of MAPK signaling pathway and contribute to the epithelial-mesenchymal transition (EMT) (19). However, we found that overexpression of TACC3 alone does not lead to increased MAPK activity (HEK293) or cell transformation (NIH3T3). Our results indicate that the fusion of FGFR3 and TACC3 is required for gain of oncogenic function.

Also missing from the FGFR3-TACC3 fusion breakpoint is the Aurora-A phosphorylation sites on TACC3. Aurora-A has been shown to phosphorylate TACC3 WT at S558 which is required for the localization of a TACC3-chTOG-clathrin complex to mitotic spindle microtubules and spindle poles (6,20,21). Localization of TACC3 to kinetochore fibers in complex with chTOG and clathrin is believed to assist with stabilization and formation of the mitotic spindle (21). However, previous studies have found the FGFR3-TACC3 fusion protein localized only to the mitotic spindle poles during mitosis, and relocated during late stage mitosis to the midbody. A mechanism for this change in recruitment and the role of FGFR3-TACC3 during interphase remains unclear (22).

Although not analyzed in regards to the cell cycle, we show a strong indication of nuclear localization for the fusion protein. Additionally, localization of FGFR3-TACC3 to the nucleus is not dependent on kinase activity as shown by K508R mutation, indicating that this localization is solely due to the fused TACC domain. Since the Aurora A phosphorylation sites are no longer present in the fusion protein, there must be another nuclear recruitment mechanism occurring. This delocalized kinase could be interacting with novel proteins that lead to cancer progression.

The detection of phosphorylated TACC3 residues (Y798, Y853 and Y867 corresponding to Y684, Y739, and Y753 in native TACC3) could indicate the ability of a highly activated FGFR3 kinase to self-phosphorylate the TACC domain and potentially lead to increased downstream signaling. Phosphorylation of Y878 was unable to be recovered by MS, but is presumably phosphorylated as it is located in a conserved 9 amino acid tyrosine phosphorylation motif within the TACC family (10). Our results, in which mutation to phenylalanine of all four tyrosine residues within the TACC3 domain leads to increased focus

formation and IL3-independent cell proliferation, leads to the conclusion that phosphorylation at these sites, while it does occur, fails to contribute significantly to the oncogenic potential of the FGFR3-TACC3 fusion oncogene.

Recently, it has been shown that chTOG (colonic and hepatic tumor overexpressed gene), a centrosomal localizing protein, recruits TACC3 to microtubule plus-ends during interphase. This localization is dependent on chTOG, not TACC3, and is independent of Aurora A phosphorylation (21). TACC3 residues 672-688 contain the binding site of ch-TOG and are present in the FGFR3-TACC3 fusion protein (at residues 786-802). Within this region is Y798, which we have found to be highly phosphorylated in the FGFR3-TACC3 and FGFR3(K650E)-TACC3 fusion proteins by LC-MS/MS. In the K650E background, when the phosphorylation site is removed by mutation Y798F, we did not observe a significant change in biologic activity, suggesting that the specific phosphorylation of Y798 occurs adventitiously and is extrinsic to the biological properties of the FGFR3-TACC3 fusion..

Introduction of Tyr-to-Phe mutations at all of the retained TACC3-derived residues Y798, Y853, Y867, or Y878 resulted in changes in biologic activity that were statistically insignificant, again indicating that the phosphorylation we observed at these sites is biologically inconsequential. An inhibitory phosphorylation site has been shown to occur in FGFR3 WT at Y770 which, upon phosphorylation, inhibits cell transformation (16). Residue Y770 has been removed from the FGFR3-TACC3 fusion, but the significance of this change was not explored here.

We have presented overwhelming evidence of the high oncogenicity of the FGFR3-TACC3 fusion protein. The presence of the TACC coiled-coil domain leads to increased and altered levels of FGFR3 activation, fusion protein phosphorylation, downstream signaling,

and cellular transformation, proliferation, and viability. The existence of FGFR3-TACC3 fusions in human cancers creates additional challenges and opportunities for identifying effective treatment strategies. Further study of novel pathways activated by the FGFR3-TACC3 fusion protein, and a deeper understanding of the molecular details exploited by FGFR3-TACC3 to achieve its biologic potency, can be expected lead to novel therapeutic paradigms.

2.4 MATERIALS AND METHODS

DNA constructs

The TACC3 gene was purchased from Sino Biological Inc (pMD-TACC3) and was subcloned into pcDNA3. FGFR3, FGFR3(K650E), and FGFR3(K508R) were developed as previously described (23). To construct FGFR3-TACC3 fusion gene a unique ClaI site was introduced by PCR based site directed mutagenesis after residue 758 in FGFR3 and before residue 648 in TACC3. This unique site was used to subclone TACC3 3' of FGFR3 in pcDNA3, creating a fusion breakpoint of FGFR3 exon 18 to TACC3 exon 11 with a 3 amino acid linker of residues ASM containing the ClaI site.

Fragments containing K650E or K508R mutations were subcloned into the FGFR3-TACC3 fusion gene. Single and multiple tyrosine mutations in the TACC3 region (Y798F, Y853F, Y867F, Y878F) were introduced by PCR based site directed mutagenesis. DNA constructs were then subcloned into pLXSN vector (24) for focus, proliferation, and MTT assays. All clones were confirmed by DNA sequencing.

Cell culture

HEK293, HEK293T, and NIH3T3 cells were maintained in DMEM plus 10% fetal bovine serum (FBS) and 1% penicillin/streptomycin in 10% CO_2, 37°C. MCF7 cells were maintained at 5% CO2 in DMEM plus 10% FBS and 1% penicillin/streptomycin in 37°C. 32D clone 3 (ATCC CRL-11346) cells were maintained in RPMI 1640 medium with 10% FBS, 1% penicillin/streptomycin, and 5 ng/mL mouse IL-3 in 5% CO_2 37°C.

Mass Spectrometry Sample Preparation

HEK293T cells were plated one day prior to transfection at 3.0 x 10^6 cells per 15-cm tissue culture plate. 10 plates per sample were transfected by calcium phosphate precipitation with 9μg of FGFR3 or FGFR3-TACC3 derivatives. After 18-20 hr, cells were treated with 10 μM MG132 for 4-6 hr, washed once in 1xPBS + 1mM Na_3VO_4 before being lysed in RIPA. Clarified lysates were immunoprecipitated with FGFR3 antisera overnight at 4°C with rocking. Immune complexes were collected with Pierce protein A/G magnetic beads as per manufactures directions. Samples were taken to The Sanford Burnham Prebys Medical Discovery Institute mass spectrometry facility for proteasome on bead digestion and liquid chromatography (LC)-high mass accuracy tandem mass spectrometry (MS/MS) analysis.

Following immunoprecipitation, proteins were digested directly on-beads using Trypsin/Lys-C mix. Briefly, the samples (IP's and controls) were washed with 50 mM ammonium bicarbonate, and then resuspended with 8M urea, 50 mM ammonium bicarbonate, and cysteine disulfide bonds were reduced with 10 mM tris(2-carboxyethyl)phosphine (TCEP) at 30°C for 60 min followed by cysteine alkylation with 30 mM iodoacetamide (IAA) in the dark at room temperature for 30 min. Following alkylation, urea was diluted to 1 M

urea using 50 mM ammonium bicarbonate. The samples were finally subjected to overnight digestion with mass spec grade Trypsin/Lys-C mix (Promega, Madison, WI). Finally, peptides were collected into a new tube, and the magnetic beads were washed once with 50mM ammonium bicarbonate to increase peptide recovery. The digested samples were partially dried to approximately 50% of the total volume, and desalted using a C_{18} TopTip (PolyLC) according to the manufacturer's recommendations. The desalted peptide sample was split into 2 aliquots, 'Total' and 'Phospho' containing 10% and 90% of the sample, respectively. Both aliquots were then dried using a SpeedVac system.

The 'Phospho' aliquot was resuspended in 80% acetonitrile, 5% trifluoroacetic acid in 1M glycolic acid and incubated with TiO_2 magnetic beads (GE) for 30 min in a Thermomix at room temperature and 900 rpm. The unbound peptides were removed and the magnetic beads were washed twice with 80% acetonitrile, 5% trifluoroacetic acid to remove non-phosphorylated peptides. Finally, phosphopeptides were eluted with 5% ammonium hydroxide and dried down using a SpeedVac system.

LC-MS/MS Analysis

Both the 'Total' and 'Phospho' were analyzed by LC-MS/MS. Fifty percent of each sample was used for LC-MS/MS, a 0.180 x 20 mm C_{18} trap Symmetry column (Waters corp., Milford, MA) connected to an analytical C_{18} BEH130 PicoChip column 0.075 x 100 mm, 1.7µm particles (NewObjective, MA) mounted on a nanoACQUITY Ultra Performance Liquid Chromatography system (Waters corp., Milford, MA), directly coupled to an Orbitrap Velos Pro mass spectrometer (Thermo Fisher Scientific). The peptides were separated with a 90-min non-linear gradient of 2-35% solvent B at a flow rate of 400nL/min. The mass

spectrometer was operated in positive data-dependent acquisition mode. MS1 spectra were measured with a resolution of 60,000, an AGC target of 10^6 and a mass range from 350 to 1400 m/z. Up to 5 MS2 spectra per duty cycle were triggered, and each precursor was fragmented twice by collisium-induced dissociation (with multiple stage activation enabled) and electron transfer dissociation (ETD), and acquired in the ion trap with an AGC target of 10^4, an isolation window of 2.0 m/z and a normalized collision energy of 35. Dynamic exclusion was set to 5 seconds to allow multiple fragmentation of phosphopeptides.

Proteomics data analysis

All mass spectra from were analyzed with MaxQuant software version 1.5.2.8 (Cox et al). Briefly, MS/MS spectra were searched against the cRAP protein sequence database (http://www.thegpm.org/crap/) indexed with corresponding FGFR3 or FGFR3-TACC3 derivative sequences. Precursor mass tolerance was set to 20ppm and 4.5ppm for the first search where initial mass recalibration was completed and for the main search, respectively. Product ions were searched with a mass tolerance 0.5 Da. The maximum precursor ion charge state used for searching was 7. Carbamidomethylation of cysteines was searched as a fixed modification, while phosphorylation of serines, threonines and tyrosines, and oxidation of methionines was searched as variable modifications. Enzyme was set to trypsin in specific mode and a maximum of two missed cleavages was allowed for searching. The target-decoy-based false discovery rate (FDR) filter for spectrum and protein identification was set to 1%. Second peptide mode of MaxQuant software was also enabled.

Antibodies and Reagents

Antibodies were obtained from the following sources: FGFR3 (B-9), mSin3A (K-20), β-tubulin (H-235), STAT1 (E-23), STAT3 (C-20) from Santa Cruz Biotechnology; phosphotyrosine (4G10) from Millipore; TACC3 C-terminal (SAB4500103) from Sigma; Phospho-STAT1 (Tyr701) (9171), Phospho-STAT3 (Tyr705) (D3A7), Phospho-p44/42 MAPK (Erk1/2) (T202/Y204) (E10), p44/42 MAPK (Erk1/2) (9102) from Cell Signaling Technology; horseradish peroxidase (HRP) anti-mouse, HPR anti-rabbit from GE Healthcare. Enhanced chemiluminence (ECL and Prime-ECL) reagents were from GE Healthcare. MG132, aFGF, and recombinant mouse Interleukin-3 (IL-3) were obtained from R&D systems; Heparin was from Sigma; Geneticin (G418) was from Gibco. Lipofectamine 2000 Reagent was from Invitrogen.

Transfection, Immunoprecipitation, Immunoblot

HEK293 were plated at a density of 1 x 10^6 cells/100-mm plate and transfected with 3 μg plasmid DNA using calcium phosphate transfection in 3% CO_2 as previously described (25). 20 to 24 hr after transfection, media was changed to DMEM with 0% FBS. Cells were starved for 20 hr before collecting and lysis.

Transfected HEK293 cells were collected, washed once in PBS, and lysed in 1% NP40 Lysis Buffer [20 mmol/L Tris-HCl (pH 7.5), 137 mmol/L NaCl, 1% Nonidet P-40, 5 mmol/L EDTA, 50 mmol/L NaF, 1 mmol/L sodium orthovanadate, 1 mmol/L phenylmethylsulfonyl fluoride (PMSF), and 10 μg/mL aprotinin] or radioimmunoprecipitation assay buffer [RIPA; 50 mmol/L Tris-HCl (pH 8.0), 150 mmol/L NaCl, 1% TritionX-100, 0.5% sodium deoxycholate, 0.1% SDS, 50 mmol/L NaF, 1 mmol/L sodium orthovanadate, 1 mmol/L

PMSF, and 10 μg/mL aprotinin]. Bradford assay or Lowry assay was used to measure total protein concentration. Antibodies were added to lysates for overnight incubation at 4°C with rocking, followed by immunoprecipitation, as described previously (24). Samples were separated by 10% or 12.5% SDS-PAGE and transferred to Immobilon-P membranes (Millipore). Membranes were blocked in 3% milk/TBS/0.05% Tween 20 or 3% bovine serum albumin (BSA)/TBS/0.05% Tween 20 (for anti-phosphotyrosine, anti–phospho-STAT1, and anti–phospho-STAT3 blots). Immunoblotting was performed as previously described (26).

Focus Assay

Focus assays were performed using NIH3T3 cells plated at a density of 2×10^5 cells/60-mm plates in DMEM with 10% FBS 24 hr before transfection. Cells were transfected by Lipofectamine 2000 Reagent per manufacturer directions with 10 μg plasmid DNA. Between 22 and 24 hr after transfection cells were re-fed with DMEM 10% FBS. Cells were split 1:12 onto 100-mm plates between 22 and 24 hr later. Foci were scored at 12-14 days, fixed in methanol, stained with Geimsa stain, and photographed. Efficiency of transfection was determined by Geneticin (G418, 0.5 mg/ml)-resistant colonies plated at a dilution of 1:240.

Fractionation

MCF7 cells were plated at a density of 1.5×10^6 cells/100-mm plates 24 hr before transfection. Immediately prior to transfection, media was changed to DMEM 0% FBS with no antibiotic. Cells were transfected with 8 μg of plasmid DNA using Lipofectamine 2000 Reagent, per manufacturer's directions. 23 hr after transfection cells were collected in PBS

and 1 mM EDTA for fractionation as described previously (27). Separated fractions were analyzed for protein content by Bradford assay, separated by 10% SDS-PAGE, and transferred to Immobilon-P membrane for Western Blot analysis.

IL-3 independent growth in 32D cells

$1x10^6$ exponentially growing 32D cells were electroporated (1500 V, 10 ms, 3 pulse) by the Neon Transfection System (Invitrogen) using 30 µg of FGFR3, FGFR3-TACC3 or PR/neu* derivatives in pLXSN in triplicate. Twenty-four hours after transfection cells were selected with 1.5 mg/ml Geneticin (G418) sulfate for 10 days to generate stable cell lines. For IL-3 independent proliferation assays, $2x10^5$ cells were seeded in 12 well plates in the absence of IL-3 or 6 well plates in the presence of IL-3. The media also contained 1 nM aFGF and 30 µg/ml heparin (28). Cell numbers were determined in triplicate, with a hemocytometer and trypan blue exclusion on days 2, 4, 6 and 7. Media was added to cultures when cell numbers reached ~$1x10^6$ cells/mL during the assays to maintain at viable concentrations. To measure cell viability MTT assays were performed. A stock solution of 5mg/ml in PBS of MTT 3-(4, 5-dimethylthiazol-2-yl)-2,5-diphenyltetrazolium bromide (Sigma) was added at 1:10 to the cultures. After incubation at 37°C, 5% CO_2 for approximately 4 hrs equal volume of 0.04 M HCl in isopropanol was added and mixed well and incubated again for at least 30 min (29). Cultures were transferred to microfuge tubes, spun for 30 sec at room temperature and supernatant absorbance was measured in a Beckman DU 350 UV/Vis spectrophotometer at 570 nm. $5x10^4$ cells per well were plated in triplicate in 24-well plates in the presence or absence of IL-3 and 1nM aFGF and 30ug/ml heparin and assayed 3 days later. The cell

viability at day 7 was measured using the cultures from the proliferation assay. In triplicate, 0.5 ml of the cultures were transferred to 24 well plates and treated with the MTT reagent.

2.5 ACKNOWLEDGMENTS

Chapter 2 was published as “Oncogenic Gene Fusion FGFR3-TACC3 Is Regulated by Tyrosine Phosphorylation”, in Molecular Cancer Research in 2016, with the authors of Nelson KN, Meyer AN, Siari A, Campos AR, Motamedchaboki K, Donoghue DJ.. The dissertation author was the primary investigator and author of this material.

2.6 REFERENCES

1. Gallo LH, Nelson KN, Meyer AN, Donoghue DJ. Functions of Fibroblast Growth Factor Receptors in cancer defined by novel translocations and mutations. Cytokine Growth Factor Rev 2015;26(4):425-49.

2. Carneiro BA, Elvin JA, Kamath SD, Ali SM, Paintal AS, Restrepo A, et al. FGFR3-TACC3: A novel gene fusion in cervical cancer. Gynecol Oncol Rep 2015;13:53-6.

3. Parker BC, Annala MJ, Cogdell DE, Granberg KJ, Sun Y, Ji P, Li X, Gumin J, Zheng H, Hu L, Yli-Harja O, Haapasalo H, Visakorpi T, Liu X, Liu CG, Sawaya R, Fuller GN, Chen K, Lang FF, Nykter M, Zhang W. The tumorigenic FGFR3-TACC3 gene fusion escapes miR-99a regulation in glioblastoma. J Clin Invest 2013;123(2):855-65.

4. Gergely F, Karlsson C, Still I, Cowell J, Kilmartin J, Raff JW. The TACC domain identifies a family of centrosomal proteins that can interact with microtubules. Proc Natl Acad Sci U S A 2000;97(26):14352-7.

5. Williams SV, Hurst CD, Knowles MA. Oncogenic FGFR3 gene fusions in bladder cancer. Hum Mol Genet 2013;22(4):795-803.

6. Thakur HC, Singh M, Nagel-Steger L, Kremer J, Prumbaum D, Fansa EK, Ezzahoini H, Nouri K, Gremer L, Abts A, Schmitt L, Raunser S, Ahmadian MR, Piekorz RP. The centrosomal adaptor TACC3 and the microtubule polymerase chTOG interact via defined C-terminal subdomains in an Aurora-A kinase-independent manner. J Biol Chem 2014;289(1):74-88.

7. Hornbeck PV, Kornhauser JM, Tkachev S, Zhang B, Skrzypek E, Murray B, Latham V, Sullivan M. PhosphoSitePlus: a comprehensive resource for investigating the structure and function of experimentally determined post-translational modifications in man and mouse. Nucleic Acids Res 2012;40(Database issue):D261-70.

8. Olsen JV, Vermeulen M, Santamaria A, Kumar C, Miller ML, Jensen LJ, Gnad F, Cox J, Jensen TS, Nigg EA, Brunak S, Mann M. Quantitative phosphoproteomics reveals widespread full phosphorylation site occupancy during mitosis. Science signaling 2010;3(104):ra3.

9. Petti LM, Irusta PM, DiMaio D. Oncogenic activation of the PDGF beta receptor by the transmembrane domain of p185neu*. Oncogene 1998;16(7):843-51.

10. McKeveney PJ, Hodges VM, Mullan RN, Maxwell P, Simpson D, Thompson A, Winter PC, Lappin TR, Maxwell AP. Characterization and localization of expression of an erythropoietin-induced gene, ERIC-1/TACC3, identified in erythroid precursor cells. Br J Haematol 2001;112(4):1016-24.

11. Roll JD, Reuther GW. ALK-activating homologous mutations in LTK induce cellular transformation. PLoS One 2012;7(2):e31733.

12. Kawai H, Matsushita H, Suzuki R, Sheng Y, Lu J, Matsuzawa H, Yahata T, Tsuma-Kaneko M, Tsukamoto H, Kawada H, Ogawa Y, Ando K. Functional analysis of the SEPT9-ABL1 chimeric fusion gene derived from T-prolymphocytic leukemia. Leuk Res 2014;38(12):1451-9.

13. Tao W, Leng X, Chakraborty SN, Ma H, Arlinghaus RB. c-Abl activates janus kinase 2 in normal hematopoietic cells. J Biol Chem 2014;289(31):21463-72.

14. Ronchetti D, Greco A, Compasso S, Colombo G, Dell'Era P, Otsuki T, Lombardi L, Neri A. Deregulated FGFR3 mutants in multiple myeloma cell lines with t(4;14): comparative analysis of Y373C, K650E and the novel G384D mutations. Oncogene 2001;20(27):3553-62.

15. Webster MK, D'Avis PY, Robertson SC, Donoghue DJ. Profound ligand-independent kinase activation of fibroblast growth factor receptor 3 by the activation loop mutation responsible for a lethal skeletal dysplasia, thanatophoric dysplasia type II. Mol Cell Biol 1996;16(8):4081-7.

16. Hart KC, Robertson SC, Donoghue DJ. Identification of tyrosine residues in constitutively activated fibroblast growth factor receptor 3 involved in mitogenesis, Stat activation, and phosphatidylinositol 3-kinase activation. Mol Biol Cell 2001;12(4):931-42.

17. Huang Z, Chen H, Blais S, Neubert TA, Li X, Mohammadi M. Structural mimicry of a-loop tyrosine phosphorylation by a pathogenic FGF receptor 3 mutation. Structure 2013;21(10):1889-96.

18. Wu YM, Su F, Kalyana-Sundaram S, Khazanov N, Ateeq B, Cao X, Lonigro RJ, Vats P, Wang R, Lin SF, Cheng AJ, Kunju LP, Siddiqui J, Tomlins SA, Wyngaard P, Sadis S, Roychowdhury S, Hussain MH, Feng FY, Zalupski MM, Talpaz M, Pienta KJ, Rhodes DR, Robinson DR, Chinnaiyan AM. Identification of targetable FGFR gene fusions in diverse cancers. Cancer discovery 2013;3(6):636-47.

19. Ha GH, Park JS, Breuer EK. TACC3 promotes epithelial-mesenchymal transition (EMT) through the activation of PI3K/Akt and ERK signaling pathways. Cancer Lett 2013;332(1):63-73.

20. Fu W, Tao W, Zheng P, Fu J, Bian M, Jiang Q, Clarke PR, Zhang C. Clathrin recruits phosphorylated TACC3 to spindle poles for bipolar spindle assembly and chromosome alignment. J Cell Sci 2010;123(Pt 21):3645-51.

21. Gutierrez-Caballero C, Burgess SG, Bayliss R, Royle SJ. TACC3-ch-TOG track the growing tips of microtubules independently of clathrin and Aurora-A phosphorylation. Biol Open 2015;4(2):170-9.

22. Singh D, Chan JM, Zoppoli P, Niola F, Sullivan R, Castano A, Liu EM, Reichel J, Porrati P, Pellegatta S, Qiu K, Gao Z, Ceccarelli M, Riccardi R, Brat DJ, Guha A, Aldape K, Golfinos JG, Zagzag D, Mikkelsen T, Finocchiaro G, Lasorella A, Rabadan R, Iavarone A. Transforming fusions of FGFR and TACC genes in human glioblastoma. Science 2012;337(6099):1231-5.

23. Webster MK, Donoghue DJ. Enhanced signaling and morphological transformation by a membrane-localized derivative of the fibroblast growth factor receptor 3 kinase domain. Mol Cell Biol 1997;17(10):5739-47.

24. Bell CA, Tynan JA, Hart KC, Meyer AN, Robertson SC, Donoghue DJ. Rotational coupling of the transmembrane and kinase domains of the Neu receptor tyrosine kinase. Mol Biol Cell 2000;11(10):3589-99.

25. Gallo LH, Meyer AN, Motamedchaboki K, Nelson KN, Haas M, Donoghue DJ. Novel Lys63-linked ubiquitination of IKKbeta induces STAT3 signaling. Cell Cycle 2014;13(24):3964-76.

26. Meyer AN, McAndrew CW, Donoghue DJ. Nordihydroguaiaretic acid inhibits an activated fibroblast growth factor receptor 3 mutant and blocks downstream signaling in multiple myeloma cells. Cancer Res 2008;68(18):7362-70.

27. Meyer AN, Drafahl KA, McAndrew CW, Gilda JE, Gallo LH, Haas M, Brill LM, Donoghue DJ. Tyrosine Phosphorylation Allows Integration of Multiple Signaling Inputs by IKKbeta. PLoS One 2013;8(12):e84497.

28. Chen J, Williams IR, Lee BH, Duclos N, Huntly BJ, Donoghue DJ, Gilliland DG. Constitutively activated FGFR3 mutants signal through PLC{gamma}-dependent and -independent pathways for hematopoietic transformation. Blood, in press 2005.

29. Mosmann T. Rapid colorimetric assay for cellular growth and survival: application to proliferation and cytotoxicity assays. J Immunol Methods 1983;65(1-2):55-63.

CHAPTER 3

Oncogenic Driver FGFR3-TACC3 is dependent on membrane trafficking and ERK signaling

ABSTRACT

Chromosomal translocations have been identified as oncogenic drivers in many cancers, allowing them to serve as potential drug targets in clinical practice. The involvement of FGFR genes in such translocations is becoming increasingly common, with FGFR3-TACC3 fusion protein becoming frequently identified in many cancer types. We demonstrate that the oncogenic effect of FGFR3-TACC3 is dependent on entrance to the secretory pathway or plasma membrane localization, leading to overactivation of canonical MAPK/ERK pathway. FGFR3-TACC3 leads to cell transformation which can be enhanced by the introduction of different breakpoints of TACC3 but not by association with canonical TACC3 interacting proteins, Aurora-A, clathrin, and ch-TOG. We have shown that kinase inhibitors for MEK (Trametinib) and FGFR (BGJ398) are effective in blocking cell transformation and MAPK pathway upregulation. The development of personalized medicines will be essential in treating patients who harbor oncogenic drivers such as FGFR3-TACC3.

3.1 INTRODUCTION

Oncogenic driver mutations have taken a front seat in the world of cancer research. These drivers are often chromosomal rearrangements resulting in fusion proteins. A recently identified fusion protein is FGFR3-TACC3 (R3T3), which has been discovered in glioblastoma, lung cancer, bladder cancer, oral cancer, head and neck squamous cell carcinoma, gallbladder cancer, and cervical cancer (1,2). This fusion protein is formed by a tandem duplication on chromosome 4 resulting in a fusion of the fibroblast growth factor receptor 3 (FGFR3) gene with transforming acidic coiled-coil containing protein 3 (TACC3) gene.

The FGFR family exhibits homologous domains of three immunoglobulin-like (Ig) domains, a transmembrane (TM) domain, and a split tyrosine kinase (TK) domain. FGFRs are activated by binding of fibroblast growth factor (FGF) ligands and heparin sulfate proteoglycans (HSPG) to the extracellular Ig-like domains. This induces FGFR dimerization and activation by trans-autophosphorylation of tyrosine residues in the kinase domain activation loop. FGFR activation leads to upregulation of RAS-MAPK, PI3K-AKT, and JAK/STAT pathways. This upregulation results in cellular proliferation, migration, angiogenesis and anti-apoptosis. In cancer, oncogenic fusion proteins involving FGFRs are becoming increasingly prevalent, with over 40 different FGFR fusion proteins detected so far (1). In such fusion proteins, the FGFR becomes constitutively activated by the dimerizing domain of the partner protein which brings the FGFR monomers close enough together to induce activation. In FGFR3-TACC3, the coiled-coil domain of TACC3 allows for autophosphorylation and activation of FGFR3 without the need for ligand binding (3).

TACC3 belongs to the TACC family, which provides stability of the mitotic spindle. Aurora-A phosphorylation of TACC3 results in a complex formation of TACC3, clathrin and ch-TOG. This complex localizes to the mitotic spindle microtubules and assists in their stability and cross-linking of microtubules to kinetochores. Formation of this complex is essential for mitotic spindle stability and proper cell division (4,5). Alteration of TACC3 expression levels has been found in many cancer types and leads to chromosomal segregation errors (6,7). These mitotic defects can contribute to aneuploidy and cancer progression (8).

It has been demonstrated that the involvement of TACC3 in the fusion protein R3T3 leads to an increased rate of aneuploidy and severe mitotic defects. Localization of R3T3 to the centrosome and mitotic spindle leads to chromosomal segregation errors and a reduction of TACC3 presence at the mitotic spindle (9,10). R3T3 has also been found to co-localize with phospho-PIN4 to induce preoxisome biogenesis and protein synthesis (11). Although altered cellular localization and effects on mitotic defects have been well explored, it is unclear if these effects are the drivers of cancer progression. It has also been demonstrated that the fusion protein R3T3 leads to an upregulation of PI3K/AKT, STAT and MAPK pathways (1,12). We demonstrate that the oncogenic mechanism initiated by R3T3 is through the overactivation of canonical FGFR pathways by entrance of R3T3 to the secretory pathway or localization to the plasma membrane.

3.2 RESULTS

Exploring the contribution of TACC3 in FGFR3-TACC3

TACC3 has been shown to localize to spindle microtubules and centrosomes during mitosis and to the cytoplasm and nucleus during interphase (13,14). The presence of the C-

terminal coiled-coil domain of TACC3 in the R3T3 fusion protein has been shown to be responsible for the localization of R3T3 to the nucleus and to mitotic spindle poles (3,9). R3T3 has been reported to increase the rate of aneuploidy and chromosomal separation errors, due to the presence of R3T3 at the mitotic spindle and the absence of TACC3 WT at spindle microtubules (9,10). These data suggest that a nuclear-localized R3T3 could significantly accelerate cancer progression. To further examine the function of R3T3 localization, we employed a bipartite Nuclear Localization Signal (NLS) from *Xenopus* nucleoplasmin fused in frame with the kinase and coiled-coil domains of R3T3 in order to direct a nuclear-localized population of R3T3 (NLS-R3T3) (15) (Figure 9A, 9D). Additionally, mutation of select positively charged residues to Gln in the NLS abrogates the nuclear localizing, resulting in a cytoplasmic-localized population of R3T3 (Figure 9A, 9D). Using these populations, which are designed to mimic TACC3 wild-type (WT) behavior during interphase (14), we investigated the effects of each R3T3 population on oncogenicity. Surprisingly, neither the nuclear- nor cytoplasmic-targeted populations of R3T3 resulted in cellular transformation, as shown by NIH3T3 focus assay (Figure 9B, 9C). This indicates that the previously identified nuclear localization of an overactivated FGFR3 receptor due to R3T3 fusion formation is not the driving force of NIH3T3 cell transformation. During interphase, the R3T3 fusion appears in vesicle-like structures, which is expected for a transmembrane protein and consistent with previous reports (10) (Figure 9D). However, the addition of the TACC3 domain does alter cellular localization, as FGFR3 *wild*-type (WT) displays both cytoplasmic and plasma membrane (PM) localization (Figure 9D). While the presence of R3T3 may contribute to mitotic chromosomal segregation errors and aneuploidy (9,10), this may not be the initial oncogenic driver of focus formation.

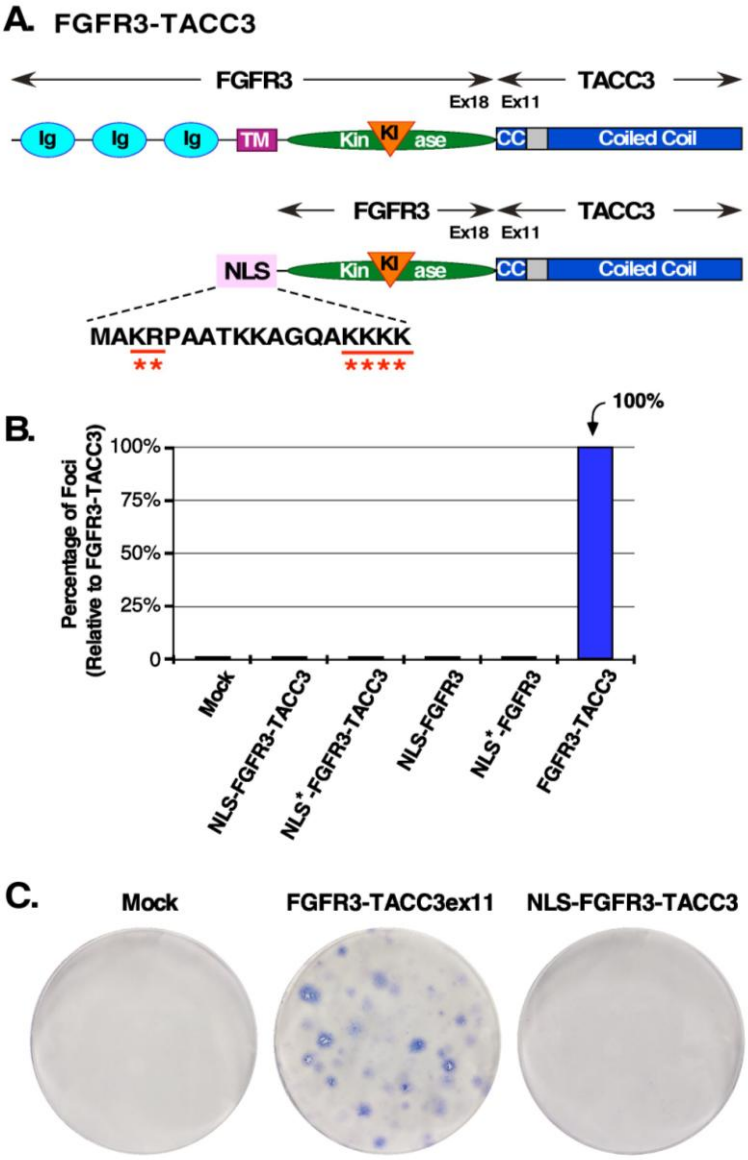

Figure 9: Nuclear-localized FGFR3-TACC3 does not convey cell transformation. **(A)** Schematic of FGFR3-TACC3 and NLS-FGFR3-TACC3 fusion proteins. For the nuclear-localized fusion construct, the extracellular and TM domains of FGFR3 are replaced with a bipartite Nuclear Localization Sequence (NLS) (NLS-FGFR3-TACC3). Mutation of underlined residues to Q results in cytoplasmic-localized FGFR3-TACC3 (NLS*-FGFR3-TACC3). **(B)** Transformation of NIH3T3 cells by FGFR3 and FGFR3-TACC3 derivatives. Number of foci were scored, normalized by transfection efficiency, and quantitated relative to FGFR3-TACC3 +/- SEM. **(C)** Representative plates from a focus assay are shown, with transfected constructs indicated. **(D)** Representative confocal micrographs of NIH3T3 cells stably expressing the indicated constructs. Secondary antibodies were either donkey anti-goat AlexFluor488 or donkey anti-goat AlexaFluor594. Nucleus is visualized with Hoechst 33342.

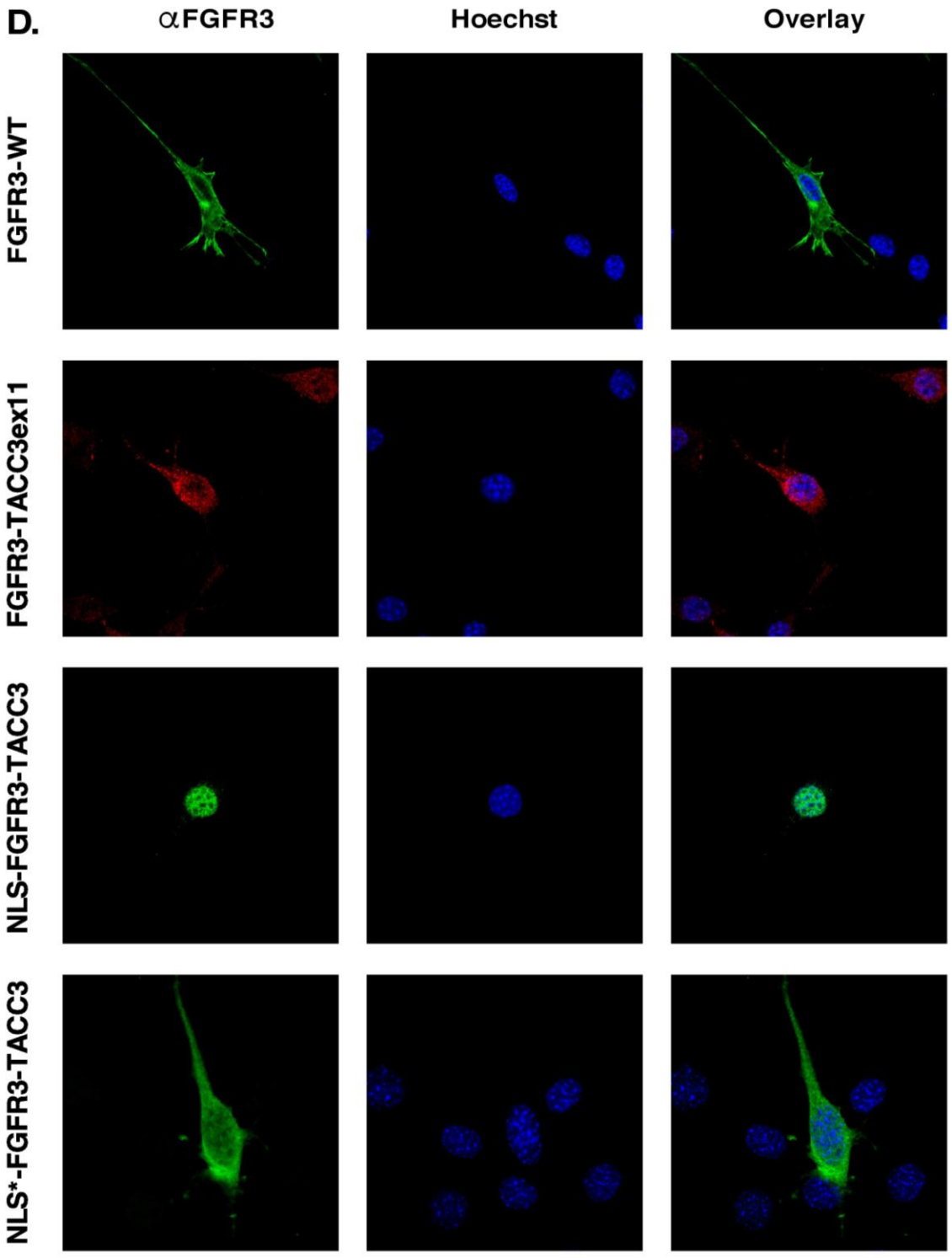

Figure 9. Nuclear-localized FGFR3-TACC3 does not convey cell transformation, continued.

Membrane localization is essential for FGFR3-TACC3 oncogenic activity

Following our results with the NLS signal, we replaced the extracellular and transmembrane domains of FGFR3 in R3T3 with a myristoylation sequence derived from the N-terminus of c-Src (Myr-R3T3) (16,17) (Figure 10A). The addition of this sequence results in myristoylation of R3T3; myristoylation is a post-translational modification that adds myristic acid, a 14-carbon saturated fatty acid, to an N-terminal Gly residue, which directs R3T3 to the inner surface of the plasma membrane, in order to mimic an integral membrane protein (Figure 10B). This membrane association represents a non-covalent type of interaction with the membrane but is distinctly different from the membrane insertion of a classic type 1 integral membrane protein such as FGFR3. FGFR3 requires an N-terminal signal sequence to direct entry into the secretory pathway, eventually reaching the cell surface after post-translation modifications such as di-sulfide bonding and glycosylation. A mutant Gly2Ala myristoylation signal results in cytoplasmic localization of R3T3 (18) (Figure 10A,B). NIH3T3 cell focus assay demonstrates that only the plasma membrane-localized R3T3 leads to focus formation, while the cytoplasmic localized fusion protein was negative in this assay (Figure 10C,D). Additionally, transfection of Myr-R3T3 into HEK293T cells leads to significant upregulation of the MAPK pathway, suggesting a key mechanism of cell transformation (Figure 10E). This increase in MAPK phosphorylation is comparable to Myr-FGFR3-K650E, which is a constitutively active myristoylated FGFR3 produced by the mutation K650E. This mutation was originally discovered as the cause of Thanatophoric Dysplasia type II, a skeletal disorder (1). Localization to the inner membrane face can produce a comparable level of cell pathway activation and transformation to R3T3, suggesting

that the driving oncogenic force of R3T3 is connected to the localization of a highly active FGFR3 kinase to the membrane in order to overactivate canonical RTK pathways.

Figure 10. Plasma membrane-localized FGFR3-TACC3 conveys cell transformation. **(A)** Schematic of FGFR3-TACC3 and Myr-FGFR3-TACC3 fusion proteins. For the membrane-localized fusion construct, the extracellular and TM domains of FGFR3 are replaced with a myristoylation sequence (Myr) derived from c-Src (Myr-FGFR3-TACC3). Mutation of underlined residue to A results in cytoplasmic-localized FGFR3-TACC3 (Myr*-FGFR3-TACC3). **(B)** Representative confocal micrographs of NIH3T3 cells stably expressing the indicated constructs, using FGFR3 immunostaining directed against an intracellular kinase domain peptide of FGFR3. Secondary antibodies were either donkey anti-goat AlexFluor488 or donkey anti-goat AlexaFluor594. Nucleus is visualized with Hoechst 33342. **(C)** Transformation of NIH3T3 cells by FGFR3 and FGFR3-TACC3 derivatives. Number of foci were scored, normalized by transfection efficiency, and quantitated relative to FGFR3-TACC3 +/- SEM. Assays were performed a minimum of three times per DNA construct. **(D)** Representative plates from a focus assay are shown, with transfected constructs indicated. **(E)** HEK293T cell lysates expressing FGFR3 or FGFR3-TACC3 derivatives were immunoblotted for phospho-MAPK (T202/Y204; top), MAPK (second panel), and FGFR3 (bottom).

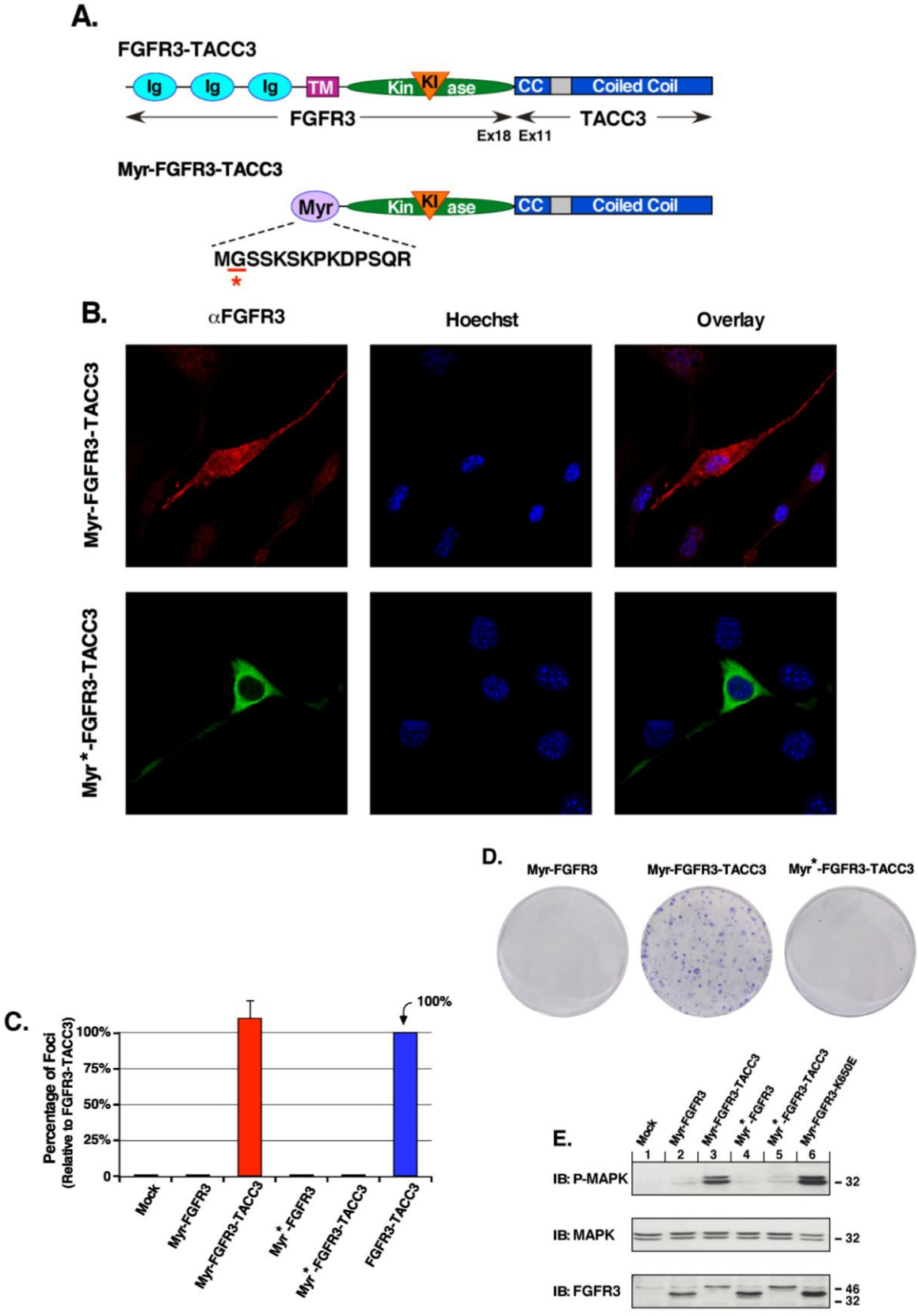
A.
FGFR3-TACC3
Ig
Ig
Ig
TM
Kin
KI
ase
CC
Coiled Coil
FGFR3
Ex18 Ex11
TACC3
Myr-FGFR3-TACC3
Myr
MGSSKSKPKDPSQR
*
B.
αFGFR3
Hoechst
Overlay
Myr-FGFR3-TACC3
Myr*-FGFR3-TACC3
C.
Percentage of Foci
(Relative to FGFR3-TACC3)
100%
75%
50%
25%
0
Mock
Myr-FGFR3
Myr-FGFR3-TACC3
Myr*-FGFR3
Myr*-FGFR3-TACC3
FGFR3-TACC3
D.
Myr-FGFR3
Myr-FGFR3-TACC3
Myr*-FGFR3-TACC3
E.
Mock
Myr-FGFR3
Myr-FGFR3-TACC3
Myr*-FGFR3
Myr*-FGFR3-TACC3
Myr-FGFR3-K650E
1
2
3
4
5
6
IB: P-MAPK
IB: MAPK
IB: FGFR3
32
32
46
32

Dual-targeted membrane associated fusion protein reinstates cell transformation

To assess if oncogenic activity can be restored to the biologically inactive nuclear-localized R3T3, the myristoylation sequence was fused in frame 5' of the NLS-FGFR3-TACC3 gene, creating the fusion construct Myr-NLS-FGFR3-TACC3 (Figure 11A). Our goal was to determine if it is possible to override the function of the NLS using a myristoylation signal to reinstate plasma membrane association and cell transformation. Immunofluorescence analysis determined that in this dual-targeted construct, the myristoylation signal is able to supersede the NLS signal, localizing R3T3 to the plasma membrane (Figure 11B). Consequently, shifting the biologically inactive NLS construct to the membrane restores biological activity and cell transformation as indicated by focus assay (Figure 11C). Also restored is the overactivation of MAPK pathway signaling by expression of Myr-NLS-FGFR3-TACC3 in HEK293T cells, furthering the connection between this pathway and cell transformation (Figure 11D). These results indicate the importance of FGFR3-TACC3 plasma membrane localization and MAPK pathway overactivation to cell transformation.

Figure 11. Re-localization to the plasma membrane reinstates NLS-FGFR3-TACC3 oncogenic activity. **(A)** Schematic of FGFR3-TACC3, NLS-FGFR3-TACC3 and Myr-NLS-FGFR3-TACC3 fusion proteins. NLS-FGFR3-TACC3 is the same fusion construct identified in Fig. 1A. For the Myr-NLS derivative, the c-Src Myr sequence is fused in front of the NLS-FGFR3-TACC3 (Myr-NLS-FGFR3-TACC3). **(B)** Representative confocal micrographs of NIH3T3 cells stably expressing the indicated constructs, using FGFR3 immunostaining directed against intracellular kinase domain peptide of FGFR3. Secondary antibodies were donkey anti-goat AlexFluor488 or donkey anti-goat AlexaFluor594. Nucleus is visualized with Hoechst 33342. **(C)** Transformation of NIH3T3 cells by the indicated constructs. Number of foci were scored, normalized by transfection efficiency, and quantitated relative to FGFR3-TACC3 +/- SEM. Assays were performed a minimum of three times per DNA construct. **(D)** HEK293T cell lysates expressing FGFR3 or FGFR3-TACC3 derivatives were immunoblotted for phospho-MAPK (T202/Y204; top), MAPK (second panel) and FGFR3 (bottom).

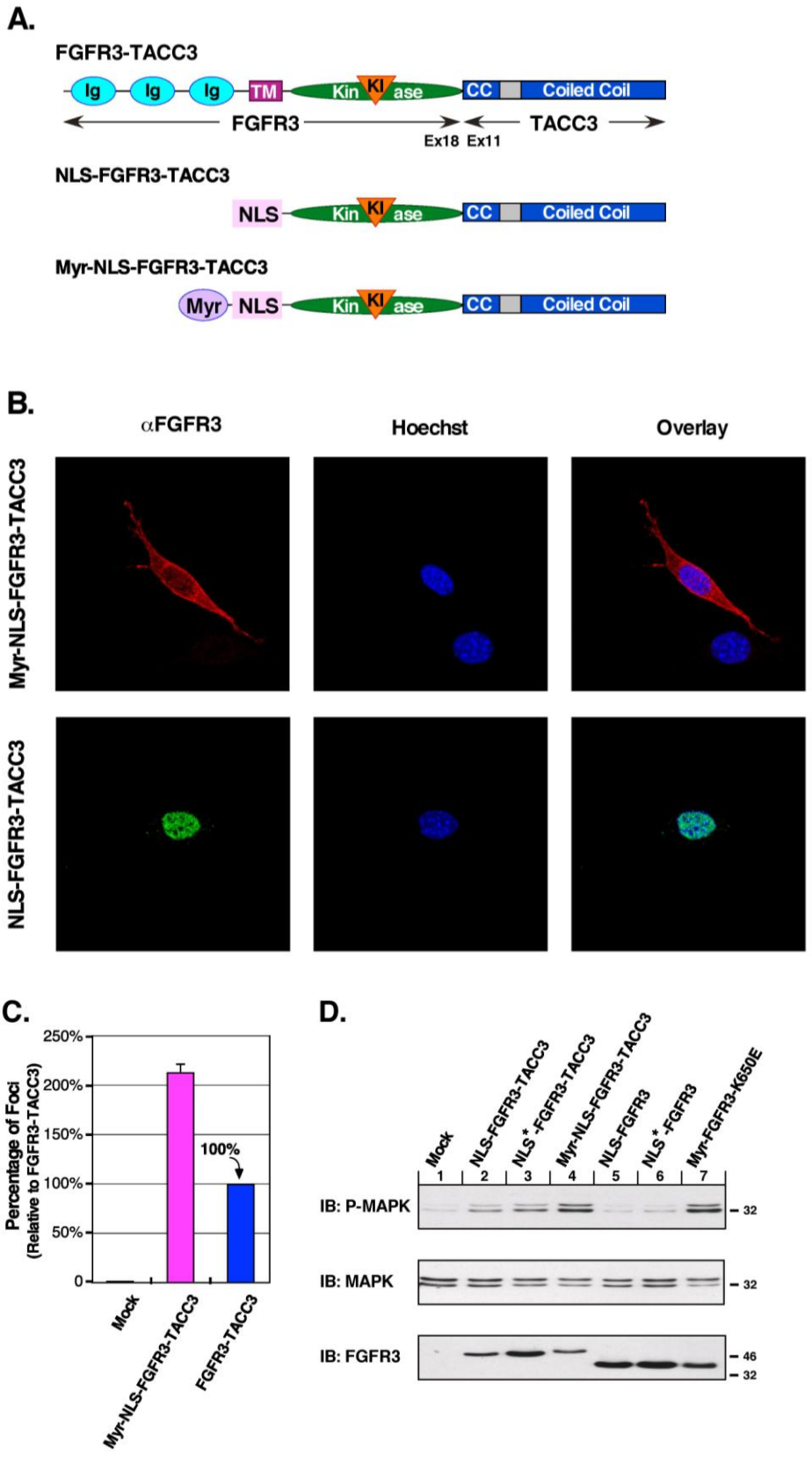
A.
FGFR3-TACC3
Ig
Ig
Ig
TM
Kin
KI
ase
CC
Coiled Coil
FGFR3
Ex18
Ex11
TACC3
NLS-FGFR3-TACC3
NLS
Myr-NLS-FGFR3-TACC3
Myr
B.
αFGFR3
Hoechst
Overlay
Myr-NLS-FGFR3-TACC3
NLS-FGFR3-TACC3
C.
Percentage of Foci
(Relative to FGFR3-TACC3)
250%
200%
150%
100%
50%
0
100%
Mock
Myr-NLS-FGFR3-TACC3
FGFR3-TACC3
D.
Mock
NLS-FGFR3-TACC3
NLS*-FGFR3-TACC3
Myr-NLS-FGFR3-TACC3
NLS-FGFR3
NLS*-FGFR3
Myr-FGFR3-K650E
1
2
3
4
5
6
7
IB: P-MAPK
IB: MAPK
IB: FGFR3
32
32
46
32

Cell transformation is dependent on entrance to the secretory pathway

The appearance of R3T3 in vesicle-like structures (Figure 9D) could indicate secretory vesicles en route to the membrane and that the fusion protein is capable of being inserted in the membrane as an integral membrane protein. To explore this, we blocked entrance of R3T3 to the secretory pathway by deletion of the FGFR3 signal sequence contained in the first 22 amino acids of the receptor (named ΔSS-FGFR3-TACC3) (19). The extracellular domain, transmembrane domain and kinase domain of FGFR3 and the coiled-coil domain of TACC3 remain intact (Figure 12A). The N-terminal signal peptide is homologous in the FGFR family and is responsible for targeting the FGFR for secretion.

We assessed co-localization of R3T3 and ΔSS-FGFR3-TACC3with a secretory pathway marker for early endosomes, EEA1, by confocal microscopy. Co-localization of R3T3 with this marker indicates its participation in membrane trafficking (Figure 12B, white arrows). Contrastingly, ΔSS-FGFR3-TACC3 does not co-localize with early endosomal EEA1 marker, confirming that entrance to the secretory pathway is blocked (Figure 12B). Analysis between R3T3 and markers for lysosomes (LAMP1), recycling endosomes (Rab11), or clathrin did not display co-localization (data not shown). As seen in Figure 12C, the multiple banding pattern of R3T3 (labeled with black arrow, lane 3) indicates different levels of glycosylation while ΔSS-FGFR3-TACC3 does not display this. Treatment of immunoprecipitated R3T3 with PNGase F to remove N-linked oligosaccharides results in a deglycosylated form of R3T3 with an electrophoretic mobility pattern identical to ΔSS-FGFR3-TACC3 (Figure 12C, lanes 5 and 6). This confirms that ΔSS-FGFR3-TACC3 does not exist as a glycosylated protein and is therefore not undergoing post-translation modifications of the secretory pathway.

As determined by focus assay and immunoblot, blocking entrance to the secretory pathway also blocks focus formation, cell transformation, and MAPK pathway activation by R3T3. This demonstrates the need for R3T3 to enter the secretory pathway and undergo post-translational processing, presumably reaching the plasma membrane in order to show oncogenic effects (Figure 12D, 12E). Some detectable MAPK pathway activation by ΔSS-FGFR3-TACC3 indicates the FGFR kinase domain is able to activate this pathway in HEK293T cells, but not enough to initiate to cell transformation in NIH3T3 cells (Figure 12E). Black arrows again demonstrate R3T3 has a multiple banding pattern indicating different levels of post-translational processing by the secretory pathway, where as ΔSS-FGFR3-TACC3 does not display this (Figure 12E).

Figure 12. FGFR3-TACC3 presence in the secretory pathway produces oncogenic effects. **(A)** Schematic of FGFR3-TACC3 with detail of signal peptide. SS-FGFR3-TACC3 indicates FGFR3-TACC3 with signal peptide deleted. **(B)** Confocal analysis of NIH3T3 cells stably expressing the indicated constructs reveals that FGFR3-TACC3 (red) co-localizes (yellow) with EEA1 early endosome marker (green) suggesting involvement in the secretory pathway. **(C)** HEK293T cell lysates expressing indicated constructs were immunoprecipitated with FGFR3 antibody, divided, treated with PNGase F enzyme and immunoblotted with FGFR3 antibody. **(D)** Transformation of NIH3T3 cells by the indicated constructs. Number of foci were scored, normalized by transfection efficiency and quantitated relative to FGFR3-TACC3 +/- SEM. Assays were performed a minimum of three times per DNA construct. **(E)** HEK293T cell lysates expressing SS-FGFR3-TACC3 or FGFR3-TACC3 were immunoblotted for phospho-MAPK (T202/Y204; top), MAPK (second panel), and FGFR3 (bottom).

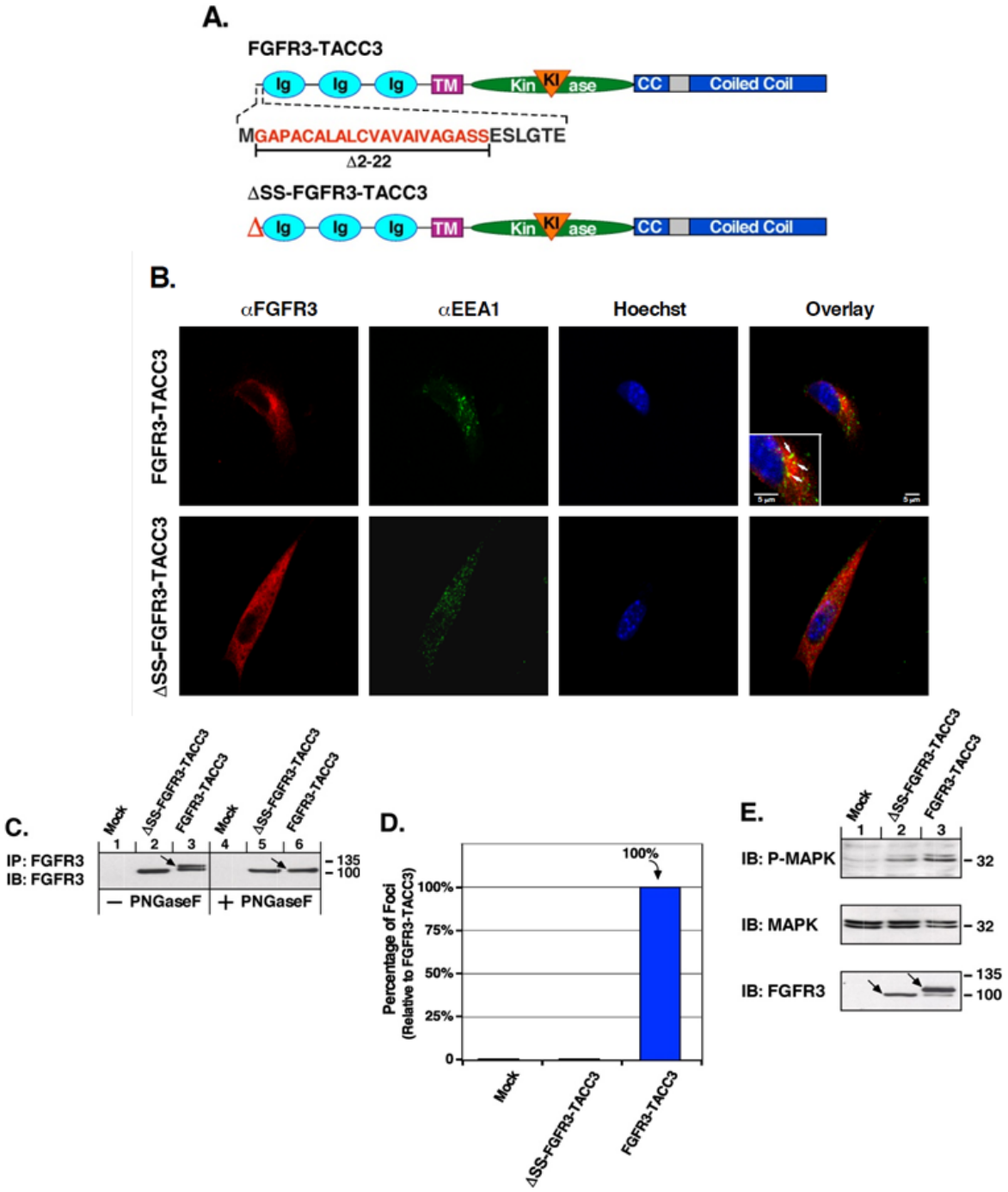
A.
FGFR3-TACC3
Ig
Ig
Ig
TM
Kin
KI
ase
CC
Coiled Coil
MGAPACALALCVAVAIVAGASSESLGTE
Δ2-22
ΔSS-FGFR3-TACC3
B.
αFGFR3
αEEA1
Hoechst
Overlay
FGFR3-TACC3
ΔSS-FGFR3-TACC3
C.
Mock
ΔSS-FGFR3-TACC3
FGFR3-TACC3
IP: FGFR3
IB: FGFR3
135
100
— PNGaseF
+ PNGaseF
D.
Percentage of Foci
(Relative to FGFR3-TACC3)
100%
75%
50%
25%
0
E.
IB: P-MAPK
IB: MAPK
IB: FGFR3
32

Different TACC3 breakpoints produce altered and elevated cell transformation

FGFR3-TACC3 has been identified in human cancer with many different breakpoints between the two fused genes. Breakpoints have been found to occur within exon 16 to 19 of FGFR3 gene and within exon 4 to 11 of TACC3 (1). The most commonly identified R3T3 fusion breakpoint is exon 18 of FGFR3 to exon 11 of TACC3, which this manuscript has focused on thus far. The second most common breakpoint of R3T3 is exon 18 of FGFR3 to exon 8 of TACC3. The introduction of the larger TACC3 gene introduces regulatory sites which are key to TACC3 *wild-type* (WT) function, including S558 Aurora-A phosphorylation site and LL566/567 clathrin binding domain, corresponding to S771 and LL779/780 in fusion protein R3T3 (Figure 13A). Upon Aurora-A phosphorylation, TACC3 WT will coordinate with ch-TOG (also named CKAP5) and clathrin to form a TACC3-ch-TOG-clathrin complex to assist with mitotic spindle binding (4,5). Immunofluorescence shows localization of R3T3ex8 to be very similar to R3T3ex11 during interphase (data not shown). However, by focus assay, R3T3ex8 displays 3-fold higher cell transformation level than R3T3ex11 (Figure 13B). Interestingly, R3T3ex8 and R3T3ex11 display comparable levels of MAPK activation, indicating the increase in cell transformation is through an additional oncogenic mechanism (data not shown).

To investigate factors contributing to the difference in focus formation between the two fusion breakpoints, abrogation of Aurora-A phosphorylation site or clathrin binding site by mutation to Ala was performed (Figure 13A). While abrogation of these two sites individually did lead to a significant decrease by Student's T test (*$p<0.05$), mutation of both of these sites within the same fusion protein did not lead to a significant reduction in focus formation (Figure 13B). This would indicate that association with clathrin or phosphorylation

by Aurora-A via TACC3's canonical pathway does not significantly contribute to cell transformation or the oncogenic mechanism of FGFR3-TACC3.

TACC3 has been shown to interact with ch-TOG regardless of Aurora-A phosphorylation. This interaction allows the TACC3-ch-TOG complex to stabilize microtubule dynamics by binding to growing microtubule ends during interphase (20). The binding domain of ch-TOG has been mapped to a break in the coiled-coil domain of TACC3, residues 678 to 688 in TACC3 WT. The implications of the interaction between ch-TOG and R3T3 have not been investigated. Previous studies have shown that deletion of the first 4 residues of this binding domain (RFEE) successfully disrupts the ch-TOG and TACC3 interaction and prevents TACC3 from localizing to growing microtubule ends (4,20). Deletion of these 4 residues in R3T3ex11 (ex11-Δch-TOG) yielded a 3-fold increase in focus formation relative to non-mutated R3T3ex11 (**$p<0.01$). Contrastingly, the same deletion in R3T3ex8 (ex8-Δch-TOG) did not yield a significant change in the amount of foci formed (Figure 13B). This could indicate that interaction of R3T3ex11 and ch-TOG inhibits the ability of R3T3 to convey cell transformation.

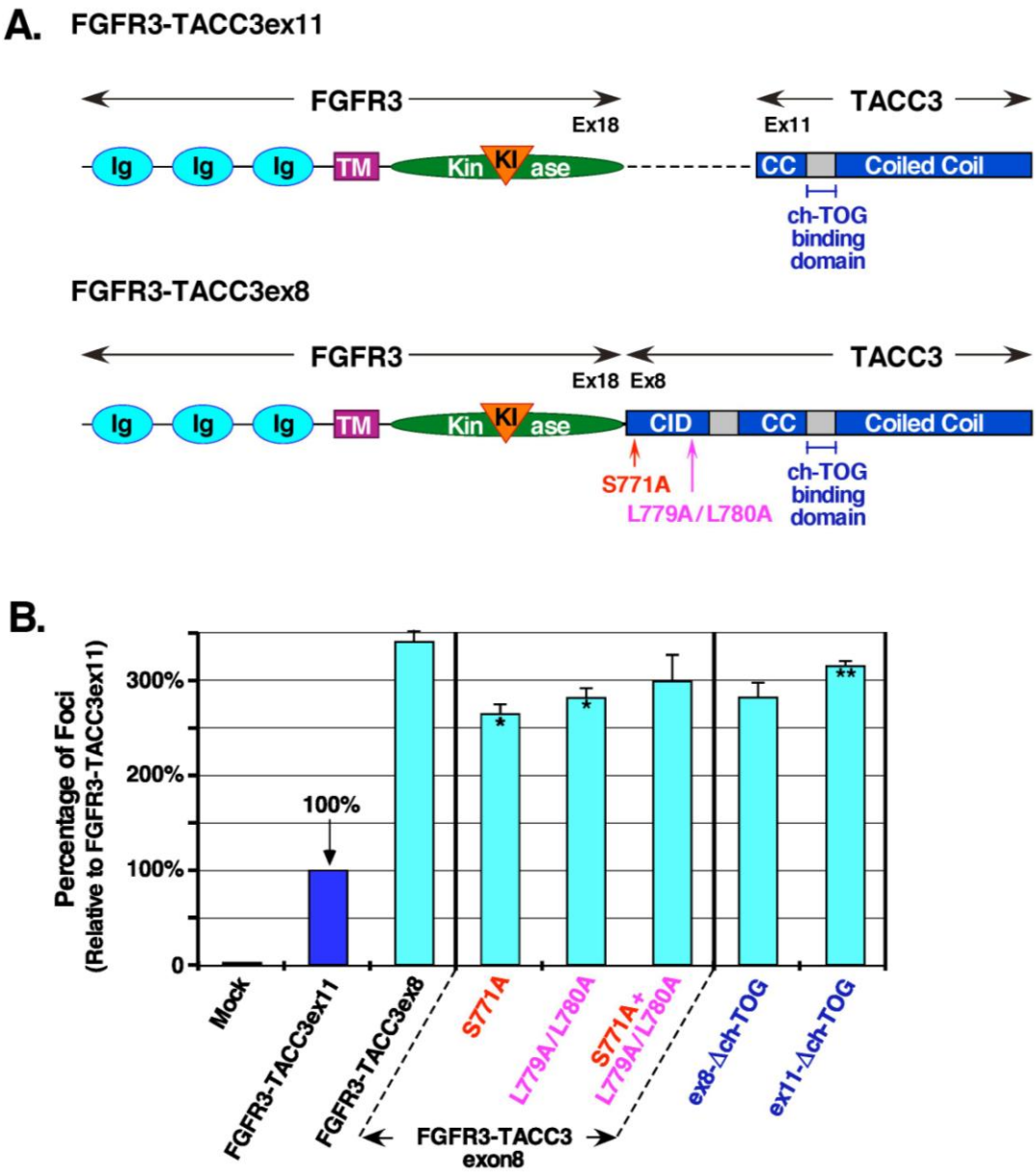

Figure13. TACC domain mutations and their contribution to cell transformation. **(A)** Schematic of FGFR3-TACC3ex11 and FGFR3-TACC3ex8 with ch-TOG binding domain indicated. Location of Aurora-A phosphorylation site (S771) and clathrin binding site (L779/L780) in FGFR3-TACC3ex8 are shown. **(B)** Transformation of NIH3T3 cells by the indicated constructs. Number of foci were scored, normalized by transfection efficiency, and quantitated relative to FGFR3-TACC3ex11 +/- SEM. Statistical analysis by Student's *t*-test identifies significant changes in focus counts (*$p<0.05$, **$p<0.01$). Assays were performed a minimum of three times per DNA construct.

FGFR3 kinase activity and MAPK pathway upregulation are key to oncogenicity

Our data indicates a distinct mechanism of action, in which cell transformation by R3T3 corresponds with MAPK pathway upregulation. A connection between these findings is further demonstrated by NIH3T3 cell focus assay, transfected with FGFR3-TACC3ex11, FGFR3-TACC3ex8 or FGFR3 K650E activating mutation and treated with increasing concentrations of either MEK1/2 inhibitor Trametinib (GSK1120212) or FGFR kinase inhibitor BGJ398 (Figure 14B, 14C). Both inhibitors individually block focus formation leading to antitumor effects, demonstrating two potential therapeutic strategies. Interestingly, differences in sensitivity to BGJ398 can be seen between the two most common breakpoints of the fusion protein, R3T3ex11 and R3T3ex8 (Figure 14C). Complete inhibition of focus formation was achieved with 2.5nM of BGJ398 in cells transfected with R3T3ex11, while complete inhibition of R3T3ex8 required 5nM of BGJ398 indicating that distinctive fusion breakpoints respond to the inhibitor differently. Similar effects were seen for the two fusion breakpoints treated with Trametinib (Figure 14B). Combination of BGJ398 and Trametinib was effective in reducing cell transformation, but with less sensitivity than expected, suggesting that these inhibitors are not additive in this assay (Figure 14D). For FGFR3 K650E, both inhibitors were successful in reducing focus formation, although with less sensitivity than seen with FGFR3-TACC3ex11 and FGFR3-TACC3ex8 (Figure 14B-D).

To further demonstrate the importance of the MAPK pathway, R3T3ex11 was transfected into HEK293T cells and treated with increasing concentrations of either BGJ398 or Trametinib. Both inhibitors effectively decrease phosphorylated MAPK, as determined by immunoblot (Figure 14A). Collectively, this data indicates a direct link between FGFR3 activation by fusion to TACC3, upregulation of the MAPK pathway, and cell transformation.

Figure 14. Effect of MEK and FGFR inhibitors on cell transformation and MAPK pathway. **(A)** HEK293T cells expressing FGFR3-TACC3ex11 were treated with Trametinib or BGJ398 at indicated concentrations and immunoblotted for phospho-MAPK (T202/Y204; top), MAPK (second panel), and FGFR3 (bottom). **(B)** Transformation of NIH3T3 cells expressing FGFR3-TACC3ex8, FGFR3-TACC3ex11 or FGFR3 K650E followed by treatment with indicated concentrations of MEK inhibitor (MEKi) Trametinib. **(C)** NIH3T3 cells expressing FGFR3-TACC3ex8, FGFR3-TACC3ex11 or FGFR3 K650E were treated with indicated concentrations of FGFR inhibitor (FGFRi) BGJ398. **(D)** NIH3T3 cells expressing indicated constructs were treated with a 1.25 nM Trametinib and varying concentrations of BGJ398. Number of foci were scored, normalized by transfection efficiency, and quantitated relative to FGFR3-TACC3ex8 +/- SEM. Assays were performed three times per DNA construct.

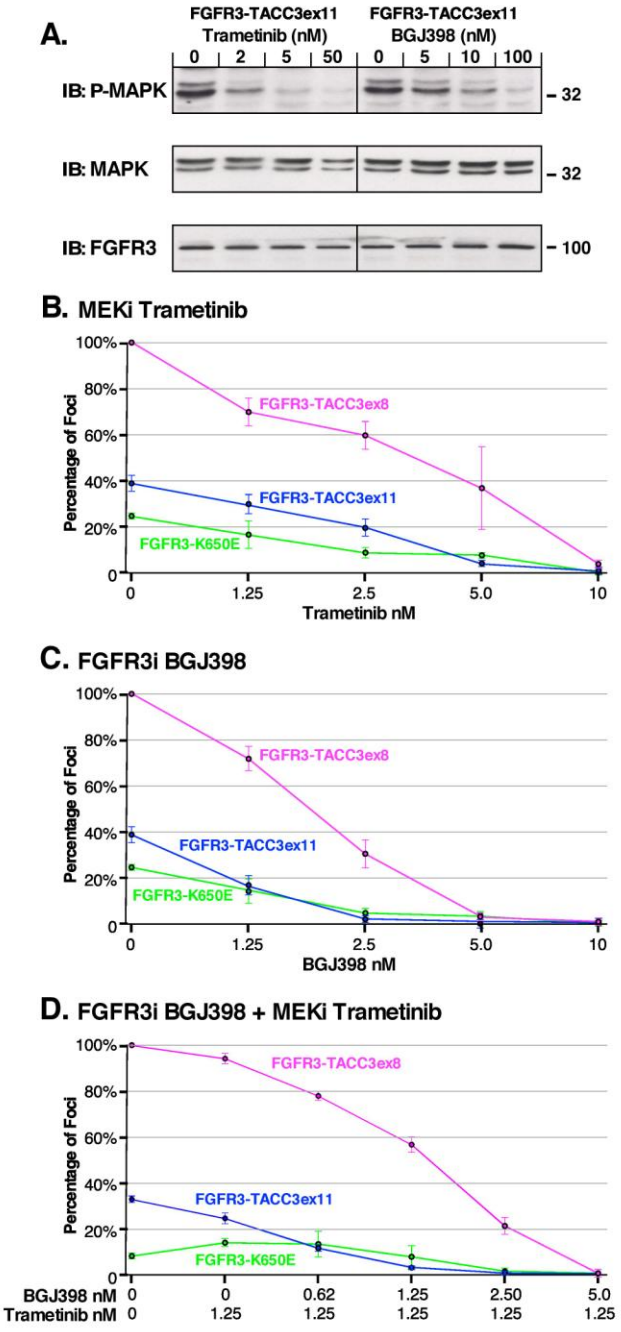
A.
FGFR3-TACC3ex11
Trametinib (nM)
0 2 5 50
FGFR3-TACC3ex11
BGJ398 (nM)
0 5 10 100
IB: P-MAPK
32
IB: MAPK
32
IB: FGFR3
100
B. MEKi Trametinib
Percentage of Foci
100%
80%
60%
40%
20%
0
FGFR3-TACC3ex8
FGFR3-TACC3ex11
FGFR3-K650E
0 1.25 2.5 5.0 10
Trametinib nM
C. FGFR3i BGJ398
Percentage of Foci
FGFR3-TACC3ex8
FGFR3-TACC3ex11
FGFR3-K650E
0 1.25 2.5 5.0 10
BGJ398 nM
D. FGFR3i BGJ398 + MEKi Trametinib
Percentage of Foci
FGFR3-TACC3ex8
FGFR3-TACC3ex11
FGFR3-K650E
BGJ398 nM 0 0 0.62 1.25 2.50 5.0
Trametinib nM 0 1.25 1.25 1.25 1.25 1.25

3.3 DISCUSSION

We have clarified the cellular location of R3T3 required to initiate cell transformation and overactivation of the canonical MAPK pathway. We have demonstrated that R3T3 must enter the secretory pathway and reach the plasma membrane to lead to oncogenic cell growth (Figure 9-12). Post-translational processing and plasma membrane localization is also required for the overactivation of MAPK in HEK293T cells. MAPK overactivation in HEK293T cells is only seen for our R3T3 derivatives that induce cell transformation in NIH3T3 cells, indicating a link between this pathway and cell transformation (Figure 10, 11). The essentiality of the MAPK pathway activation to cell transformation is demonstrated by the use of Trametinib, a MEK inhibitor, which blocks cell transformation by R3T3 in NIH3T3 cells. FGFR inhibitor BGJ398 is also able to block focus formation indicating kinase activity is required for cell transformation. Both inhibitors display unique levels of inhibition against different R3T3 fusion protein breakpoints, specifically R3T3ex11 and R3T3ex8, demonstrating the need for personalized treatment of cancers depending on the fusion breakpoint (Figure 14). Additionally, R3T3 contains TACC3 functional sites, the Aurora-A phosphorylation site, clathrin binding site and ch-TOG binding site. However, interaction with these proteins does not significantly contribute to the ability of R3T3 to induce cell transformation (Figure 13).

The appearance of R3T3 in vesicle-like structures by IF in NIH3T3 cells is an indicator of secretory vesicles en route to the membrane and that the fusion protein is capable of being inserted in the membrane as a type 1 integral membrane protein (Figure 9, 12). Upon reaching the membrane, internalization of the fusion protein could occur quickly due to its high level of activation without the need for ligand binding. Additionally, nuclear and

cytoplasmic localization of R3T3 does not contribute to cell transformation (Figure 9, 10). Our results indicate that in order to induce cell transformation in NIH3T3 cells, R3T3 must undergo post-translational processing via the secretory pathway, presumably reaching the membrane in order for cell transformation and MAPK pathway overactivation to occur. Prevention of entrance to the secretory pathway also blocks post-translational modifications, cell transformation and reduces MAPK overactivation (Figure 12). Myristoylation of R3T3 indicates the importance of plasma membrane association for inducing cell transformation and overactivation of canonical FGFR3 pathways. Previous studies by our lab and others have identified R3T3-induced overactivation of MAPK and PI3K/AKT pathways, which drives of cell proliferation leading to acceleration of the cell cycle and cancer progression (3,21). This indicates that R3T3 increases oncogenic growth by overactivation of cell growth pathways, not by an altered localization of R3T3 by the TACC3 domain to the nucleus, centrosome, or mitotic spindle, as previous studies have suggested (3,9,10).

Our work with R3T3ex8 demonstrates the fusion protein's oncogenic effects are not due to mitotic involvement via TACC3's canonical pathway. Abrogation of Aurora-A phosphorylation, clathrin and ch-TOG binding sites in R3T3ex8 displayed no significant change in focus formation demonstrating that interaction with these proteins does not effect the biological activity of R3T3ex8. In R3T3ex11, deletion of ch-TOG binding site increases focus formation, further demonstrating that interaction with ch-TOG does not contribute to oncogenic activity (Figure 13). Interaction between R3T3 and ch-TOG may in fact have an inhibitory role in cell growth. Previous studies have found that it is a removal of TACC3 from the mitotic spindle or a presence of R3T3 at the centrosomes that leads to chromosomal segregation errors during mitosis (9,10). However, incorrect cell division due to R3T3 does

not appear to be the key oncogenic driver in cells expressing this fusion. Consistently, studies analyzing the recruitment of other tyrosine kinases to the centrosome by fusion protein formation found centrosomal targeting to be unessential to oncogenic progression (22). We have demonstrated that involvement with TACC3 canonical interacting proteins is not the driving force of oncogenicity.

Interestingly, we demonstrate a difference in oncogenic activity between two breakpoints of R3T3 (R3T3ex8, R3T3ex11) and how those breakpoints respond differently to the same inhibitor treatment. The use of kinase inhibitors stresses the importance of personalized treatment not only for knowing if a specific RTK inhibitor is useful, but also how that inhibitor affects various fusion breakpoints or cancer genotypes. We demonstrated inhibition of MEK and FGFR as two potential therapeutic strategies for cancers that harbor the R3T3 rearrangement. This data is also supported by inhibition of MEK and FGFR in cervical cancer cell lines to reduce cell proliferation (23). Assessment of several FGFR inhibitors against R3T3 or other FGFR alterations in clinical trials is currently underway [clinicaltrials.gov]. A clinical trial enrolling patients with similar genomic alterations but various cancer types may prove useful in determining the efficacy of an inhibitor against different genomic backgrounds (23). The fact that inhibitors display different levels of effectiveness against varied genomic backgrounds is supported not only by our work but also by those exploring inhibition of R3T3 in concert with PI3K inhibition (24). This demonstrates a need for personalized cancer treatment and precision medicine.

This manuscript characterizes the need for R3T3 to be in the secretory pathway or at the cell membrane to induce cell transformation. The activation of the MAPK pathway is essential for cell transformation but involvement in the cell cycle via TACC3's canonical

pathways is not. We have shown that kinase inhibitors for MEK and FGFR are effective in blocking cell transformation and MAPK pathway upregulation. The need for precision medicine is evidenced by the different inhibitory effects these inhibitors have against various R3T3 breakpoints. The development of such personalized medicines will be essential in treating patients who harbor oncogenic drivers such as FGFR3-TACC3.

3.4 MATERIALS AND METHODS

DNA constructs

FGFR3-TACC3 gene was constructed as previously described (3). For derivation of plasma membrane- and nuclear-localizing constructs, myristoylation signal from c-Src or nuclear localization signal from *Xenopus* nucleoplasmin was utilized as previously described (18). Briefly, each sequence was ligated in place of the extracellular and transmembrane domains of FGFR3 resulting in fusion to residues 400 to 806 of FGFR3 or residues 400 to 953 in FGFR3-TACC3. For deletion of signal sequence of FGFR3, residue 2 to 22 were deleted following the site-directed mutagenesis protocol of Liu and Naismith. Deletion of ch-TOG domain followed the same protocol and deleted TACC3 residues RFEE, 792-795 in FGFR3-TACC3 or 678-681 in TACC3 (25). Aurora-A and clathrin mutations were achieved by Quikchange site-directed mutagenesis.

Cell culture

HEK293T cells were cultured in 10% FBS DMEM plus 1% penicillin/streptomycin in 10% CO2 at 37°C. NIH3T3 cells were maintained in 10% CS DMEM and 1% penicillin/streptomycin in 10% CO2 at 37°C.

Antibodies and reagents

Antibodies were purchased from: FGFR3 (B-9), FGFR3 (P18) from Santa Cruz Biotechnology; FGFR3 (OAAB11172) from Aviva Systems Biology; phospho-p44/42 MAPK (ERK 1/2; T202/Y204; D13.14.4E), p44/42 MAPK (ERK 1/2, 9102) from Cell Signaling Technology; EEA1 (610456) from BD Biosciences; Alexa Fluor 488 donkey anti-goat (A11055), Alexa Fluor 594 donkey anti-goat (A11058), Alexa Fluor 488 donkey anti-mouse (A21202) from Invitrogen; horseradish peroxidase (HRP) anti-mouse, HRP anti-rabbit, and Enhanced Chemiluminence (ECL) reagents were from GE Healthcare. Geneticin (G418) was from Gibco, and Lipofectamine 2000 was from Invitrogen. PNGase F was purchased from NEB (P0704S) and Pierce Protein A/G Magnetic Beads (88802) were purchased from Thermo Fisher. Inhibitors BGJ398 (S2183) and Trametinib (S2673) were purchased from Selleckchem.

Immunoprecipitation and immunoblot analysis

24 h before transfection, HEK293T cells were plated at $1x10^6$ cells/100-mm plate. Calcium phosphate method was used to transfect 3 μg plasmid DNA in 3% CO_2 as described previously (3). For immunoblot analysis, after cell starvation and collection, cells were lysed in RIPA buffer [50 mmol/l Tris-HCl (pH 8.0), 150 mmol/l NaCl, 1% TritionX-100, 0.5% sodium deoxycholate, 0.1% SDS, 50 mmol/l NaF, 1 mmol/l sodium orthovanadate, 1 mmol/l PMSF, and 10 mg/ml aprotinin]. Total protein concentration was measured using Lowry assay. For immunoprecipitation, cells were lysed in 1% NP40 Lysis Buffer [20 mmol/l Tris-HCl (pH 7.5), 137 mmol/l NaCl, 1% Nonidet P-40, 5 mmol/l EDTA, 50 mmol/l NaF, 1 mmol/l sodium orthovanadate, 1 mmol/l phenylmethylsulfonylfluoride (PMSF), and 10

mg/ml aprotinin]. Protein concentration was measured by Bradford assay. Lysates were incubated overnight with antibodies at 4°C with rocking. Complexes were collected with Pierce Protein A/G Magnetic Beads (88802) according to manufacturers protocol. For PNGase digest, PNGase F Protocol from manufacturer NEB was followed.

10% or 12.5% SDS-PAGE separated samples before transfer to Immobilon-P PVDF membranes (Millipore). Membranes were blocked in 3% bovine serum albumin (BSA)/TBS/0.05% Tween 20 or 3% milk/TBS/0.05% Tween 20. Immunoblotting was completed as previously described (26).

Immunofluorescence

Stable cell lines were created by transfecting NIH3T3 cells with Lipfectamine 2000 with FGFR3-TACC3 derivatives in pLXSN vector with Geneticin as the selectable marker. Cells were grown in 500 μg/ml G418 supplemented media for 14 days. Cell lines were created for all constructs except FGFR3 WT and ΔSS-FGFR3-TACC3. Stable cell lines were plated on 60mm plates with 6 coverslips at 1 x 10^5 cells per plate. Coverslips were PLL coated (Neuvitro, GG-12-1.5-PLL). 24 h after plating, cells were starved with 0% serum DMEM for additional 24 h. Coverslips were fixed with 4% paraformaldehyde/PBS for 10 min.

For FGFR3 WT and ΔSS-FGFR3-TACC3, NIH3T3 cells were plated at 2 x 10^5. 24 h after plating, cells were transfect with Lipofectamine 2000. 18-20 h after transfection, cells were refed with 10% CS DMEM for 6 h until media was changed to 0% serum DMEM for 24 h. Cells were fixed with 4% paraformaldehyde/PBS for 10 min.

For immunofluorescence staining, cells were permeabilized with 0.1% Triton X-100/PBS for 20 min, blocked with 5% BSA/PBS before incubation with primary antibodies, goat anti-FGFR3 (1:500 or 1:1500) or EEA1 (1:25). After washes, cells were treated with secondary antibodies, donkey anti-goat Alexafluor488 (1:2000), donkey anti-goat Alexafluor594 (1:1500), or donkey anti-mouse Alexafluor 488 (1:250). Nucleus is visualized with Hoechst 33342 (1μg/ml, 15 min). Cells were examined on Leica SP5 Confocal/MultiPhoton microscope (UC San Diego Neuroscience Core Facility). Images were processed with Leica LAS Lite and FIJI software.

Focus assay

NIH3T3 cells were plated at a density of $4x10^5$ cells/60-mm plates in 10% CS DMEM 24 h before transfection. Lipofectamine 2000 Reagent was used to transfect cells with 10 μg plasmid DNA. Cells were re-fed with DMEM 10% CS 22-24 h after transfection. Cells were split 1:12 onto duplicate 100-mm plates 24 h later with 2.5% CS DMEM. Cells were refed every 3-4 days. After 14 days, foci were scored, fixed with methanol, and Geimsa stained. Transfection efficiency was determined by Geneticin (G418, 0.5 mg/ml)-resistant colonies plated at 1:240 dilution. Number of foci were scored, normalized by transfection efficiency, and quantitated relative to FGFR3-TACC3 +/- SEM. Assays were performed a minimum of three times per DNA construct. Statistical analysis by Student's *t*-test identifies significant changes in focus counts and a two-tailed P-value of 0.05 was considered significant.

For inhibitor treatment, 24 h after splitting cells 1:12 onto 100-mm plates, cells were refed with 2.5% CS DMEM containing indicated concentrations of BGJ398 or Trametinib. Cells were refed with 2.5% CS DMEM with the same inhibitor concentrations every 3-4 days.

After 14 days, foci were scored, fixed with methanol, and Geimsa stained. Transfection efficiency was determined by Geneticin (G418, 0.5 mg/ml)-resistant colonies plated at 1:240 dilution.

3.5 ACKNOWLEDGMENTS

Chapter 3, in part is currently being prepared for submission for publication of the material, with the authors of Nelson KN, Meyer AN, Wang CG, Donoghue DJ. The dissertation author was the primary investigator and author of this material.

The author would also like to acknowledge Seth Field and Matt Buschman for immunofluorescence assistance and antibody gifts. Microscope facilities were supported by UC San Diego Neuroscience Microscope Shared Facility Grant (NS047101).

3.6 REFERENCES

1. Gallo, L. H., Nelson, K. N., Meyer, A. N. & Donoghue, D. J. Functions of Fibroblast Growth Factor Receptors in cancer defined by novel translocations and mutations. Cytokine and Growth Factor Reviews 2015. 13:53-6.

2. Carneiro BA, Elvin JA, Kamath SD, Ali SM, Paintal AS, Restrepo A, Berry E, Giles FJ, Johnson ML. FGFR3-TACC3: A novel gene fusion in cervical cancer. Gynecol. Oncol. Reports 2015. 06.05-11

3. Nelson KN, Meyer AN, Siari A, Campos AR, Motamedchaboki K, Donoghue DJ. Oncogenic Gene Fusion FGFR3-TACC3 Is Regulated by Tyrosine Phosphorylation. Mol. Cancer Res. 2016. 14(5):458-69.

4. Hood FE, Williams SJ, Burgess SG, Richards MW, Roth D, Straube A, Pfuhl M, Bayliss R, Royle SJ. Coordination of adjacent domains mediates TACC3-ch-TOG-clathrin assembly and mitotic spindle binding. J. Cell Biol. 2013. 202(3):463-78.

5. Hood, F. E. & Royle, S. J. Pulling it together: The mitotic function of TACC3. Bioarchitecture 2011. 1(3)16518

6. Nixon FM, Gutiérrez-Caballero C, Hood FE, Booth DG, Prior IA, Royle SJ. The mesh is a network of microtubule connectors that stabilizes individual kinetochore fibers of the mitotic spindle. Elife 2015,4.

7. Schmidt S, Schneider L, Essmann F, Cirstea IC, Kuck F, Kletke A, Jänicke RU, Wiek C, Hanenberg H, Ahmadian MR, Schulze-Osthoff K, Nürnberg B, Piekorz RP. The centrosomal protein TACC3 controls paclitaxel sensitivity by modulating a premature senescence program. Oncogene 2010. 29(46):6184-92.

8. Sansregret, L. & Swanton, C. The role of aneuploidy in cancer evolution. Cold Spring Harbor Perspectives in Medicine 2017.

9. Singh D, Chan JM, Zoppoli P, Niola F, Sullivan R, Castano A, Liu EM, Reichel J, Porrati P, Pellegatta S, Qiu K, Gao Z, Ceccarelli M, Riccardi R, Brat DJ, Guha A, Aldape K, Golfinos JG, Zagzag D, Mikkelsen T, Finocchiaro G, Lasorella A, Rabadan R, Iavarone A. Transforming fusions of FGFR and TACC genes in human glioblastoma. Science. 2012. 337(6099):1231-5.

10. Sarkar, S., Ryan, E. L. & Royle, S. J. FGFR3-TACC3 cancer gene fusions cause mitotic defects by removal of endogenous TACC3 from the mitotic spindle. Open Biol. 2017. 7(8).

11. Frattini V, Pagnotta SM, Tala, Fan JJ, Russo MV, Lee SB, Garofano L, Zhang J, Shi P, Lewis G, Sanson H, Frederick V, Castano AM, Cerulo L, Rolland DCM, Mall R, Mokhtari K, Elenitoba-Johnson KSJ, Sanson M, Huang X, Ceccarelli M, Lasorella A, Iavarone A. A metabolic function of FGFR3-TACC3 gene fusions in cancer. Nature 2018. 553(7687):222-227.

12. Daly C, Castanaro C, Zhang W, Zhang Q, Wei Y, Ni M, Young TM, Zhang L, Burova E, Thurston G. FGFR3-TACC3 fusion proteins act as naturally occurring drivers of tumor resistance by functionally substituting for EGFR/ERK signaling. Oncogene 2017. 36(4):471-481.

13. Gergely F, Karlsson C, Still I, Cowell J, Kilmartin J, Raff JW. The TACC domain identifies a family of centrosomal proteins that can interact with microtubules. Proc. Natl. Acad. Sci. 2000. 97(26):14352-7.

14. Peset, I. & Vernos, I. The TACC proteins: TACC-ling microtubule dynamics and centrosome function. Trends in Cell Biology 2008. 06.005

15. Robbins, J., Dilwortht, S. M., Laskey, R. A. & Dingwall, C. Two interdependent basic domains in nucleoplasmin nuclear targeting sequence: Identification of a class of bipartite nuclear targeting sequence. Cell 1991. (91)90.245

16. Kamps, M. P., Buss, J. E. & Sefton, B. M. Mutation of NH2-terminal glycine of p60src

prevents both myristoylation and morphological transformation. Proc. Natl. Acad. Sci. U. S. A. 1985. 82.14.4625

17. Aronheim A, Engelberg D, Li N, al-Alawi N, Schlessinger J, Karin M. Membrane targeting of the nucleotide exchange factor Sos is sufficient for activating the Ras signaling pathway. Cell 1994. (94) 78(6):949-61.

18. Webster, M. K. & Donoghue, D. J. Enhanced signaling and morphological transformation by a membrane-localized derivative of the fibroblast growth factor receptor 3 kinase domain. Mol. Cell. Biol. 1997.

19. Käll, L., Krogh, A. & Sonnhammer, E. L. L. A combined transmembrane topology and signal peptide prediction method. J. Mol. Biol. 2004. 03.016

20. Gutierrez-Caballero, C., Burgess, S. G., Bayliss, R. & Royle, S. J. TACC3-ch-TOG track the growing tips of microtubules independently of clathrin and Aurora-A phosphorylation. Biol. Open 2015. 10843

21. Yuan L, Liu ZH, Lin ZR, Xu LH, Zhong Q, Zeng MS. Recurrent FGFR3-TACC3 fusion gene in nasopharyngeal carcinoma. Cancer Biol. Ther. 2014. 15(12):1613-21.

22. Bochtler T, Kirsch M, Maier B, Bachmann J, Klingmüller U, Anderhub S, Ho AD, Krämer A. Centrosomal targeting of tyrosine kinase activity does not enhance oncogenicity in chronic myeloproliferative disorders. Leukemia 2012. 26(4):728-35.

23. Tamura R, Yoshihara K, Saito T, Ishimura R, Martínez-Ledesma JE, Xin H, Ishiguro T, Mori Y, Yamawaki K, Suda K, Sato S, Itamochi H, Motoyama T, Aoki Y, Okuda S, Casingal CR, Nakaoka H, Inoue I, Verhaak RGW, Komatsu M, Enomoto T. Novel therapeutic strategy for cervical cancer harboring FGFR3-TACC3 fusions. Oncogenesis 2018. 7(1):4.

24. Wang L, Šuštić T, Leite de Oliveira R, Lieftink C, Halonen P, van de Ven M, Beijersbergen RL, van den Heuvel MM, Bernards R, van der Heijden MS. A Functional Genetic Screen Identifies the Phosphoinositide 3-kinase Pathway as a Determinant of Resistance to Fibroblast Growth Factor Receptor Inhibitors in FGFR Mutant Urothelial Cell Carcinoma. Eur. Urol. 2017. 71(6):858-862.

25. Liu, H. & Naismith, J. H. An efficient one-step site-directed deletion, insertion, single and multiple-site plasmid mutagenesis protocol. BMC Biotechnol. 2008. 6750-8-91

26. Meyer, A. N., McAndrew, C. W. & Donoghue, D. J. Nordihydroguaiaretic acid inhibits an activated fibroblast growth factor receptor 3 mutant and blocks downstream signaling in multiple myeloma cells. Cancer Res. 2008. 08-0575

CHAPTER 4

Receptor Tyrosine Kinases: Translocation Partners in Hematopoietic Disorders

ABSTRACT

Receptor tyrosine kinases (RTKs) activate various signaling pathways and regulate cellular proliferation, survival, migration and angiogenesis. Malignant neoplasms often circumvent or subjugate these pathways by promoting RTK over-activation through mutation or chromosomal translocation. RTK translocations create a fusion protein containing a dimerizing partner fused to an RTK kinase domain, resulting in constitutive kinase domain activation, altered RTK cellular localization, upregulation of downstream signaling and novel pathway activation. While RTK translocations in hematological malignancies are relatively rare, clinical evidence suggests patients with these genetic abnormalities benefit from RTK-targeted inhibitors. This chapter presents a timely review of an exciting field by examining RTK chromosomal translocations in hematological cancers, particularly ALK, FGFR, PDGFR, RET, CSF1R and NTRK3 fusions, and current therapeutic options.

4.1 RECEPTOR TYROSINE KINASE TRANSLOCATIONS IN CANCER

Malignant genetic events can often be sorted in two categories: gene inactivation and gene activation or deregulation. Chromosomal translocations have been detected in all cancer

types and account for approximately 20% of all malignant neoplasms (1). Moreover, there is a close correlation between the translocations and the tumor phenotypes in which they occur (1).

Translocations usually arise by multiple erroneous double stranded breaks (DSB) in chromosomes which may occur for various reasons. The translocation also relies on spatial proximity of the DSB and the ability of the damaged region to rearrange in the nucleus, which can allow the chromosomes to incorrectly repair (2, 3). These translocations can result in a translatable fusion protein, some of which have oncogenic potential. While the percentage of chromosomal translocations in hematological disorders is generally lower than solid tumors (1.4% of all hematological cancers) their occurrence is nevertheless significant, especially in diseases such as chronic myeloid leukemia (CML), where 100% of cases harbor the t(9;22)(q34;q11) translocation, resulting in the gene fusion of breakpoint cluster region (*BCR*) and *ABL1*, a non-receptor tyrosine kinase (1). CML is a classic example of a translocation-driven disease that is amenable to treatment with a tyrosine kinase inhibitor (TKI). Imatinib, also known as Gleevec, has been widely used to treat CML and diseases presented by some of the fusion proteins discussed in this review. CML treatment with imatinib has ushered in a new era of rational drug development to identify TKIs with therapeutic value.

This chapter will focus on translocations involving receptor tyrosine kinases (RTKs) in hematological cancers (Figure 15). Of the 58 known human RTKs, the following have been identified as fusion partners resulting from chromosomal translocations in hematopoietic cancer cells: Anaplastic Lymphoma Kinase (ALK), Fibroblast Growth Factor Receptor (FGFR), Platelet-Derived Growth Factor Receptor (PDGFR), REarranged during Transfection (RET), Colony Stimulating Factor 1 Receptor (CSF1R) and Neurotrophic Tyrosine Kinase

Receptor Type 3 (NTRK3). As reviewed in this chapter, the most common hematopoietic cancer RTK translocations include the genes that encode ALK, FGFR and PDGFR. As discussed, these translocations results in cancers that present with different proliferative effects and treatment options, which highlights the importance of determining cancer-causing genetic alterations in patients.

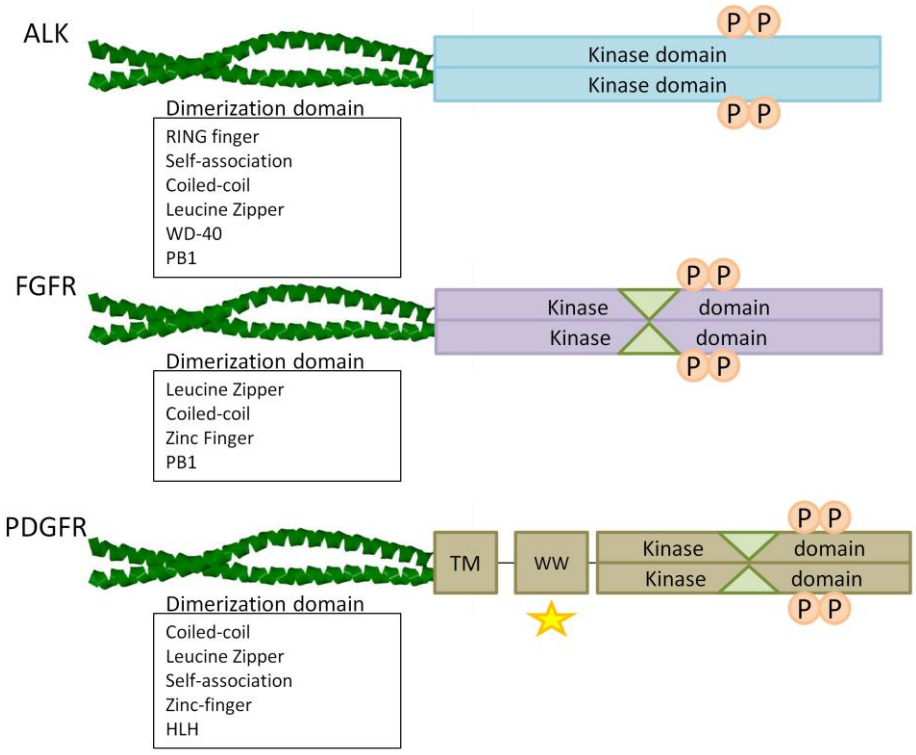

Figure 15. General Structural Schematic of RTK Fusion Proteins. Depicted are ALK, FGFR, and PDGFR fusion proteins, showing a generic dimerization domain for each. A star indicates an alternate breakpoint; a triangle indicates kinase insert domain; TM is transmembrane domain; WW is WW-like domain; P is phosphorylation site. Each of these RTK fusion proteins displays a dimerization domain fused to a C-terminal kinase domain provided by the respective RTK. The dimerization domains commonly associated with each RTK fusion protein are shown in the outlined box.

4.2 ALK TRANSLOCATIONS: FUSION PROTEINS INVOLVING THE ONLY RTK NAMED FOR A DISEASE

ALK regulation normally occurs by ligand binding to its extracellular domain. ALK expression occurs in the central and peripheral nervous system, primarily during development, as shown in multiple species, including human (4). After birth, as shown in mouse studies, ALK mRNA and protein levels reach a minimum in all tissues and remain at low levels in adult animals (4). As such, *Alk*-knockout (KO) mice display only mild behavioral phenotypes and ALK inhibitors appear to be well tolerated in patients presenting with ALK-positive lymphoma (4). ALK was initially identified in a human t(2;5)(p23;q35) translocation, fusing Nucleophosmin (NPM1) to ALK, expressing the fusion protein NPM-ALK leading to overexpression and constitutive activation of NPM-ALK kinase activity (5). This fusion protein occurs in 50-60% of anaplastic large cell lymphomas (ALCL) (6). The two main forms of ALCL are primary cutaneous, which affects the skin, and systemic, which can be divided into ALK-positive and ALK-negative subgroups. ALK fusion-positive ALCL tends to occur in younger patients and has a greater disease-free and overall survival rates than patients with ALK fusion-negative ALCL (7).

ALK fusion proteins are a recurring abnormality in ALCL, accounting for 2% of adult non-Hodgkin's lymphomas (NHL) and 13% of pediatric NHL (8). Some of the N-terminal ALK fusion partners in ALCL include clathrin heavy chain gene (CLTC), nucleophosmin (NPM), tropomyosin 3 (TPM3), TPM4, and TNF receptor-associated factor 1 (TRAF1) (4, 5, 7, 9). A complete list is shown in Table 2. All ALK fusion partners contain dimerization domains in the N-terminal fusion partner fused to the C-terminal ALK kinase domain (4) (Figure 15). While NPM-ALK is the most common translocation, 15-28% of ALK fusion-

positive cases display an alternative ALK fusion protein (5). ALK fusion proteins have also been detected in diffuse large B cell lymphoma (DLBCL), a rare but aggressive B cell lymphoma. The most common ALK translocation partner in this disease is CLTC (4). In addition, the translocation partner must exhibit active promoter activity, as ALK is not typically expressed outside of the nervous system or after birth (4, 6). The initiation of transcription of the fusion protein thus relies on the promoter sequence of the 5' fusion gene.

The most common hematological ALK fusion, NPM-ALK, arises from the translocation t(2;5)(p23;q35) between *ALK* on human chromosome 2 and *NPM1* on chromosome 5. The ALK tyrosine kinase domain becomes constitutively activated by formation of homodimers mediated by the self-associating domain of nucleophosmin (NPM). This dimerization is essential for oncogenic transformation by NPM-ALK, which is capable of transformation of various cell types, IL-3 independent proliferation of Ba/F3 lymphocytes by interaction with PLCγ, and activation of PI3K, AKT and STAT5. Additionally, a human lymphoblastic Jurkat T cell line stably expressing NPM-ALK displays PI3K and PLCγ-independent inhibition of doxorubicin-induced apoptosis (5).

Although the NPM1 domain is essential to oncogenic activity, this domain is also responsible for nuclear localization of the fusion protein, as its normal role is an RNA-binding nucleolar phosphoprotein. NPM-ALK is the only ALK fusion protein identified so far that displays nuclear localization (5, 10) (Figure 16). While NPM-ALK is detected in the cytoplasm and the nucleus, only the cytoplasmic fusion protein exhibits an active ALK kinase domain (10). The nuclear population is inactivated by dimerization with WT NPM1, which includes nuclear (NLS) and nucleolar localization signals (NuLS) not included in the NPM-ALK fusion protein. Formation of NPM-ALK/NPM1 heterodimers does not allow the ALK

kinase to become activated by trans-phosphorylation but does result in nuclear localization. Cytoplasmic expression appears to be a requirement for cell transformation, as this is the location of many other ALK fusion proteins (11) (Figure 16). Altered localization of a strongly activated tyrosine kinase may result in interaction with and phosphorylation of novel proteins and pathways.

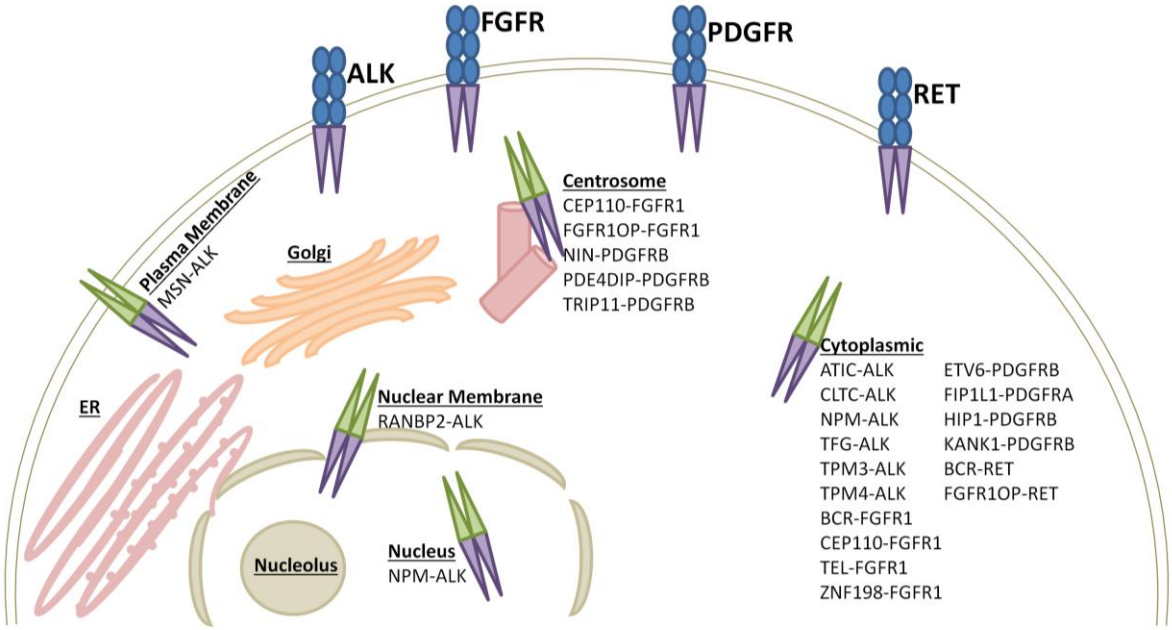

Figure 16. Cellular localization of various RTK fusion proteins. The identified localization of the parent RTKs and the resulting fusion proteins are shown. The RTK fusion proteins are depicted in their corresponding localization site. These RTK fusions may localize in the plasma membrane, centrosome, nuclear membrane, nucleus or cytoplasm.

Studies have emerged identifying spatial organization of the genome as a cause for recurring translocations in lymphomas (12). Specifically, in ALCL there are several dysregulated genes surrounding the chromosomal breakpoints for *ALK* and *NPM1*. In ALK fusion-negative cells, the breakpoint regions of the t(2;5) translocation are in close proximity

within the nucleus but not yet fused. This allows for the experimental generation of this translocation. The spatial proximity of NPM and ALK genes does not exist in non-ALCL cells, such as Jurkat and KE-37 (T-cell leukemia) cell lines (13). The t(2;5) translocation may not be the initial transformation event for the development of ALCL, a hypothesis supported by the fact that not all ALCL cases display this NPM-ALK fusion protein (13). Nevertheless, the presence of ALK fusion proteins in cancer cells leads to increased proliferation and cancer viability presenting a potential therapeutic target.

4.3 FGFR TRANSLOCATIONS: RELATIVELY RARE BUT PROVIDING IMPORTANT INSIGHTS

FGFRs are often aberrantly activated in cancer by overexpression, mutation, or translocation (14). In early hematopoietic cells, FGFRs are usually poorly expressed but as cells mature, FGFR expression generally increases. Human leukemia cells have been shown to express at least one type of receptor (FGFR1, FGFR3, or FGFR4) (15, 16).

FGFR1 is involved in 8p11 myeloproliferative syndrome (EMS), also known as stem cell leukemia-lymphoma syndrome (SCLL). EMS involves a chromosomal translocation that produces a dimerizing protein partner fused N-terminally to the kinase domain of FGFR1, normally encoded at the 8p11 locus. EMS is a rare, aggressive myeloproliferative disorder that can quickly progress into acute myeloid leukemia (AML) (17).

FGFR1 fusion partners in EMS are many and varied (Table 2), some of which include breakpoint cluster region (BCR), cut-like homeobox 1 (CUX1), FGFR1 oncogenic partner (FGFR1OP) and zinc finger 198 (ZNF198) (14). Interestingly, many of these partners also contain leucine zipper, leucine rich and coiled-coil domains. The contribution of a

dimerization domain by each fusion partner is necessary for the phosphorylation and activation of the FGFR1 kinase domain, resulting in a gain-of-function fusion protein. Additionally, given that biologically active translocations result from the in-frame fusion of two coding sequences that are normally distinct, this dictates that expression of the FGFR1 kinase domain in these fusions is reliant on the promoter sequence of the partner N-terminal protein.

In patients with EMS, the presence of an 8p11 translocation does not always mean an *FGFR1* rearrangement. Studies have identified a small subset of 8p11 translocations as rearrangements of the histone lysine acetyltransferase KAT6A (*KAT6A* gene), also located at the same chromosomal region as *FGFR1*. *KAT6A* has several translocation partners occurring in 2% of AML cases (18). FISH analysis is recommended for patients with EMS and 8p11 rearrangements in order to identify the correct translocation, allowing treatment with TKI therapeutics, such as ponatinib and dovitinib, for those expressing FGFR1 fusion proteins (19-21).

Though not as common, FGFR3 is also involved in translocations in hematopoietic disorders. Ets variant 6 (ETV6, previously known as TEL, translocation-ets-leukemia) is fused to FGFR3, and is found in T-cell lymphomas which progress to AML. Wild type (WT) ETV6 contains a helix-loop-helix (HLH) domain and serves as a transcription factor. The fusion of ETV6 to FGFR3 arises from the t(4; 12)(p16;p13) translocation and leads to the HLH domain of ETV6 fused to the transmembrane domain of FGFR3. The HLH domain is a dimerization domain, allowing constitutive activation of the FGFR3 kinase domain. The ETV6-FGFR3 fusion leads to IL-3 independent growth in Ba/F3 cells, activation of STAT3, STAT5, MAPK and PI3K, and exhibits cytoplasmic localization (22).

Multiple myeloma (MM) commonly contains a t(4;14) translocation between *IgH* promoter to the MMSET and FGFR3 genes, a translocation which does not result in a novel FGFR3 fusion protein but rather overexpression. MMSET overexpression is observed in all translocation-positive cases and FGFR3 overexpression in 70% of translocation-positive cases, which often exhibit activating point mutations in FGFR3 as well (14, 23). This overexpression leads to IL-6 independent growth in murine B9 cells, upregulated MAPK and PI3K signaling, and induced lymphoid malignancies in mice (15, 23). In chronic lymphocytic leukemia (CLL), rare translocations between FGFR3 and IgH (t(4;14)(p16;q32)) and IgL (t(4;22)(p16;q11.2) have been identified (14, 24). These types of translocations resulting in altered FGFR3 expression are medically important, yet they are distinct from the other translocations reviewed here which fuse two distinct reading frames to create a novel fusion protein.

The most commonly identified FGFR1 fusion protein is ZNF198-FGFR1, found in 48% of EMS cases (17). Endogenous ZNF198, also known as ZMYM2, contains a zinc finger related motif, a proline rich domain and a MYM domain, and is suggested to serve as a transcription factor (17, 25). The fusion of ZNF198 and FGFR1 arises from the t(8;13)(p11;q12) human translocation, in which *ZMYM2*, the gene encoding ZNF198 on chromosome 13, is fused 5' to *FGFR1* on chromosome 8. This fusion occurs in both myeloid and lymphoid cells, suggesting a multipotent hematopoietic progenitor cell origin. The N-terminal ZNF198 domain, particularly the proline rich domain, facilitates dimerization and activation of the FGFR1 kinase domain (17). The ZNF198-FGFR1 fusion is oncogenic, as shown by IL-3 independent Ba/F3 cell proliferation, increased tyrosine phosphorylation of STAT1 and STAT5, as well as activation of PLC-γ, PI3K/AKT and notch signaling pathways

(26-28). While WT ZNF198 displays nucleolar localization, the fusion protein exhibits cytoplasmic localization (25) (Figure 16).

BCR-FGFR1 is another commonly identified fusion protein in EMS. BCR contains a coiled-coil domain, possesses serine/threonine kinase activity and is a GTPase activating protein for Rac1 (29). BCR is more commonly found fused to ABL to form the BCR-ABL oncogene, where ABL encodes a non-receptor tyrosine kinase. This BCR-ABL fusion results from the Philadelphia chromosome, where exon 1 of BCR is fused to exon 2 of ABL, found in 95% of CML patients (30, 31). Cases positive for other fusion proteins, including BCR-FGFR1 fusion, are considered atypical CML (aCML). Both CML and aCML share similar phenotypes, as both are myeloproliferative disorders of hematopoietic stem cells, characterized by leukocytosis and a high number of immature granulocytes (30).

The fusion of BCR and FGFR1, resulting from a t(8;22) (p11;q11) translocation, occurs commonly in EMS but is also observed in AML and B-cell lymphomas. The BCR-FGFR1 fusion differs from the BCR-ABL fusion, as BCR exon 4 is fused to FGFR exon 9 (32). This fusion gives rise to a kinase-kinase fusion product, with the serine-threonine kinase domain of BCR fused to the tyrosine kinase domain of FGFR1. The kinase domain of FGFR1 becomes constitutively activated as a result of this fusion, leading to activation of STAT3, STAT5 and MAPK3/1 pathways and IL-3-independent proliferation of Ba/F3 cells (33). The BCR-FGFR1 fusion protein localizes to the cytoplasm, but it is unknown what role this plays in its oncogenicity (34) (Figure 16). The discovery and further characterization of FGFR fusion proteins arising from translocations is vital to determine the extent of signaling and proliferation that occurs due to different fusion partners.

Table 2: RTK Fusion Proteins in Hematological Cancers

C-terminal fusion partner	N-terminal fusion partner	Protein name	N-terminal domain	Cancer type	Pathway	Refs
ALK: kinase domain	ATIC	Aminoimidazole Carboxamide Ribonucleotide Transformylase	Self-association	ALCL	STAT	[55]
	CLTC	Clathrin, Heavy Chain	Self-association	ALCL, DLBCL, BPDCN, LBCL	STAT	[80–82]
	MSN	Moesin	FERM	ALCL	TBD	[83]
	MYH9	Myosin, Heavy Chain 9	Coiled-coil	ALCL	TBD	[84]
	NPM	Nucleophosmin	Self-association	ALCL, DLBCL	PI3K, AKT, STAT, JUNB	[4,10,55]
	RANBP2	RAN Binding Protein 2	Leucine zipper	AMMoL, AML, DLBCL	TBD	[85–87]
	RNF213/ALO17	Ring Finger Protein 213/ALK Lymphoma Oligomerization partner on chromosome 17	Ring finger	ALCL	TBD	[80]
	SEC31A	SEC31 Homolog A	WD-40	DLBCL	AKT, MAPK, STAT	[88]
	SQSTM1	Sequestosome 1	PB1	LBCL	STAT	[89]
	TFG	TRK-Fused Gene	Coiled-coil	ALCL	STAT, PLCγ	[55]
	TPM3	Tropomyosin 3	Coiled-coil	ALCL	PI3K, AKT, STAT	[55]
	TPM4	Tropomyosin 4	Coiled-coil	ALCL	TBD	[90]
	TRAF1	TNF Receptor-Associated Factor 1	Coiled-coil	ALCL	NFκB	[91]
CSF1R: kinase domain	MEF2D	Myocyte Enhancer Factor 2D	MADS-box	ALL	TBD	[92]
FGFR1: kinase domain	BCR	Breakpoint Cluster Region	Ser/Thr kinase, coiled-coil	EMS	STAT, MAPK	[29,33]
	CEP110	Centriolin	Leucine zipper, coiled-coil	EMS	TBD	[14]
	CPSF6	Cleavage and Polyadenylation Specific Factor 6	RNA recognition motif	EMS	TBD	[14]

Nelson KN, Peiris MN, Meyer AN, Siari A, Donoghue DJ. Receptor Tyrosine Kinases: Translocation Partners in Hematopoietic Disorders. Trends in Molecular Medicine. 2017.

Table 2: RTK Fusion Proteins in Hematological Cancers. Continued

C-terminal fusion partner	N-terminal fusion partner	Protein name	N-terminal domain	Cancer type	Pathway	Refs
	CUX1	Cut Like Homeobox 1	Coiled-coil	EMS	STAT, RPS6K	[14,93]
	FGFR1OP	Fibroblast Growth Factor 1 Oncogenic Partner	Leucine-rich	EMS	STAT, MAPK	[14,17]
	HERV-K	Human Endogenous Retrovirus Group K 6	HERV-K Rec open reading frame	EMS	TBD	[14]
	LRRFIP1	Leucine-Rich Repeat (in FLII) Interacting Protein 1	Coiled-coil	EMS	TBD	[14,94]
	MYO18A	Myosin XVIIIA	Coiled-coil	EMS	TBD	[14]
	NUP98	Nucleoporin 98kDa	Coiled-coil	EMS	TBD	[14]
	RANBP2	RAN Binding Protein 2	Leucine zipper	EMS	TBD	[14,95]
	SQSTM1	Sequestosome 1	PB1	EMS	TBD	[96,97]
	TPR	Translocated Promoter Region, Nuclear Basket Protein	Coiled-coil	EMS	TBD	[14]
	TRIM24	Tripartite Motif Containing 24	Coiled-coil	EMS	TBD	[14]
	ZNF198	Zinc Finger MYM-Type Containing 2	Zinc finger motif, proline-rich domain	EMS	STAT, PLCγ, Notch, PI3K/AKT	[17,27,28]
FGFR3: TM kinase domain	ETV6	Ets Variant 6	HLH	AML	STAT, PI3K, MAPK	[98]
NTRK3: kinase domain	ETV6	Ets Variant 6	HLH	AML	MAPK	[98]
PDGFRA: kinase domain	BCR	Breakpoint Cluster Region	Ser/Thr kinase, coiled-coil	aCML/T-ALL/CEL	TBD	[39,40]
	CDK5RAP2	CDK5 Regulatory Subunit Associated Protein 2	Coiled-coil	CEL	TBD	[99]
	EVT6/TEL	Ets Variant 6	HLH	CEL	TBD	[41]
	FIP1L1	FIP1-Like 1	Self-association	CEL, HES, Eos-MPN, AML, T-cell NHL	MAPK, STAT, NFκB	[50,59,61,100]
	FOXP1	Forkhead Box P1	Zinc-finger	MPN	TBD	[101]
	KI5B	Kinesin family member 5B	Coiled-coil	IHES	TBD	[102]
	STRN	Striatin	Coiled-coil	CEL	TBD	[41]

Table 2: RTK Fusion Proteins in Hematological Cancers, Continued

C-terminal fusion partner	N-terminal fusion partner	Protein name	N-terminal domain	Cancer type	Pathway	Refs
PDGFRB: kinase domain	c6orf204/ CEP85L	Centrosomal Protein 85 kDa-Like	Coiled-coil	Precursor T lymphoblastic lymphoma/MPN	TBD	[103,104]
	NIN	Ninein	Coiled-coil	MPN	TBD	[105]
	PRKG2	Protein Kinase, CGMP-Dependent, Type II	Coiled-coil	MPN	TBD	[106]
PDGFRB: TM kinase domain	CEV14/TRIP11	Thyroid Hormone Receptor Interactor 11	Leucine zipper	CMML, AML, T-ALL, APL	TBD	[107,108]
	DTD1	D-Tyrosyl-TRNA Deacylase 1	Unknown	MPN	TBD	[109]
	ERC1	ELKS/RAB6-Interacting/CAST Family Member 1	Coiled-coil	AML	TBD	[110]
	EVT6/TEL	Ets Variant 6	HLH	CMML, HES, aCML, AML (APL)	STAT, MAPK, PI3K, NFκB	[42,43,59]
	GIT2	G-Protein-Coupled Receptor Kinase Interacting ArfGAP 2	Ankyrin protein interaction motif	MPN	TBD	[106]
	GPIAP1/ CAPRIN1	Cell Cycle Associated Protein 1	Coiled-coil	MPN	TBD	[106]
	H4/D10S170/ CCDC6	Coiled-Coil Domain Containing 6	Leucine zipper	aCML, CMML	TBD	[111,112]
	HCMOGHT1/ SPECC1	Sperm Antigen with Calponin Homology and Coiled-Coil Domains 1	Coiled-coil	MPN	TBD	[113]
	HIP1	Huntingtin Interacting Protein 1	Leucine zipper	CMML	SHIP1, STAT	[64,65]
	KANK1	KN Motif And Ankyrin Repeat Domains 1	Coiled-coil; KOD	MPN	STAT, MAPK, PLCγ	[42,63]
	KIAA1509/ CCDC88C	Coiled-Coil Domain Containing 88C	Coiled-coil	MPN	TBD	[109]
	MYO18A	Myosin 18A	Coiled-coil	MPN	TBD	[114]

Table 2: RTK Fusion Proteins in Hematological Cancers, Continued

C-terminal fusion partner	N-terminal fusion partner	Protein name	N-terminal domain	Cancer type	Pathway	Refs
	NDE1	NudE Neurodevelopment Protein 1	Coiled-coil	CML	TBD	[115]
	PDE4DIP/ myomegalin	Phosphodiesterase 4D Interacting Protein	Coiled-coil	MPN	TBD	[116]
	RAB5A	RAS-Associated Protein RAB5A	Coiled-coil	CMML	TBD	[117]
	RABEP1	Rabaptin, RAB GTPase Binding Effector Protein 1	Coiled-coil	CMML	TBD	[117]
	TP53BP1	Tumor Protein P53 Binding Protein 1	Coiled-coil	aCML	TBD	[118]
RET: kinase domain	FGFR1OP	Fibroblast Growth Factor 1 Oncogenic Partner	Leucine-rich domain	CMML	PI3K, STAT	[119]
	BCR	Breakpoint Cluster Region	Ser/Thr kinase, coiled-coil	CMML	MAPK, STAT, AKT	[119]

[a]Abbreviations: aCML, atypical chronic myeloid leukemia; AML, acute myeloid leukemia; AMMoL, acute myelomonocytic leukemia; APL, acute promyelocytic leukemia; BPDCN, blastic plasmacytoid dendritic cell neoplasm; CEL, chronic eosinophilic leukemia; CMML, chronic myelomonocytic leukemia; DLBCL, diffuse large B cell lymphoma; Eos-MPD, eosinophilia-associated myeloproliferative disorders; HES, hypereosinophilic syndrome; HLH, helix-loop-helix; IHES, idiopathic HES; JUNB, Jun B proto-oncogene; LBCL, large B cell lymphoma; MAPK, mitogen-activated protein kinase; MPN, myeloproliferative neoplasms; NFκB, nuclear factor kappa B; PI3K, phosphatidylinositide 3-kinase; PLCγ, phospholipase C gamma 1; RPS6K, ribosomal protein S6 kinase beta-1; SHIP1, inositol polyphosphate-5-phosphatase D; STAT, signal transducer and activator of transcription; T cell NHL, lymphoblastic T cell non-Hodgkin lymphoma; TM, transmembrane domain.

4.4 PDGFR TRANSLOCATIONS: FUSION PROTEINS AND THEIR CANCERS

Similar to other hematopoietic translocations, PDGFR fusion proteins express the RTK kinase domain as the C-terminal fusion protein partner whose expression is now reliant on the promoter of the gene encoding the N-terminal fusion protein. Unlike ALK receptors, WT PDGFRs are expressed at constant low levels in hematopoietic human and mouse cells (35). However, as shown using murine hematopoietic chimeras reconstituted with *pdgfrb*(-/-) fetal liver cells, PDGFR expression is not required for normal hematopoiesis (36).

Although translocations creating PDGFR fusion proteins is low, a number of different fusion protein partners have been reported. Translocations have been reported that result in PDGFRA fused to BCR, FIP1-like 1 (FIP1L1) and striatin (STRN). For fusions with PDGFRB, many fusion partners have been reported including myosin 18A (MYO18A), Rab5A, tropomyosin 3 (TPM3) and others (Table 2). Both PDGFRA and PDGFRB have been found fused to ETV6. In myelodysplastic/myeloproliferative neoplasms (MDS/MPNs), 1.8% of cases appear to contain translocations encoding PDGFRB fusions proteins (37). As with ALK and FGFR translocations, most of these fusion partners contain dimerization domains which are essential for constitutive activation of the PDGFR receptor -- an exception being FIP1L1-PDGFRα.

For WT PDGFR, dimerization alone is not enough to constitute receptor activation. Activation of the kinase domain also relies on reorganization and homotypic interaction of the extracellular Ig-like domain D4 between PDGFR receptors (38). However, in PDGFR fusion proteins, the extracellular domains are no longer present, yet the kinase domain is constitutively active (Figure 15). This indicates that an altered mechanism of activation which relies on the fused N-terminal dimerization domain is taking place.

One potentially interesting rearrangement results in the kinase domain of BCR fused to the kinase domain of PDGFRα, similar to the BCR-FGFR1 and BCR-ABL fusion proteins. This t(17;13) translocation between BCR and PDGFRA was reported in atypical CML (aCML), CEL, B/myeloid mixed phenotype leukemia and T acute lymphoblastic leukemia (T-ALL). Only a few cases of BCR-PDGFRα have been reported with varying breakpoints: exon 7, 12, or 17 for BCR fused to exon 12 or 13 of PDGFR (39, 40). In order to determine the extent of activation, signaling and proliferative differences contributed by the different fusion partners, a molecular analysis of BCR-PDGFRα with BCR-FGFR1 or BCR-ABL, comparing their relative extents of oncogenicity or clinical disease, may prove interesting.

The most common PDGFRB fusion partner is ETV6, defined by t(5;12)(q33;p13) and identified in chronic myelomonocytic leukemia (CMML). ETV6 has also been found fused to PDGFRA in one patient (41). The ETV6 domain contains a HLH dimerization domain which allows for ligand-independent activation of the PDGFR receptor. Increased cell proliferation and transformation demonstrated by ETV6-PDGFRβ is reliant on increased fusion protein stability by reduced ubiquitination and increased STAT5 activation in Ba/F3 cells and mouse models (42). Murine stem cell differentiation is induced by the ETV6-PDGFRβ fusion protein through MAPK and STAT5 pathway activation (43).

The ETV6-PDGFRβ fusion protein, along with FIP1L1-PDGFRα and ZNF198-FGFR1, displays increased stability by evading ubiquinitation and degradation (44). To prevent overactivation, RTKs are often controlled by proteosomal degradation, negative feedback signals and, upon ligand binding, the complex is internalized and degraded. Additionally, the PDGFR juxtamembrane domain acts as an inhibitory domain by interacting with and inhibiting the kinase domain when ligand is not present (42, 45). The C-terminal tail

of PDGFR also functions as an allosteric inhibitor of the kinase domain (46). Despite these processes, overactivation occurs through PDGFR translocations in myeloid malignancies (47).

Most of the PDGFR fusion proteins, including ETV6-PDGFRβ, involve a breakpoint occurring just before the transmembrane (TM) domain of PDGFRβ, although some contain a breakpoint in between the transmembrane and kinase domains (Table 2, Figure 15). Experimental deletion of the transmembrane domain in the ETV6-PDGFRβ fusion does not hinder dimerization or kinase domain activation, but does result in a decrease of cell proliferation and STAT5 and MAPK activation in Ba/F3 cells, suggesting that cell transformation relies not only on activation, but also proper alignment of the kinase domain (42). The inhibitory effects that the intracellular-juxtamembrane domain and C-terminal tail have on the WT receptor are lost or subdued in this fusion protein.

Another common PDGFRα fusion protein is FIP1L1-PDGFRα discovered in myeloproliferative diseases associated with hypereosinophilia, sometimes referred to as chronic eosinophilic leukemia (CEL). This fusion protein is estimated to occur in 10-20% of eosinophilia cases (37). This chromosomal rearrangement is caused by an 800-kb deletion in chromosome 4 (del(4)(q12g12)), a segment including the cysteine-rich hydrophobic domain 2 (*CHIC2*) locus (48). This fusion protein poses an exception to previously discussed RTK fusion proteins, as FIP1L1 is dispensable for PDGFRα dimerization, as shown by Ba/F3 cell transformation assays and by murine bone marrow transplantation using transduced bone marrow cells with various deletion constructs of FIP1L1-PDGFRα, where all or most of FIP1L1 was deleted (49). However, the FIP1 motif is involved in protein-protein interactions and is essential for homodimer formation of a fusion protein between FIP1L1 and retinoic acid receptor α (FIP1L1-RARA) in leukemia. The FIP1L1 domain does play a role in human

progenitor cell proliferation and contains two phosphotyrosine sites that may provide protein binding sites (50). The IL-3 independent proliferation of Ba/F3 cells and the dispensability of the FIP1L1 domain was also recently confirmed by CRISPR/Cas genome editing in Ba/F3 cells to create the fusion at endogenous levels (51).

The breakpoint of FIP1L1-PDGFRα lies within the juxtamembrane domain of PDGFRα and disrupts an inhibitory WW-like domain, which may be the key to constitutive receptor activation and transforming potential. The WW-like domain contains two conserved tryptophan residues in the juxtamembrane domain. When truncated by fusion protein formation, absence of one of the tryptophan residues results in constitutive receptor activation (49). The disruption of this domain has been noted in BCR-PDGFRα and STRN-PDGFRα (41, 49). Fusion proteins with the transmembrane and juxtamembrane domains intact most likely require an alternative dimerization and activation mechanism provided by the N-terminal fusion partner. Although PDGFR translocations are relatively rare compared to other hematological translocations, their existence potentially provides an effective therapeutic target for cancer patients.

4.5 SIGNALING ALTERATIONS RESULTING FROM RTK TRANSLOCATIONS

ALK and ALK Fusions

Aberrant expression of highly active RTK kinases in tissues will result in novel pathway activation, and may present novel therapeutic possibilities. For instance, WT ALK results in the activation of multiple pathways including PLCγ, JAK/STAT, PI3K/AKT, JUNB, MAPK, and MYCN. ALK activation of ERK and PI3K can lead to MYCN expression, and high MYCN levels have been linked to neuroblastoma oncogenesis (52, 53).

The NPM-ALK fusion protein specifically activates JUNB, Y-box transcription factor (YBX1), BCL2A1, matrix metalloproteinase 9 (MMP9), CDKN2A and hypoxia-inducible factor 1α (HIF1A) as shown in various studies using either Ba/F3 cells or ALK-positive ALCL human cell lines (4).

NPM-ALK downregulates STAT1 in ALCL cells. STAT1 is known to function as a tumor suppressor in some cancer cell types and phosphorylation of STAT1 at Y701 leads to its proteasomal degradation. Tumor suppression in ALCL cells can be restored by increasing STAT1 by transfection with a constitutively activated STAT1 expression plasmid (54). A correlation is seen between invasive cell ability and the PI3K/AKT pathway activation, implicated in cell migration. For the fusion proteins NPM-ALK, TPM3-ALK, TFG-ALK, CLTC-ALK and ATIC-ALK, their ability to stimulate PI3K and AKT phosphorylation as shown by immunoblotting correlates with their transendothelial migration ability (55). Among these fusion proteins, ATIC-ALK displays the highest phosphorylation of STAT3 in mouse NIH3T3 cells (55).

NPM-ALK, TPM3-ALK, TFG-ALK, CLTC-ALK and ATIC-ALK fusion proteins result in cell transformation, proliferation, invasion, transendothelial cell migration and tumor development in nude mice (55, 56). In general, the oncogenic effects of these proteins increase as expression levels increase; an exception is provided by the TPM3-ALK fusion protein, for which increased expression results in lower proliferation rates in NIH3T3 cells but increased invasiveness (55). Confocal microscopy and fractionation of NIH3T3 cells showed TPM3-ALK fusion proteins localized to the cytoskeletal fraction; thus, this effect may be due to the role of TPM3 as an actin filament stabilizer, potentially altering cell shape and movement (56). Of note, TPM3-ALK, TFG-ALK, CLTC-ALK and ATIC-ALK all

display cytoplasmic localization, while NPM-ALK displays both nuclear and cytoplasmic localization (55, 56) (Figure 16).

FGFR and FGFR Fusions

WT FGFRs result in the activation of multiple signaling pathways including PLCγ, PI3K/AKT, MAPK and STAT, and are important in cell proliferation and differentiation as demonstrated in mouse models (57). However, the signaling differences between WT FGFRs and FGFR fusion proteins are not completely understood. Both the ZNF198-FGFR1 and BCR-FGFR1 fusion proteins induce aberrant signaling through the dimerization of the kinase domain of FGFR1. Activation of FGFR1 through the ZNF198-FGFR1 fusion leads to phosphorylation or activation of FGFR1 targets such as STATs, PI3K, PLC-γ, AKT and MAPK as shown by expression in Ba/F3 cells. In addition, ZNF198-FGFR1 is able to activate a pathway involving plasminogen activator inhibitor 2 gene (PAI-2/SERPINB2), which is not observed in native FGFR1 signaling. The PAI-2 gene induces resistance to TNFα, which could suggest an alternative pathway contributing to the oncogenic potential of the ZNF198-FGFR1 fusion, as shown by assays in HEK293 and Ba/F3 cells (58). The BCR-FGFR1 fusion is dependent on adaptor protein Grb2. This translocation binds Grb2 through BCR Y177, and was shown to induce CML-like leukemia in mice. However, BCR-FGFR1 with a mutated Y177 lacks Grb2 binding and causes an EMS like disease (34).

PDGFR and PDGFR Fusions

Upon activation by ligand binding, PDGFRs bind various signal transduction molecules via phosphotyrosine interaction motifs such as SH2 or PTB, resulting in activation

of downstream signaling. Some key interacting proteins include PI3K, PLCγ, Src family tyrosine kinases, SHP2 tyrosine phosphatase and STAT proteins (47).

Although few PDGFR fusion proteins have been analyzed for biological function, a study analyzing ETV6-PDGFRβ and FIP1L1-PDGFRα found that NFκB activation was required for human CD34(+) cell proliferation and differentiation with a bias towards eosinophil lineage (59). These fusions play a large role in human hypereosinophilia development in the absence of growth factors IL-3 and IL-5, whose expression usually supports hematopoietic stem cell differentiation to form eosinophils. IL-5 expression is increased in cells expressing these PDGFR fusions and, in patients, an IL-5 gene polymorphism was linked to a more severe disease development as shown by eosinophil counts and increased tissue infiltration (59).

Multiple tyrosine phosphorylation sites (Y579/581) in PDGFRβ of ETV6-PDGFRβ are responsible for myeloproliferative neoplasm (MPN) development in mice. Mutation to phenylalanine in Y579F/Y581F mutants results in development of T-cell lymphoma, but not MPN (60). For FIP1L1-PDGFRα, it was identified that tyrosine 720 of PDGFRα is critical for SHP2 recruitment, which results in MAPK activation and Ba/F3 hematopoietic cell transformation. Interestingly, SHP2 recruitment represents an altered mechanism compared to WT PDGFR, as cell proliferation and MAPK activation occurs regardless of SHP2 interaction with WT receptor, as shown by expression of the human FIP1L1-PDGFRα fusion protein in murine Ba/F3 cells (61). Indeed, SHP2 is involved in JAK/STAT, PI3K, MAPK and other signaling pathway regulation, and has been implicated in leukemogenesis caused by mutations in KIT and FLT3 receptors (61).

Both ETV6-PDGFRβ and FIP1L1-PDGFRα display cytosolic expression and result in the activation of STAT1, STAT3 and STAT5 (Figure 16, Figure 17). STAT5 plays an important role in myeloproliferation by PDGFR fusion proteins as shown in both human and murine cell lines (59, 61, 62). STAT5 activation was also demonstrated by KANK1-PDGFRβ fusion protein, despite an inactivity of JAK2 and inability of JAK inhibitor to affect cell growth. This fusion protein is found in MPN and arises because of a t(5;9) translocation that results in KN Motif and Ankyrin Repeat Domains (KANK1) fused to PDGFRB. KANK1 contributes three coiled-coil domains and an oligomerization domain, both of which are required for cell proliferation and upregulation of signaling (63). Interestingly, this fusion protein was shown to exist as a homotrimer, of which either the coiled-coil or the oligomerization domain may be present to allow for this motif formation (63). KANK1-PDGFRβ also activates PLCγ and MAPK pathways, and displays cytosolic expression as shown in human and murine cell lines (63) (Figure 16, Figure 17).

STAT5 activation was also shown to be essential for Ba/F3 cell transformation by the fusion protein Huntingtin Interacting Protein (HIP1)-PDGFRβ (64). This fusion protein also co-localizes with Src Homology 2-containing Inositol 5-Phosphatase (SHIP1) and displays cytosolic localization as shown in human HEK293T cells (64) (Figure 16). As SHIP1 is only expressed in hematopoietic tissues and developing spermatogonia, SHIP1 could serve as a potential therapeutic target (65).

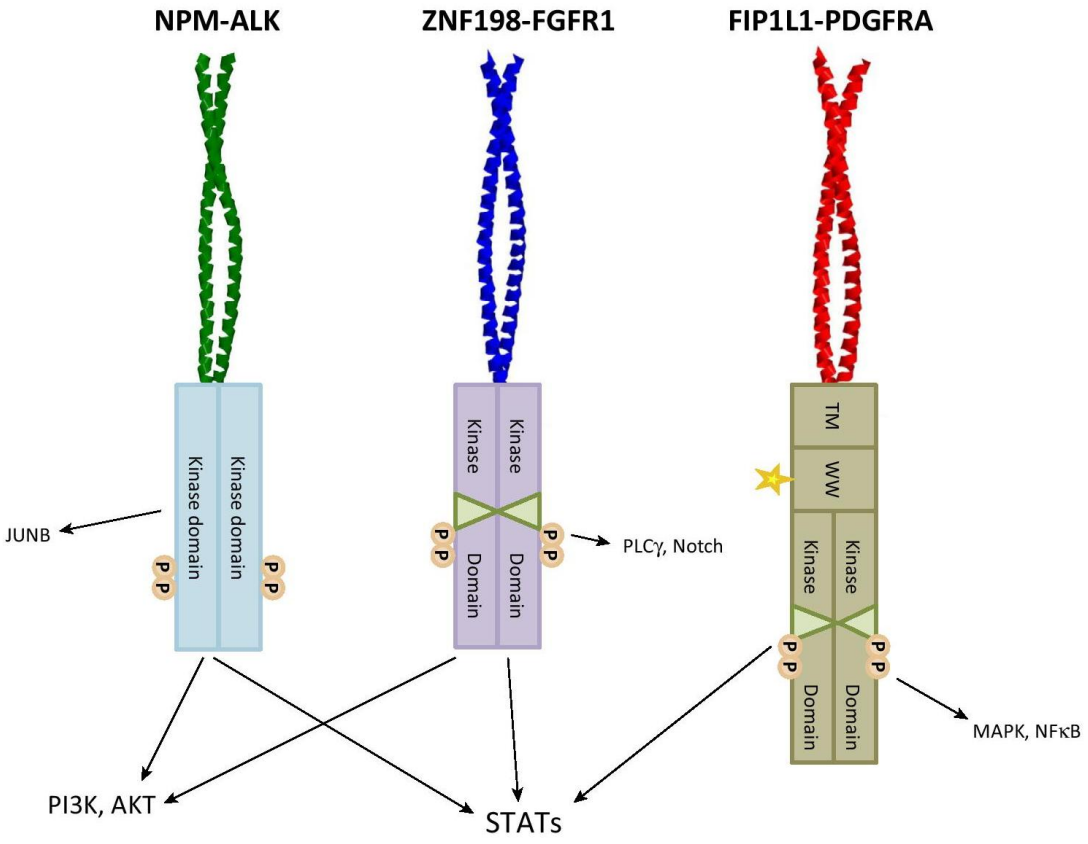

Figure 17. Major signaling pathways activated by common RTK fusion proteins. Activation of STAT signaling is a commonly seen occurrence. The arrows indicate activated pathways; the activation of these pathways lead to cell survival and proliferation. A star indicates an alternate breakpoint; a triangle indicates kinase insert domain; TM is transmembrane domain; WW is WW-like domain; P is phosphorylation site.

4.6 THERAPEUTICS FOR HEMATOPOIETIC CANCERS WITH RTK TRANSLOCATIONS

There are a number of drugs that have been characterized for their potential to inhibit the fusion proteins discussed in this review in Table 3. These function to inhibit or reduce the kinase activity of the RTK fusion partner leading to reduced proliferation, increased apoptosis and altered downstream signaling.

ALK Fusions

Crizotinib, the first ALK inhibitor to be clinically tested, is a potent, ATP-competitive, small molecule inhibitor initially designed against the hepatocyte growth factor receptor (c-Met) to inhibit phosphorylation. It inhibits ALK phosphorylation and signal transduction leading to apoptosis in lymphoma cell lines that express the NPM-ALK fusion protein (4, 66). This ALK inhibitor also shows an antitumor activity in ALCL Karpas299 mouse xenograft models expressing the NPM-ALK fusion by inhibiting c-Met and ALK downstream signaling, resulting in reduction of tumor growth (66). Crizotinib has been extensively used to treat solid tumors containing EML4-ALK and STRN-ALK fusions in thyroid cancer and EML4-ALK rearrangements in non-small cell lung cancer (NSCLC) (67-69). Crizotinib is currently in multiple clinical trials for treating patients with ALCL (Table 3).

Unfortunately, resistance and relapse can occur with crizotinib treatment leading to secondary mutations in ALK, rendering the drug ineffective (70). For instance, after treating human cell lines expressing the NPM-ALK fusion with high doses of crizotinib, the mutations L1196Q and I1171N were identified in the ALK kinase domain and shown to confer resistance to crizotinib in NPM-ALK expressing Ba/F3 cells (71). The L1196Q is a **gatekeeper mutation** within the ATP binding pocket, in the hinge region between the N and C lobes. Point mutation of this region prevents or reduces the binding of the inhibitory molecules and is a common occurrence in inhibitor-resistant cancers (71). The I1171N mutation is part of the hydrophobic spine of the kinase domain critical for tyrosine kinase activity (71). In RANBP2-ALK the kinase domain mutation G1269A was found in patients with AML and NSCLS after crizotinib treatment (70), and again this occurs in the ATP binding pocket and acts by decreasing TKI affinity (70).

An alternative selective ALK inhibitor, ceritinib, has been approved for treatment of NSCLC with the NPM-ALK fusion and is in a phase II trial for relapsed/refractory ALK+ hematologic malignancies (Table 3) (72). Another alternative, brigatinib, also leads to resistance through point mutations in the ALK kinase domain in NPM-ALK-amplified ALCL cells (73). One study finds that removal of the kinase inhibitor actually leads to apoptosis of the brigatinib-resistant ALCL cells by hyperactivation of the MAPK pathway (10). This suggests that a periodic suspension of drug treatment might potentially be beneficial for cancer patients with ALK translocations/amplifications. Additionally, since NPM-ALK fusion proteins are only active in the cytoplasm, blocking nuclear export of the fusion with selective inhibitors of nuclear export (SINE), such as selinexor, are currently under investigation in clinical trials for hematological cancers (Table 3) (10). Interestingly, a non-toxic naturally-occurring compound found in extracts from the plant silybum marianum (milk thistle) seeds, silibinin, which has known anti-tumor effects, is able to inhibit NPM-ALK activation leading to reduced proliferation and increased apoptosis in Karpas299 and SupM2 cell lines (74).

FGFR Fusions

The importance of inhibiting aberrant FGFR signaling in FGFR-dependent malignancies is a well-established therapeutic target; however, specific FGFR inhibitors have been elusive (75). The classic FGFR inhibitor, dovitinib is a multi-targeted RTK inhibitor which targets FGFR, PDGFR, VEGFR, FLT3 and c-KIT. When the fusion proteins ZNF198-FGFR1 and BCR-FGFR1 are expressed in Ba/F3 cells, treatment with dovitinib results in the inhibition of STAT5, MAPK, IL-3 independence and phosphorylation of the fusion proteins (20). Proliferation of FGFR1OP2-FGFR1 cell lines is also inhibited by dovitinib (20). A

phase II trial for dovitinib was recently completed in 2015 for patients with solid or hematologic malignancies with mutations or translocations of FGFR and other RTKs (Table 3). The FDA-approved FGFR inhibitor, ponatinib, is also a multi-RTK inhibitor that is currently in multiple trials for AML and CML (75). Ponatinib shows potential for EMS treatment in the murine Baf3 cell lines expressing the ZNF198-FGFR1 and BCR-FGFR1 fusions, and in the human KG1A cell line expressing the FGFR1OP2-FGFR1 fusion, leading to reduced proliferation, survival and phosphorylation of the FGFR1 fusion proteins and downstream substrates and induction of apoptosis (76). In addition, cells from EMS patients show reduced colony growth when treated with ponatinib (21). The specific pan-FGFR inhibitor, infigratinib, shows potential for EMS treatment as it is able to reduce survival and proliferation of TPR-FGFR1 expressing murine 32Dcl3 cells (77). It is currently in clinical trials for patients with FGFR genetic alterations (Table 3).

In order to overcome the resistance that can occur with kinase inhibitors, FGFR irreversible inhibitors 2 (FIIN-2) and 3 (FIIN-3), have recently been developed which target cysteines in the ATP binding pocket. They inhibit the proliferation of transformed Ba/F3 cells dependent upon the gatekeeper mutants of FGFR1 or FGFR2 which often lead to drug resistance (78).

PDGFR Fusions

Imatinib is a multikinase inhibitor selective for ABL, PDGFR and c-Kit and is the most common treatment for malignancies associated with activated PDGFR. Hematolymphiod neoplasms associated with PDGFRα and PDGFRβ fusions such as FIP1L1-PDGFRα and ETV6-PDGFRβ respond well to treatment with imatinib, with secondary

resistance being uncommon. In contrast, patients with rare and aggressive neoplasms containing FGFR1 fusions tend not be responsive to imatinib treatment (37). BCR-PDGFRα fusions found in aCML become undetectable when treated with imatinib. Diagnosing the difference between CML and aCML, both of which display highly similar phenotypes, is important to prevent treatment with an inadequate TKI (39).

When resistance does occur, mutations have been found in the ATP binding site gatekeeper residue, T674I, of FIP1L1-PDGFRα. A novel TKI, S116836, has recently been found to be effective in inhibiting both FIP1L1-PDGFRα and FIP1L1-PDGFRα T674I downstream signaling, and reducing xenograft tumors in nude mice formed in response to BaF3 cells expressing FIP1L1-PDGFRα T674I (79). The fusion proteins driving hematopoietic cancers often becoming resistant, leading to additional mutations, thus highlighting the putative need for multiple types of drugs at various times during treatment.

Table 3. TKIs: Therapeutics for Hematopoietic Disorders

RTK	Drug	Mechanism	www.ClinicalTrials.gov
ALK	Crizotinib (PF02341066)	Multi-target TKI against ALK, MET, ROS-1; ATP binding pocket	NCT02487316; NCT01979536; NCT01606878; NCT02419287; NCT00939770; NCT00585195; NCT01524926
ALK	Ceritinib (LDK378)	TKI against ALK; ATP binding pocket	NCT01742286; NCT0729961; NCT02465528; NCT02186821; NCT02343679
ALK	Brigatinib (AP26113)	TKI against ALK and EGFR; ATP binding pocket	NCT01449461
ALK	Selinexor (KPT330)	Selective inhibitor of nuclear export; modifies CRM1-cargo binding cysteine residue	NCT02530476; NCT02573363; NCT02093403; NCT02416908; NCT02088541; NCT02299518; NCT02403310; NCT02249091; NCT02485535; NCT02212561; NCT02091245
ALK	Silibinin	Antioxidant; biochemical activity under investigation	No trials with Lymphomas
FGFR	Dovitinib (TKI258)	Multi-target TKI against FGFR, PDGFR, VEGFR, FLT3, c-KIT; ATP binding pocket	NCT01831726
FGFR	Ponatinib (AP24534)	Multi-target TKI against FGFR, PDGFR, VEGFR; ATP binding pocket	NCT02627677; NCT02467270; NCT00660920; NCT01667133; NCT01746836; NCT02398825; NCT01207440; NCT01620216
FGFR	Infigratinib (BGJ398)	pan FGFR inhibitor; ATP binding pocket	NCT02160041
FGFR	FIIN2 and FIIN3	TKI against FGFR and EGFR; targets Cys residue(s) in ATP binding pocket	No trials
PDGFR	Imatinib (STI571)	Multi-target TKI against PDGFR, ABL, c-KIT; ATP binding pocket	NCT00044304; NCT00038675
PDGFR	S116836	Multi-target TKI against gatekeeper residue of PDGFR, FLT, TIE2, KIT, SRC family kinases; ATP binding site	No trials

4.7 CONCLUDING REMARKS

Factors that influence translocations include chromosome position, DNA damage response pathways, transcription frequency and epigenetic factors. Transcription can be a driver of translocations, possibly due to DNA supercoiling and torsional stress leading to topoisomerase-induced breaks (6). In this review, we discussed translocations involving RTKs in hematopoietic disorders including ALK, FGFR, PDGFR, RET, CSF1R and NTRK3. Although many translocations have been identified, activation pathways and mechanistic insight for many of these RTK fusions in cancer pathogenesis have yet to be elucidated.

The discovery of these translocations has already facilitated the use of novel RTK inhibitor therapies to treat patients who are positive for translocation-induced cancers. While some RTK-targeted therapies have proven to be beneficial in various malignancies, challenges remain as many cases result in drug resistance or relapse. Therefore, there is an urgent need for additional approaches to the characterization and treatment of RTK-translocation induced cancers. The identification of chromosomal translocations occurring in different cancers will be essential, and the utilization of multiple drug types during different treatment stages may prove to be efficacious. It is crucial that the robust discovery and characterization of these RTK fusions continue to allow the development of finely tuned therapies for hematopoietic disorders.

4.8 ACKNOWLEDGMENTS

Chapter 4 was published as “Receptor Tyrosine Kinases: Translocation Partners in Hematopoietic Disorders”, in Trends in Molecular Medicine in 2017, with the authors of

Nelson KN, Peiris MN, Meyer AN, Siari A, Donoghue DJ. The dissertation author was the primary investigator and author of this material.

4.9 REFERENCES

1 Mitelman, F., Johansson, B., and Mertens, F. The impact of translocations and gene fusions on cancer causation. Nat Rev Cancer 7, 2007. 233-245

2 Iwasaki, J., Kondo, T., Darmanin, S., Ibata, M., Onozawa, M., Hashimoto, D., Teshima, T. Dynamics of double strand breaks and chromosomal translocations. Molecular cancer 2014. 13, 249

3 Hakim, O., Resch, W., Yamane, A., Klein, I., Kieffer-Kwon, K.R., Jankovic, M., Casellas, R. DNA damage defines sites of recurrent chromosomal translocations in B lymphocytes. Nature 2012. 484, 69-74

4 Hallberg, B. and Palmer, R.H. Mechanistic insight into ALK receptor tyrosine kinase in human cancer biology. Nat Rev Cancer 2013. 13, 685-700

5 Scheijen, B. and Griffin, J.D. Tyrosine kinase oncogenes in normal hematopoiesis and hematological disease. Oncogene 2002. 21, 3314-3333

6 Roukos, V. and Mathas, S. The origins of ALK translocations. Front Biosci (Schol Ed) 2015. 7, 260-268

7 Barreca, A., Lasorsa, E., Riera, L., Machiorlatti, R., Piva, R., Ponzoni, M. Anaplastic lymphoma kinase in human cancer. J Mol Endocrinol 2011. 47, R11-23

8 Drexler, H.G., Gignac, S.M., von Wasielewski, R., Werner, M., and Dirks, W.G. Pathobiology of NPM-ALK and variant fusion genes in anaplastic large cell lymphoma and other lymphomas. Leukemia 2000. 14, 1533-1559

9 Lawrence, K., Berry, B., Handshoe, J., Hout, D., Mazzola, R., Morris, S.W., and Saltman, D.L. Detection of a TRAF1-ALK fusion in an anaplastic large cell lymphoma patient with chemotherapy and ALK inhibitor-resistant disease. BMC Res Notes 2015. 8, 308

10 Ceccon, M., Merlo, M.E., Mologni, L., Poggio, T., Varesio, L.M., Menotti, M., . . . Voena, C. Excess of NPM-ALK oncogenic signaling promotes cellular apoptosis and drug dependency. Oncogene 2015.

11 Toffalini, F. and Demoulin, J.B. New insights into the mechanisms of hematopoietic cell transformation by activated receptor tyrosine kinases. Blood 2010. 116, 2429-2437

12 Roix, J.J., McQueen, P.G., Munson, P.J., Parada, L.A., and Misteli, T. Spatial proximity of translocation-prone gene loci in human lymphomas. Nat Genet 2003. 34, 287-291

13 Mathas, S., Kreher, S., Meaburn, K.J., Johrens, K., Lamprecht, B., Assaf, C., . . . Dorken, B. Gene deregulation and spatial genome reorganization near breakpoints prior to formation of translocations in anaplastic large cell lymphoma. Proc Natl Acad Sci U S A 2009. 106, 5831-5836

14 Gallo, L.H., Nelson, K.N., Meyer, A.N., and Donoghue, D.J. Functions of Fibroblast Growth Factor Receptors in cancer defined by novel translocations and mutations. Cytokine Growth Factor Rev 2015. 26, 425-449

15 Moroni, E., Dell'Era, P., Rusnati, M., and Presta, M. Fibroblast growth factors and their receptors in hematopoiesis and hematological tumors. J Hematother Stem Cell Res 2002. 11, 19-32

16 Magnusson, P.U., Ronca, R., Dell'Era, P., Carlstedt, P., Jakobsson, L., Partanen, J., . . . Claesson-Welsh, L. Fibroblast growth factor receptor-1 expression is required for hematopoietic but not endothelial cell development. Arterioscler Thromb Vasc Biol 2005. 25, 944-949

17 Jackson, C.C., Medeiros, L.J., and Miranda, R.N. 8p11 myeloproliferative syndrome: a review. Hum Pathol 2010. 41, 461-476

18 Chinen, Y., Taki, T., Tsutsumi, Y., Kobayashi, S., Matsumoto, Y., Sakamoto, N., . . . Taniwaki, M. The leucine twenty homeobox (LEUTX) gene, which lacks a histone acetyltransferase domain, is fused to KAT6A in therapy-related acute myeloid leukemia with t(8;19)(p11;q13). Genes Chromosomes Cancer 2014. 53, 299-308

19 Baldazzi, C. FGFR1 and KAT6A rearrangements in patients with hematological malignancies and chromosome 8p11 abnormalities: biological and clinical features. Am J Hematol 2016. 91, E14-16

20 Chase, A., Grand, F.H., and Cross, N.C. Activity of TKI258 against primary cells and cell lines with FGFR1 fusion genes associated with the 8p11 myeloproliferative syndrome. Blood 2007. 110, 3729-3734

21 Khodadoust, M.S. Clinical activity of ponatinib in a patient with FGFR1-rearranged mixed-phenotype acute leukemia. Leukemia 2016. 30, 947-950

22 Maeda, T. Transforming property of TEL-FGFR3 mediated through PI3-K in a T-cell lymphoma that subsequently progressed to AML. Blood 2005. 105, 2115-2123

23 Geller, M.D., Pei, Y., Spurgeon, S.E., Durum, C., and Leeborg, N.J. (2014) Chronic lymphocytic leukemia with a FGFR3 translocation: case report and literature review of an uncommon cytogenetic event. Cancer genetics 207, 340-343

24 Cerny, J., Yu, H., and Miron, P.M. Novel FGFR3 rearrangement t(4;22)(p16;q11.2) in a patient with chronic lymphocytic leukemia/small lymphocytic lymphoma. Ann Hematol 2013. 92, 1433-1435

25 Guzzo, C.M., Ringel, A., Cox, E., Uzoma, I., Zhu, H., Blackshaw, S. Characterization of the SUMO-binding activity of the myeloproliferative and mental retardation (MYM)-type zinc fingers in ZNF261 and ZNF198. PLoS One 2014. 9, e105271

26 Demiroglu, A., Steer, E.J., Heath, C., Taylor, K., Bentley, M., Allen, S.L. (2001) The t(8;22) in chronic myeloid leukemia fuses BCR to FGFR1: transforming activity and specific inhibition of FGFR1 fusion proteins. Blood 98, 3778-3783

27 Ren, M. and Cowell, J.K. Constitutive Notch pathway activation in murine ZMYM2-FGFR1-induced T-cell lymphomas associated with atypical myeloproliferative disease. Blood 2011. 117, 6837-6847

28 Chen, J., Deangelo, D.J., Kutok, J.L., Williams, I.R., Lee, B.H., Wadleigh, M., . . . Gilliland, D.G. PKC412 inhibits the zinc finger 198-fibroblast growth factor receptor 1 fusion tyrosine kinase and is active in treatment of stem cell myeloproliferative disorder. Proc Natl Acad Sci U S A 2004. 101, 14479-14484

29 Park, A.R., Regulation of dendritic arborization by BCR Rac1 GTPase-activating protein, a substrate of PTPRT. J Cell Sci 2012. 125, 4518-4531

30 Hernandez, J.M., del Canizo, M.C., Cuneo, A., Garcia, J.L., Gutierrez, N.C., Gonzalez, M., San Miguel, J.F. Clinical, hematological and cytogenetic characteristics of atypical chronic myeloid leukemia. Ann Oncol 2000. 11, 441-444

31 Melo, J.V. BCR-ABL gene variants. Baillieres Clin Haematol 1997. 10, 203-222

32 Dolan, M., Cioc, A., Cross, N.C., Neglia, J.P., and Tolar, J. Favorable outcome of allogeneic hematopoietic cell transplantation for 8p11 myeloproliferative syndrome associated with BCR-FGFR1 gene fusion. Pediatric blood & cancer 2012. 59, 194-196

33 Ren, M. Acute progression of BCR-FGFR1 induced murine B-lympho/myeloproliferative disorder suggests involvement of lineages at the pro-B cell stage. PLoS One 2012. 7, e38265

34 Roumiantsev, S. Distinct stem cell myeloproliferative/T lymphoma syndromes induced by ZNF198-FGFR1 and BCR-FGFR1 fusion genes from 8p11 translocations. Cancer Cell 2004. 5, 287-298

35 Demoulin, J.B. and Montano-Almendras, C.P. Platelet-derived growth factors and their receptors in normal and malignant hematopoiesis. Am J Blood Res 2012. 2, 44-56

36 Kaminski, W.E., Lindahl, P., Lin, N.L., Broudy, V.C., Crosby, J.R., Hellstrom, M., Raines, E.W. Basis of hematopoietic defects in platelet-derived growth factor (PDGF)-B and PDGF beta-receptor null mice. Blood 2001. 97, 1990-1998

37 Vega, F., Medeiros, L.J., Bueso-Ramos, C.E., Arboleda, P., and Miranda, R.N. Hematolymphoid neoplasms associated with rearrangements of PDGFRA, PDGFRB, and FGFR1. Am J Clin Pathol 2015. 144, 377-392

38 Yang, Y., Yuzawa, S., and Schlessinger, J. Contacts between membrane proximal regions of the PDGF receptor ectodomain are required for receptor activation but not for receptor dimerization. Proc Natl Acad Sci U S A 2008. 105, 7681-7686

39 Cluzeau, T., Lippert, E., Cayuela, J.M., Maarek, O., Migeon, M., Noguera, M.E., Rea, D. Novel fusion between the breakpoint cluster region and platelet-derived growth factor receptor-alpha genes in a patient with chronic myeloid leukemia-like neoplasm: undetectable residual disease after imatinib therapy. Eur J Haematol 2015. 95, 480-483

40 Yigit, N., Wu, W.W., Subramaniyam, S., Mathew, S., and Geyer, J.T. BCR-PDGFRA fusion in a T lymphoblastic leukemia/lymphoma. Cancer genetics 2015. 208, 404-407

41 Curtis, C.E., Grand, F.H., Musto, P., Clark, A., Murphy, J., Perla, G. Two novel imatinib-responsive PDGFRA fusion genes in chronic eosinophilic leukaemia. Br J Haematol 2007. 138, 77-81

42 Toffalini, F., Hellberg, C., and Demoulin, J.B. Critical role of the platelet-derived growth factor receptor (PDGFR) beta transmembrane domain in the TEL-PDGFRbeta cytosolic oncoprotein. J Biol Chem 2010. 285, 12268-12278

43 Dobbin, E., Graham, C., Corrigan, P.M., Thomas, K.G., Freeburn, R.W., and Wheadon, H. Tel/PDGFRbeta induces stem cell differentiation via the Ras/ERK and STAT5 signaling pathways. Exp Hematol 2009. 37, 111-121

44 Toffalini, F., Kallin, A., Vandenberghe, P., Pierre, P., Michaux, L., Cools, J., and Demoulin, J.B. The fusion proteins TEL-PDGFRbeta and FIP1L1-PDGFRalpha escape ubiquitination and degradation. Haematologica 2009. 94, 1085-1093

45 Irusta, P.M. Definition of an inhibitory juxtamembrane WW-like domain in the platelet-derived growth factor beta receptor. J Biol Chem 2002. 277, 38627-38634

46 Chiara, F., Bishayee, S., Heldin, C.H., and Demoulin, J.B. Autoinhibition of the platelet-derived growth factor beta-receptor tyrosine kinase by its C-terminal tail. J Biol Chem 2004. 279, 19732-19738

47 Jones, A.V. and Cross, N.C. Oncogenic derivatives of platelet-derived growth factor receptors. Cell Mol Life Sci 2004. 61, 2912-2923

48 Pardanani, A., Ketterling, R.P., Brockman, S.R., Flynn, H.C., Paternoster, S.F., Shearer, B.M., Tefferi, A.CHIC2 deletion, a surrogate for FIP1L1-PDGFRA fusion, occurs in systemic mastocytosis associated with eosinophilia and predicts response to imatinib mesylate therapy. Blood 2003. 102, 3093-3096

49 Stover, E.H., Chen, J., Folens, C., Lee, B.H., Mentens, N., Marynen, P. Activation of FIP1L1-PDGFRalpha requires disruption of the juxtamembrane domain of PDGFRalpha and is FIP1L1-independent. Proc Natl Acad Sci U S A 2006. 103, 8078-8083

50 Iwasaki, J., Kondo, T., Darmanin, S., Ibata, M., Onozawa, M., Hashimoto, D., Teshima, T. FIP1L1 presence in FIP1L1-RARA or FIP1L1-PDGFRA differentially contributes to the pathogenesis of distinct types of leukemia. Ann Hematol 2014. 93, 1473-1481

51 Vanden Bempt, M., Demeyer, S., Mentens, N., Geerdens, E., De Bock, C.E., Wlodarska, I., and Cools, J. Generation of the Fip1l1-Pdgfra fusion gene using CRISPR/Cas genome editing. Leukemia 2016. 30, 1913-1916

52 Moore, N.F. Molecular rationale for the use of PI3K/AKT/mTOR pathway inhibitors in combination with crizotinib in ALK-mutated neuroblastoma. Oncotarget 2014. 5, 8737-8749

53 Umapathy, G. The kinase ALK stimulates the kinase ERK5 to promote the expression of the oncogene MYCN in neuroblastoma. Science signaling 2014. 7, ra102

54 Wu, C., Molavi, O., Zhang, H., Gupta, N., Alshareef, A., Bone, K.M. STAT1 is phosphorylated and downregulated by the oncogenic tyrosine kinase NPM-ALK in ALK-positive anaplastic large-cell lymphoma. Blood 2015. 126, 336-345

55 Armstrong, F., Duplantier, M.M., Trempat, P., Hieblot, C., Lamant, L., Espinos, E., Touriol, C. Differential effects of X-ALK fusion proteins on proliferation, transformation, and invasion properties of NIH3T3 cells. Oncogene 2004. 23, 6071-6082

56 Armstrong, F., Lamant, L., Hieblot, C., Delsol, G., and Touriol, C. TPM3-ALK expression induces changes in cytoskeleton organisation and confers higher metastatic capacities than other ALK fusion proteins. Eur J Cancer 2007. 43, 640-646

57 Turner, N. and Grose, R. Fibroblast growth factor signalling: from development to cancer. Nat Rev Cancer 2010. 10, 116-129

58 Kasyapa, C.S., Kunapuli, P., Hawthorn, L., and Cowell, J.K. Induction of the plasminogen activator inhibitor-2 in cells expressing the ZNF198/FGFR1 fusion kinase that is involved in atypical myeloproliferative disease. Blood 2006. 107, 3693-3699

59 Montano-Almendras, C.P., Essaghir, A., Schoemans, H., Varis, I., Noel, L.A., Velghe, A.I. ETV6-PDGFRB and FIP1L1-PDGFRA stimulate human hematopoietic progenitor cell proliferation and differentiation into eosinophils: the role of nuclear factor-kappaB. Haematologica 2012. 97, 1064-1072

60 Tomasson, M.H., Sternberg, D.W., Williams, I.R., Carroll, M., Cain, D., Aster, J.C., Gilliland, D.G. Fatal myeloproliferation, induced in mice by TEL/PDGFbetaR expression, depends on PDGFbetaR tyrosines 579/581. J Clin Invest 2000. 105, 423-432

61 Noel, L.A., Arts, F.A., Montano-Almendras, C.P., Cox, L., Gielen, O., Toffalini, F., . . . Demoulin, J.B. The tyrosine phosphatase SHP2 is required for cell transformation by the receptor tyrosine kinase mutants FIP1L1-PDGFRalpha and PDGFRalpha D842V. Mol Oncol 2014. 8, 728-740

62 Cain, J.A. Myeloproliferative disease induced by TEL-PDGFRB displays dynamic range sensitivity to Stat5 gene dosage. Blood 2007. 109, 3906-3914

63 Medves, S., Noel, L.A., Montano-Almendras, C.P., Albu, R.I., Schoemans, H., Constantinescu, S.N., and Demoulin, J.B. Multiple oligomerization domains of KANK1-PDGFRbeta are required for JAK2-independent hematopoietic cell proliferation and signaling via STAT5 and ERK. Haematologica 2011. 96, 1406-1414

64 Saint-Dic, D., Chang, S.C., Taylor, G.S., Provot, M.M., and Ross, T.S. Regulation of the Src homology 2-containing inositol 5-phosphatase SHIP1 in HIP1/PDGFbeta R-transformed cells. J Biol Chem 2001. 276, 21192-21198

65 Ross, T.S. and Gilliland, D.G. Transforming properties of the Huntingtin interacting protein 1/ platelet-derived growth factor beta receptor fusion protein. J Biol Chem 1999. 274, 22328-22336

66 Christensen, J.G., Zou, H.Y., Arango, M.E., Li, Q., Lee, J.H., McDonnell, S.R., Los, G. Cytoreductive antitumor activity of PF-2341066, a novel inhibitor of anaplastic lymphoma kinase and c-Met, in experimental models of anaplastic large-cell lymphoma. Mol Cancer Ther 2007. 6, 3314-3322

67 Ji, J.H. Identification of Driving ALK Fusion Genes and Genomic Landscape of Medullary Thyroid Cancer. PLoS genetics 2015. 11, e1005467

68 Kelly, L.M., Barila, G., Liu, P., Evdokimova, V.N., Trivedi, S., Panebianco, F., . . . Nikiforov, Y.E. Identification of the transforming STRN-ALK fusion as a potential therapeutic target in the aggressive forms of thyroid cancer. Proc Natl Acad Sci U S A 2014. 111, 4233-4238

69 Kwak, E.L., Bang, Y.J., Camidge, D.R., Shaw, A.T., Solomon, B., Maki, R.G., . . . Iafrate, A.J. Anaplastic lymphoma kinase inhibition in non-small-cell lung cancer. N Engl J Med 2010. 363, 1693-1703

70 Takeoka, K., Okumura, A., Maesako, Y., Akasaka, T., and Ohno, H. Crizotinib resistance in acute myeloid leukemia with inv(2)(p23q13)/RAN binding protein 2 (RANBP2) anaplastic lymphoma kinase (ALK) fusion and monosomy 7. Cancer genetics 2015. 208, 85-90

71 Ceccon, M., Mologni, L., Bisson, W., Scapozza, L., and Gambacorti-Passerini, C. Crizotinib-resistant NPM-ALK mutants confer differential sensitivity to unrelated Alk inhibitors. Mol Cancer Res 2013. 11, 122-132

72 Marsilje, T.H., Pei, W., Chen, B., Lu, W., Uno, T., Jin, Y. Synthesis, structure-activity relationships, and in vivo efficacy of the novel potent and selective anaplastic lymphoma kinase (ALK) inhibitor 5-chloro-N2-(2-isopropoxy-5-methyl-4-(piperidin-4-yl)phenyl)-N4-(2-(isopropylsulf onyl)phenyl)pyrimidine-2,4-diamine (LDK378) currently in phase 1 and phase 2 clinical trials. J Med Chem 2013. 56, 5675-5690

73 Ceccon, M., Mologni, L., Giudici, G., Piazza, R., Pirola, A., Fontana, D., and Gambacorti-Passerini, C. Treatment Efficacy and Resistance Mechanisms Using the Second-Generation ALK Inhibitor AP26113 in Human NPM-ALK-Positive Anaplastic Large Cell Lymphoma. Mol Cancer Res 2015. 13, 775-783

74 Molavi, O. Silibinin suppresses NPM-ALK, potently induces apoptosis and enhances chemosensitivity in ALK-positive anaplastic large cell lymphoma. Leuk Lymphoma 2016. 57, 1154-1162

75 Brooks, A.N., Kilgour, E., and Smith, P.D. Molecular pathways: fibroblast growth factor signaling: a new therapeutic opportunity in cancer. Clin Cancer Res 2012. 18, 1855-1862

76 Chase, A., Grand, F.H., and Cross, N.C. Ponatinib as targeted therapy for FGFR1 fusions associated with the 8p11 myeloproliferative syndrome. Haematologica 2013. 98, 103-106

77 Malli, T. Functional characterization, localization, and inhibitor sensitivity of the TPR-FGFR1 fusion in 8p11 myeloproliferative syndrome. Genes Chromosomes Cancer 2016. 55, 60-68

78 Tan, L., Wang, J., Tanizaki, J., Huang, Z., Aref, A.R., Rusan, M. Development of covalent inhibitors that can overcome resistance to first-generation FGFR kinase inhibitors. Proc Natl Acad Sci U S A 2014. 111, E4869-4877

79 Shen, Y., Ren, X., Ding, K., Zhang, Z., Wang, D., and Pan, J. Antitumor activity of S116836, a novel tyrosine kinase inhibitor, against imatinib-resistant FIP1L1-PDGFRalpha-expressing cells. Oncotarget 2014. 5, 10407-10420

80 Cools, J., Wlodarska, I., Somers, R., Mentens, N., Pedeutour, F., Maes, B., . . . Marynen, P. Identification of novel fusion partners of ALK, the anaplastic lymphoma kinase, in anaplastic large-cell lymphoma and inflammatory myofibroblastic tumor. Genes Chromosomes Cancer 2002. 34, 354-362

81 Cerchietti, L., Damm-Welk, C., Vater, I., Klapper, W., Harder, L., Pott, C., Woessmann, W. Inhibition of anaplastic lymphoma kinase (ALK) activity provides a therapeutic approach for CLTC-ALK-positive human diffuse large B cell lymphomas. PLoS One 2011. e18436

82 Tokuda, K., Eguchi-Ishimae, M., Yagi, C., Kawabe, M., Moritani, K., Niiya, T., Eguchi, M. CLTC-ALK fusion as a primary event in congenital blastic plasmacytoid dendritic cell neoplasm. Genes Chromosomes Cancer 2014. 53, 78-89

83 Tort, F. Heterogeneity of genomic breakpoints in MSN-ALK translocations in anaplastic large cell lymphoma. Hum Pathol 2004. 35, 1038-1041

84 Lamant, L., Gascoyne, R.D., Duplantier, M.M., Armstrong, F., Raghab, A., Chhanabhai, M. Non-muscle myosin heavy chain (MYH9): a new partner fused to ALK in anaplastic large cell lymphoma. Genes Chromosomes Cancer 2003. 37, 427-432

85 Lee, S.E., Kang, S.Y., Takeuchi, K., and Ko, Y.H. Identification of RANBP2-ALK fusion in ALK positive diffuse large B-cell lymphoma. Hematol Oncol 2014. 32, 221-224

86 Lim, J.H., Jang, S., Park, C.J., Cho, Y.U., Lee, J.H., Lee, K.H. RANBP2-ALK fusion combined with monosomy 7 in acute myelomonocytic leukemia. Cancer genetics 2014. 207, 40-45

87 Maesako, Y., Okumura, A., Takeoka, K., Kishimori, C., Izumi, K., Kamoda, Y., Ohno, H. Reduction of leukemia cell burden and restoration of normal hematopoiesis at 3 months of crizotinib treatment in RAN-binding protein 2 (RANBP2)-anaplastic lymphoma kinase (ALK) acute myeloid leukemia. Leukemia 2014. 28, 1935-1937

88 Van Roosbroeck, K. ALK-positive large B-cell lymphomas with cryptic SEC31A-ALK and NPM1-ALK fusions. Haematologica 2010. 95, 509-513

89 d'Amore, E.S. STAT3 pathway is activated in ALK-positive large B-cell lymphoma carrying SQSTM1-ALK rearrangement and provides a possible therapeutic target. Am J Surg Pathol 2013. 37, 780-786

90 Meech, S.J., McGavran, L., Odom, L.F., Liang, X., Meltesen, L., Gump, J., Hunger, S.P. Unusual childhood extramedullary hematologic malignancy with natural killer cell properties that contains tropomyosin 4--anaplastic lymphoma kinase gene fusion. Blood 2001. 98, 1209-1216

91 Abate, F. A novel patient-derived tumorgraft model with TRAF1-ALK anaplastic large-cell lymphoma translocation. Leukemia 2015. 29, 1390-1401

92 Lilljebjorn, H., Agerstam, H., Orsmark-Pietras, C., Rissler, M., Ehrencrona, H., Nilsson, L. RNA-seq identifies clinically relevant fusion genes in leukemia including a novel MEF2D/CSF1R fusion responsive to imatinib. Leukemia 2014. 28, 977-979

93 Wasag, B., Lierman, E., Meeus, P., Cools, J., and Vandenberghe, P. The kinase inhibitor TKI258 is active against the novel CUX1-FGFR1 fusion detected in a patient with T-lymphoblastic leukemia/lymphoma and t(7;8)(q22;p11). Haematologica 2011. 96, 922-926

94 Soler, G. LRRFIP1, a new FGFR1 partner gene associated with 8p11 myeloproliferative syndrome. Leukemia 2009. 23, 1359-1361

95 Gervais, C., Dano, L., Perrusson, N., Helias, C., Jeandidier, E., Galoisy, A.C., Mauvieux, L. A translocation t(2;8)(q12;p11) fuses FGFR1 to a novel partner gene, RANBP2/NUP358, in a myeloproliferative/myelodysplastic neoplasm. Leukemia 2013. 27, 1186-1188

96 Burke, R.M. and Berk, B.C. The Role of PB1 Domain Proteins in Endothelial Cell Dysfunction and Disease. Antioxid Redox Signal 2015. 22, 1243-1256

97 Myeku, N. and Figueiredo-Pereira, M.E. Dynamics of the degradation of ubiquitinated proteins by proteasomes and autophagy: association with sequestosome 1/p62. J Biol Chem 2011. 286, 22426-22440

98 Kralik, J.M., Kranewitter, W., Boesmueller, H., Marschon, R., Tschurtschenthaler, G., Rumpold, H Characterization of a newly identified ETV6-NTRK3 fusion transcript in acute myeloid leukemia. Diagn Pathol 2011. 6, 19

99 Walz, C., Haferlach, C., Hanel, A., Metzgeroth, G., Erben, P., Gosenca, D. Transient response to imatinib in a chronic eosinophilic leukemia associated with ins(9;4)(q33;q12q25) and a CDK5RAP2-PDGFRA fusion gene. Genes Chromosomes Cancer 2006. 45, 950-956

100 Metzgeroth, G. Recurrent finding of the FIP1L1-PDGFRA fusion gene in eosinophilia-associated acute myeloid leukemia and lymphoblastic T-cell lymphoma. Leukemia 2007. 21, 1183-1188

101 Sugimoto, Y., Sada, A., Shimokariya, Y., Monma, F., Ohishi, K., Masuya, M., . Katayama, N. A novel FOXP1-PDGFRA fusion gene in myeloproliferative neoplasm with eosinophilia. Cancer genetics 2015. 208, 508-512

102 Score, J., Curtis, C., Waghorn, K., Stalder, M., Jotterand, M., Grand, F.H., and Cross, N.C. Identification of a novel imatinib responsive KIF5B-PDGFRA fusion gene following screening for PDGFRA overexpression in patients with hypereosinophilia. Leukemia 2006. 20, 827-832

103 Chmielecki, J. Systematic screen for tyrosine kinase rearrangements identifies a novel C6orf204-PDGFRB fusion in a patient with recurrent T-ALL and an associated myeloproliferative neoplasm. Genes Chromosomes Cancer 2012. 51, 54-65

104 Winkelmann, N., Hidalgo-Curtis, C., Waghorn, K., Score, J., Dickinson, H., Jack, A., . Cross, N.C. Recurrent CEP85L-PDGFRB fusion in patient with t(5;6) and imatinib-responsive myeloproliferative neoplasm with eosinophilia. Leuk Lymphoma 2013. 54, 1527-1531

105 Vizmanos, J.L., Novo, F.J., Roman, J.P., Baxter, E.J., Lahortiga, I., Larrayoz, M.J.,. Cross, N.C. NIN, a gene encoding a CEP110-like centrosomal protein, is fused to PDGFRB in a patient with a t(5;14)(q33;q24) and an imatinib-responsive myeloproliferative disorder. Cancer Res 2004. 64, 2673-2676

106 Walz, C., Haferlach, C., Hanel, A., Metzgeroth, G., Erben, P., Gosenca, D. Characterization of three new imatinib-responsive fusion genes in chronic myeloproliferative disorders generated by disruption of the platelet-derived growth factor receptor beta gene. Haematologica 2007. 92, 163-169

107 Gong, S.L., Guo, M.Q., Tang, G.S., Zhang, C.L., Qiu, H.Y., Hu, X.X., and Yang, J.M. Fusion of platelet-derived growth factor receptor beta to CEV14 gene in chronic myelomonocytic leukemia: A case report and review of the literature. Oncol Lett 2016. 11, 770-774

108 Kim, H.G., Jang, J.H., and Koh, E.H. TRIP11-PDGFRB fusion in a patient with a therapy-related myeloid neoplasm with t(5;14)(q33;q32) after treatment for acute promyelocytic leukemia. Mol Cytogenet 2014. 7, 103

109 Gosenca, D., Kellert, B., Metzgeroth, G., Haferlach, C., Fabarius, A., Schwaab, J., Reiter, A. Identification and functional characterization of imatinib-sensitive DTD1-PDGFRB and CCDC88C-PDGFRB fusion genes in eosinophilia-associated myeloid/lymphoid neoplasms. Genes Chromosomes Cancer 2014. 53, 411-421

110 Gorello, P., La Starza, R., Brandimarte, L., Trisolini, S.M., Pierini, V., Crescenzi, B., Mecucci, C. A PDGFRB-positive acute myeloid malignancy with a new t(5;12)(q33;p13.3) involving the ERC1 gene. Leukemia 2008. 22, 216-218

111 Drechsler, M., Hildebrandt, B., Kundgen, A., Germing, U., and Royer-Pokora, B. Fusion of H4/D10S170 to PDGFRbeta in a patient with chronic myelomonocytic leukemia and long-term responsiveness to imatinib. Ann Hematol 2007. 86, 353-354

112 Schwaller, J. H4(D10S170), a gene frequently rearranged in papillary thyroid carcinoma, is fused to the platelet-derived growth factor receptor beta gene in atypical chronic myeloid leukemia with t(5;10)(q33;q22). Blood 2001. 97, 3910-3918

113 Morerio, C., Acquila, M., Rosanda, C., Rapella, A., Dufour, C., Locatelli, F., Panarello, C. HCMOGT-1 is a novel fusion partner to PDGFRB in juvenile myelomonocytic leukemia with t(5;17)(q33;p11.2). Cancer Res 2004. 64, 2649-2651

114 Walz, C. Identification of a MYO18A-PDGFRB fusion gene in an eosinophilia-associated atypical myeloproliferative neoplasm with a t(5;17)(q33-34;q11.2). Genes Chromosomes Cancer 2009. 48, 179-183

115 La Starza, R., Rosati, R., Roti, G., Gorello, P., Bardi, A., Crescenzi, B.A new NDE1/PDGFRB fusion transcript underlying chronic myelomonocytic leukaemia in Noonan Syndrome. Leukemia 2007. 21, 830-833

116 Wilkinson, K. Cloning of the t(1;5)(q23;q33) in a myeloproliferative disorder associated with eosinophilia: involvement of PDGFRB and response to imatinib. Blood 2003. 102, 4187-4190

117 Magnusson, M.K., Meade, K.E., Brown, K.E., Arthur, D.C., Krueger, L.A., Barrett, A.J., and Dunbar, C.E. Rabaptin-5 is a novel fusion partner to platelet-derived growth factor beta receptor in chronic myelomonocytic leukemia. Blood 2001. 98, 2518-2525

118 Grand, F.H., Burgstaller, S., Kuhr, T., Baxter, E.J., Webersinke, G., Thaler, J., Cross, N.C. p53-Binding protein 1 is fused to the platelet-derived growth factor receptor beta in a patient with a t(5;15)(q33;q22) and an imatinib-responsive eosinophilic myeloproliferative disorder. Cancer Res 2004. 64, 7216-7219

119 Ballerini, P., Struski, S., Cresson, C., Prade, N., Toujani, S., Deswarte, C. RET fusion genes are associated with chronic myelomonocytic leukemia and enhance monocytic differentiation. Leukemia 2012. 26, 2384-2389

120 Weiss, A. and Schlessinger, J. Switching signals on or off by receptor dimerization. Cell 1998. 94, 277-280

121 Schlessinger, J. Cell signaling by receptor tyrosine kinases. Cell 2000. 103, 211-225

122 Grande, E., Bolos, M.V., and Arriola, E. Targeting oncogenic ALK: a promising strategy for cancer treatment. Mol Cancer Ther 2011. 10, 569-579

123 Hasan, M.K., Nafady, A., Takatori, A., Kishida, S., Ohira, M., Suenaga, Y., . Nakagawara, A. ALK is a MYCN target gene and regulates cell migration and invasion in neuroblastoma. Scientific reports 2013. 3, 3450

124 Reshetnyak, A.V., et al. Augmentor alpha and beta (FAM150) are ligands of the receptor tyrosine kinases ALK and LTK: Hierarchy and specificity of ligand-receptor interactions. Proc Natl Acad Sci U S A 2015. 112, 15862-15867

125 Guan, J. FAM150A and FAM150B are activating ligands for anaplastic lymphoma kinase. Elife 2015. 4, e09811

126 Murray, P.B. Heparin is an activating ligand of the orphan receptor tyrosine kinase ALK. Science signaling 2015. 8, ra6

127 Andrae, J., Gallini, R., and Betsholtz, C. Role of platelet-derived growth factors in physiology and medicine. Genes Dev 2008. 22, 1276-1312

128 Bonifer, C. and Hume, D.A. The transcriptional regulation of the Colony-Stimulating Factor 1 Receptor (csf1r) gene during hematopoiesis. Front Biosci 2008. 13, 549-560